Mon. Not. R. Astron. Soc. **000**, 1–?? (2009) Printed 21 October 2010 (MN LATEX style file v2.2)

Luminous Blue Variable eruptions and related transients: Diversity of progenitors and outburst properties

Nathan Smith[1,2⋆], Weidong Li[2], Jeffrey M. Silverman[2], Mohan Ganeshalingam[2], & Alexei V. Filippenko[2]
[1] *Steward Observatory, University of Arizona, 933 North Cherry Avenue, Tucson, AZ 85721, USA*
[2] *Astronomy Department, University of California, Berkeley, CA 94720-3411, USA*

Accepted 0000, Received 0000, in original form 0000

ABSTRACT

We present new light curves and spectra for a number of extragalactic optical transients or "supernova (SN) impostors" related to giant eruptions of luminous blue variables (LBVs), and we provide a comparative discussion of LBV-like giant eruptions known to date. New data include photometry and spectroscopy of SNe 1999bw, 2000ch, 2001ac, 2002bu, 2006bv, and 2010dn. SN 2010dn is a carbon copy of SN 2008S and NGC 300-OT, whereas SN 2002bu shows spectral evolution from a normal LBV at early times to a twin of these cooler transients at late times. SN 2008S, NGC300-OT, and SN 2010dn appear to be special cases of a broader eruptive phenomenon where the progenitor star was enshrouded by dust, perhaps from a previous unseen eruptive episode. Evidence suggests that their progenitors have initial masses in the range 10–20 $M_{\odot}$, extending the range of masses susceptible to violent eruptive phenomenon below the canoncial LBV mass range. Examining the full sample, SN impostors are characterized by strong photometric variability on a range of timescales from a day to decades, potentially suffering multiple eruptions of the same source. The upper end of the luminosity distribution overlaps with the least luminous core-collapse SNe, but in most cases a distinction can be made based on spectra. The low end of the luminosity distribution is far less well defined, and a distinction between LBV giant eruptions, S Doradus phases of LBVs, novae, and possible eruptions of intermediate-mass stars is not entirely clear. We discuss observational clues concerning stellar winds or shocks as the relevant mass-loss mechanism, and we evaluate possible ideas for the physical mechanism(s) of outbursts, but *there is still a great need for theoretical work on this problem.* Although known examples of these eruptions are sufficient to illustrate their remarkably wide diversity in peak absolute magnitude, duration, progenitor stars, outburst spectra, and other observable properties, their statistical distribution is an area that will benefit greatly from upcoming transient surveys. Based on the distribution of these eruptive properties, we propose that the prototypical object SN 1961V was not a member of this class of impostors after all, but was instead a true core-collapse SN IIn that was preceded by a giant LBV eruption.

Key words: instabilities — stars: evolution — stars: mass loss — stars: winds, outflows — supernovae: general

1 INTRODUCTION

This paper investigates observations of transient phenomena known variously as luminous blue variable (LBV) eruptions, supernova (SN) impostors, or other optical transients usually associated with massive stars. These are thought to be nonterminal eruptions or explosions (i.e., not core-collapse) related to the extreme brightening events observed in LBVs such as η Carinae, although the physical mechanism of the outbursts is not yet known. The naming convention is rather haphazard, with some earning official SN designations — only to be recognized later as "impostors" — while others deemed unworthy are demoted to generic optical transients

⋆ Email: nathans@as.arizona.edu

at the time of discovery.[1] When designated as a SN, their spectra are classified as Type IIn due to the strong and narrow H I emission lines that arise from their relatively slow winds or ejecta, typically moving at $\lesssim$1000 km s^{-1}.

Only two of these events have been witnessed in our own galaxy,[2] both as historical naked-eye transients: P Cygni erupted in 1600 A.D., and η Carinae suffered its so-called Great Eruption in the mid 19th century. While small in number, these nearby events have had an enormous influence on our understanding of the phenomenon, since their physical parameters are relatively well constrained and we can verify that the stars survived the eruptive events. They are the only two outbursts where we can directly measure the total mass ejected; analysis of their spatially resolved circumstellar shells implies more than 10 $M_{\odot}$ in the case of η Carinae (Smith et al. 2003b) and only about 0.1 $M_{\odot}$ for P Cygni (Smith & Hartigan 2006). The radiated and kinetic energy in these events also differed by more than two orders of magnitude, so from just these two events we can already see a wide diversity among the eruptions of LBVs, which is a major theme in this paper.

Additional examples from nearby external galaxies are also known. SN 1954J was the eruption of the bright blue irregular variable V12 in NGC 2403 (Tammann & Sandage 1968; Smith et al. 2001; Van Dyk et al. 2005), and the famously weird object SN 1961V was originally categorized as a Type V event (Zwicky 1964), but was later thought to be an extreme version of a non-terminal eruption *a la* η Car (Goodrich et al. 1989; Filippenko et al. 1995). Together with P Cygni and η Car, these four historical LBV giant eruptions have come to represent the class of SN impostors (Van Dyk 2005; Humphreys et al. 1999).[3] The eclipsing binary HD 5980 (the most luminous star in the SMC) and V1 in NGC 2366 both suffered eruptions in the mid 1990s, and over a dozen more examples have been discovered in the past decade in the course of various SN searches. A list of these events is provided later in the paper.

LBVs are thought to be massive stars that are unstable because they have reached a point in their evolution where they are dangerously close to the classical Eddington limit, partly due to core evolution and partly to mass loss in preceding phases (see e.g., Smith & Conti 2008). It was suggested long ago that cool temperatures in the stellar envelopes may lead to an opacity-modified Eddington limit that may play a role in initiating the outbursts (Lamers & Fitzpatrick 1988; Appenzeller 1986), but further progress on the physical mechanism causing LBV eruptions has been slow to enter the refereed literature. Most theoretical work on LBV eruptions so far has focussed on the physics of driving powerful winds in quasi-steady state when a star exceeds the Eddington limit (e.g., Shaviv 2000; Owocki et al. 2004; Owocki 2005; Owocki & van Marle 2007; van Marle et al. 2008, 2009). With the high mass-loss rates required for LBV eruptions, the material must be optically thick and therefore continuum driven or hydrodynamically launched, rather than line driven (Smith & Owocki 2006; van Marle et al. 2008). For this reason, these super-Eddington continuum-driven winds are of interest as a potential mode of mass loss at low metallicity (Smith & Owocki 2006). Although the underlying mechanism behind the increased luminosity remains unknown, the massive shells seen around many LBVs with nebular masses of a few to 20 $M_{\odot}$, combined with the fact that these episodes appear to recur, argue that the episodic ejection of the H envelope in LBV eruptions is a dominant mode of mass loss for massive stars (Smith & Owocki 2006).

The traditional explanation for LBV eruption light curves in historical examples (e.g., Humphreys et al. 1999; Humphreys & Davidson 1994) has been that a massive star increases its bolometric luminosity output and then reaches or exceeds the classical Eddington limit; this initiates catastrophic mass loss. Dust condensation in the ejected shell eventually obscures the star and causes the object to fade at visual wavelengths. Humphreys et al. (1999) suggested that these "giant eruptions" are different from the more typical "S Doradus variability" exhibited by LBVs in that their bolometric luminosity increases, whereas the visual brightening in a normal S Doradus episode is thought to be caused by a change in bolometric correction at constant luminosity. The traditional view has been that LBVs should be relatively cool in their bright phases, exhibiting an F supergiant-like spectrum (Humphreys & Davidson 1994). Modern observations are revealing that these and other characterizations of LBV eruptions, which are based on few examples, are not necessarily true for the class, and so our understanding of these events is still developing as we discover additional examples.

A qualitative shift in interpreting LBV giant eruptions came with the recent recogition that strong shock waves may also play a role in some of the outbursts. This became apparent following the discovery of very fast ejecta surrounding η Carinae (Smith 2008), but it had been suspected earlier based on the rough equipartition in the kinetic and radiated energy budgets of its 19th century giant eruption (Smith et al. 2003b). Smith (2008) suggested that we may expect to see X-rays or radio emission from some LBV eruptions, and that this evidence for a shock would not necessarily implicate a core-collapse event. Since then, Dessart et al. (2010) have explored weak explosions as a possible mechanism for some SN impostor events, and additional observational evidence for an explosive component in LBV eruptions is accumulating. In particular, Smith et al. (2010a) proposed that the fast ($\sim$5000 km s^{-1}) ejecta seen in absorption in SN 2009ip

[1] While none of these names are ideal, we tentatively prefer "LBV-like eruptions", since it is based on an observationally established class of objects, while we remain cognizant of the possibility that LBV-like outbursts might also occur in cool (i.e., non-blue) stars like red supergiants, or stars that are not necessarily the most massive stars. This paper attempts to provide a comparative study of the light curves and spectra for known examples of this class. One must also be careful to distinguish between "LBVs" — which refers to a particular class of variable stars, not all of which have been observed to suffer a giant eruption like η Car — and "LBV-like eruptions", which refers to the temporary brightening event that resembles the giant eruptions observed in LBVs like η Car (i.e., not all LBVs have documented giant eruptions).

[2] If V838 Mon is a similar type of event, then it would be the third example in our galaxy.

[3] As we argue in this paper, however, SN 1961V may be a true core-collapse SN IIn event. One day before submission of this paper, we learned that Kochanek et al. (private comm.) simultaneously reached a similar conclusion about SN 1961V based on the lack of an expected mid-IR counterpart.

may result from an explosion similar to that inferred for η Car, and that shock excitation may be important in explaining some of the diversity among spectral properties of LBV eruptions. Preliminary reports of a high X-ray luminosity in the very recent LBV eruption SN 2010da (Immler et al. 2010) may also suggest the influence of a shock, but this new object is still being studied at the time of writing (see below). The influence of both shocks and super-Eddington winds on observations of LBV eruptions was discussed in detail by Smith et al. (2010a). Although shocks may play a role in a few cases, strong super-Eddington winds must operate in many of the LBV eruptions.

Another key development in our interpretation of these eruptions is that their progenitors may be substantially more diverse than previously recognized. SN 2008S and the 2008 optical transient in NGC 300 (N300-OT hereafter) were similar in their observed properties to other SN impostors, but Prieto and collaborators (Prieto 2008; Prieto et al. 2008; Thompson et al. 2009) discovered that their progenitors were faint and heavily obscured. While only upper limits were available for visual wavelengths, archival *Spitzer* data suggested IR luminosities of $\lesssim 10^{4.9}$ $L_{\odot}$ before the eruptions. If the progenitor stars were cool, their observed IR luminosities could be consistent with initial masses as low as 8–10 $M_{\odot}$, suggesting the intriguing possibility that these eruptions might be associated with weak electron capture SNe in extreme AGB stars (Thompson et al. 2009; Botticella et al. 2009), or that they may be associated with obscured OH/IR stars (see also Khan et al. 2010a). On the other hand, if they were heavily obscured supergiant stars, their IR luminosities would imply initial masses of 10–20 $M_{\odot}$ (Smith et al. 2009a, 2010a; Bond et al. 2009; Berger et al. 2010). Smith et al. (2010a) discussed this debate in detail, showing that the IR luminosity of N300-OT, for example, was quite similar to the progenitor luminosity of V12/SN 1954J. For the nearby case of N300-OT, at least, studies of the surrounding stellar population favor an initial mass of 12-25 $M_{\odot}$ (Gogarten et al. 2009), apparently ruling out the low-mass option. In any case, the progenitors of SN 2008S and N300-OT were probably less massive than classical LBVs, which were thought to extend down to initial masses of only 20–25 $M_{\odot}$ (Smith et al. 2004).

Initial masses below $\sim$20 $M_{\odot}$ for some of these events have rather profound implications for the larger class of SN impostors and LBV eruptions, because stars of this mass are not expected to approach or exceed the Eddington limit during the normal course of their post-main sequence evolution. Together with evidence for explosive shock waves described above, this seems to favor a deep-seated energy injection, rather than a runaway near-Eddington instability in the outer envelope. Furthermore, if being dangerously near the Eddington limit is *not* a necessary precondition for these eruptions after all, then the same (or a related) mechanism that drives giant eruptions of luminous stars like η Car might also operate in lower mass stars as well, perhaps even below 8 $M_{\odot}$. In this context, relieved of the notion that LBV-like eruptions are exclusive to the most massive stars, it is prudent to explore the diversity in this class of non-terminal stellar eruptions. As the astronomical community embarks upon an era of more intensive transient studies, more examples will hopefully illuminate and quantify the statistical distribution across this diverse range of properties.

Table 1. New photometry for SN 1999bw

JD	B mag	V mag	R mag	I mag
2451289.69	19.27±0.14	18.45±0.06	17.99±0.07	17.60±0.10
2451291.70	...	18.36±0.05	17.98±0.08	17.67±0.06
2451292.69	...	18.39±0.14	17.87±0.12	17.69±0.13
2451295.72	...	18.37±0.10	...	17.83±0.30
2451298.72	...	18.33±0.08	17.82±0.08	17.72±0.11

Table 2. New photometry for SN 2001ac

JD	B mag	V mag	R mag	I mag
2451981.79	18.77±0.11	18.53±0.08	18.53±0.08	17.88±0.07
2451982.76	18.70±0.11	18.71±0.07	18.71±0.07	18.15±0.11
2451986.81	19.09±0.12	18.91±0.09	18.91±0.09	18.21±0.15
2451990.79	18.78±0.33	18.61±0.30	18.61±0.30	...
2451994.81	19.68±0.24	19.24±0.12	19.24±0.12	18.60±0.16
2451998.78	19.81±0.24	19.13±0.11	19.13±0.11	18.54±0.13
2452009.74	19.90±0.23	19.80±0.29	19.80±0.29	18.97±0.27
2452013.76	20.59±0.36	19.91±0.27	19.91±0.27	19.16±0.28

In this paper we collect examples of LBV giant eruptions known to date, examining their light curves, spectra, and several derived properties. In §2 we present some unpublished data on previous SN impostors as well as some recent examples. In §3 we compile a list of known events and present their light curves and spectra, and we provide a detailed comparative discussion of their various observational properties. In §4 we discuss the diversity of the sample and its implications for the physics behind these eruptions. We also briefly discuss overlap with transients that may be related but have not been considered as LBV eruptions so far, and discuss which objects should belong in the class.

Table 3. New photometry for SN 2002bu

JD	B mag	V mag	R mag	I mag
2452363.88	16.20±0.03	15.60±0.02	15.13±0.02	...
2452364.84	15.98±0.02	15.46±0.02	15.03±0.02	14.70±0.02
2452365.77	15.84±0.02	15.33±0.02	14.99±0.02	14.65±0.02
2452366.83	15.74±0.02	15.26±0.02	14.93±0.02	14.62±0.02
2452368.88	15.67±0.02	15.23±0.02	14.92±0.02	14.65±0.02
2452372.83	15.71±0.02	15.34±0.02	15.02±0.02	14.80±0.02
2452375.82	15.84±0.02	15.42±0.02	15.13±0.02	14.86±0.02
2452377.81	15.89±0.02	15.47±0.02	15.20±0.02	14.92±0.02
2452380.76	16.01±0.02	15.57±0.02	15.26±0.02	14.97±0.02
2452383.82	16.14±0.02	15.63±0.02	15.34±0.02	15.04±0.02
2452386.77	16.24±0.02	15.71±0.02	15.42±0.02	15.10±0.02
2452389.77	16.36±0.03	15.74±0.03	15.46±0.04	15.10±0.02
2452392.82	16.30±0.05	15.77±0.02	15.41±0.03	15.05±0.02
2452396.76	16.50±0.02	15.80±0.02	15.45±0.02	15.06±0.02
2452399.73	16.52±0.02	15.84±0.02	15.48±0.02	15.07±0.02
2452403.72	16.61±0.03	15.88±0.02	15.48±0.02	15.07±0.02
2452411.70	16.80±0.02	16.03±0.02	15.59±0.02	15.19±0.02
2452419.70	17.06±0.04	16.26±0.02	15.74±0.02	15.30±0.02
2452423.69	17.17±0.02	16.34±0.02	15.85±0.02	15.38±0.02
2452427.70	17.38±0.02	16.53±0.02	16.03±0.02	15.55±0.02
2452431.74	...	16.71±0.03	16.17±0.02	15.66±0.03
2452438.69	17.84±0.04	17.05±0.03	16.40±0.03	15.93±0.02
2452445.70	18.22±0.04	17.45±0.05	16.81±0.03	16.24±0.03
2452452.70	18.60±0.09	17.90±0.05	17.15±0.05	16.63±0.04

Table 4. Unfiltered KAIT photometry for SN 2006bv

JD	mag	err
2453852.80	18.51	0.15
2453864.80	18.14	0.07
2453887.74	18.70	0.07

Table 5. Additional unfiltered KAIT photometry for U2773-OT

JD	mag	err
2455181.5	17.64	0.03
2455184.5	17.57	0.03
2455188.5	17.57	0.03
2455191.5	17.60	0.03
2455199.5	17.53	0.03
2455202.5	17.58	0.03
2455205.5	17.56	0.05
2455211.5	17.48	0.05
2455227.5	17.50	0.03
2455238.5	17.42	0.04
2455241.5	17.41	0.03
2455244.5	17.49	0.03
2455256.5	17.46	0.03
2455266.5	17.41	0.03
2455269.5	17.37	0.03
2455272.5	17.43	0.05

2 NEW OBSERVATIONS

For new observational material on SN impostors, our data were collected as part of the Lick Observatory Supernova Search (LOSS). Most of our photometry comes from the Katzman Automatic Imaging Telescope (KAIT; Filippenko et al. 2001; Filippenko 2003), while our new spectra listed below were obtained using the Kast spectrograph (Miller & Stone 1993) on the Shane 3m Reflector at Lick Observatory, or at the 10m Keck Observatory using the Low Resolution Imaging Spectrograph (LRIS; Oke et al. 1995) or the Deep Imaging Multi-Object Spectrograph (DEIMOS; Faber et al. 2003). Details about the new data are given in subsequent sections.

Table 6. New spectroscopy of SN impostors

Transient	Obs. Date	Day	Tel./Inst.	$\delta\lambda$ (Å)
SN 1999bw	1999 Apr 24	4	Lick/Kast	4300-7000
SN 2000ch	2000 May 31	28	Lick/Kast	4250-6950
SN 2000ch	2004 Apr 26	1456	Keck/LRIS	3300-9400
SN 2001ac	2001 Mar 21	9	Lick/Kast	3300-7830
SN 2001ac	2001 Mar 29	17	Keck/LRIS	4350-6860
SN 2002bu	2002 Apr 08	11	Lick/Kast	3300-10400
SN 2002bu	2002 Apr 20	23	Lick/Kast	3300-10400
SN 2002bu	2002 May 07	40	Lick/Kast	3300-10400
SN 2002bu	2002 Jun 08	72	Lick/Kast	3100-10400
SN 2002bu	2002 Jun 17	81	Lick/Kast	3100-10400
SN 2010dn	2010 Jun 08	9	Lick/Kast	3430-10260
SN 2010dn	2010 Jun 11	12	Keck/DEIMOS	6101-7410
SN 2010dn	2010 Jun 18	19	Lick/Kast	3510-9920

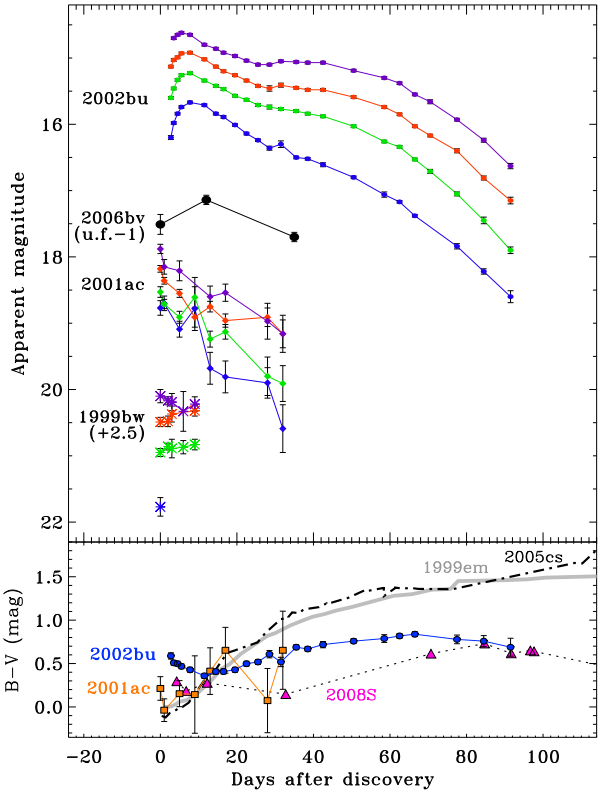

Figure 1. *Top:* Apparent magnitude light curves for SN impostor photometry from KAIT, reported here for the first time (see Tables 1, 2, 3, and 4). For SN 2002bu (filled dots) and SN 2001ac (filled diamonds), apparent $BVRI$ magnitudes obtained with KAIT are shown as observed; B, V, R, and I are plotted as blue, green, red, and purple, respectively. For clarity of display, the $BVRI$ photometry for SN 1999bw (asterisks) is shown offset by +2.5 mag. Unfiltered photometry for SN 2006bv (black dots) is offset by −1 mag. *Bottom:* $B-V$ color curves of SN 2002bu (blue circles) and 2001ac (orange squares), compared to color curves of the SN impostor SN 2008S (magenta triangles; Smith et al. 2009a), the normal SN II-P 1999em (gray; Leonard et al. 2002), and the faint SN II-P 2005cs (black dot-dashed; Pastorello et al. 2009).

2.1 New Photometry

Optical photometry of the SN impostors were obtained with KAIT. Several objects were followed in multiple passbands ($BVRI$) soon after discovery. For several other objects, no dedicated followup campaign was initiated, but their host galaxies were monitored without using a filter during the course of our SN search, so we have unfiltered data of the eruptions as a byproduct. For the objects with multi-color $BVRI$ photometry, we obtained calibrations of the fields by observing them together with several Landolt (1992) star fields at various airmasses in photometric nights. Deep template images of the fields after the objects have faded beyond detection have also been obtained. These template images and calibrations are then used in the KAIT photometry pipeline (Ganeshalingam et al. 2010) to perform image subtraction on the image data and calibration to the standard photometry system.

For the objects with only unfiltered data, we treat the

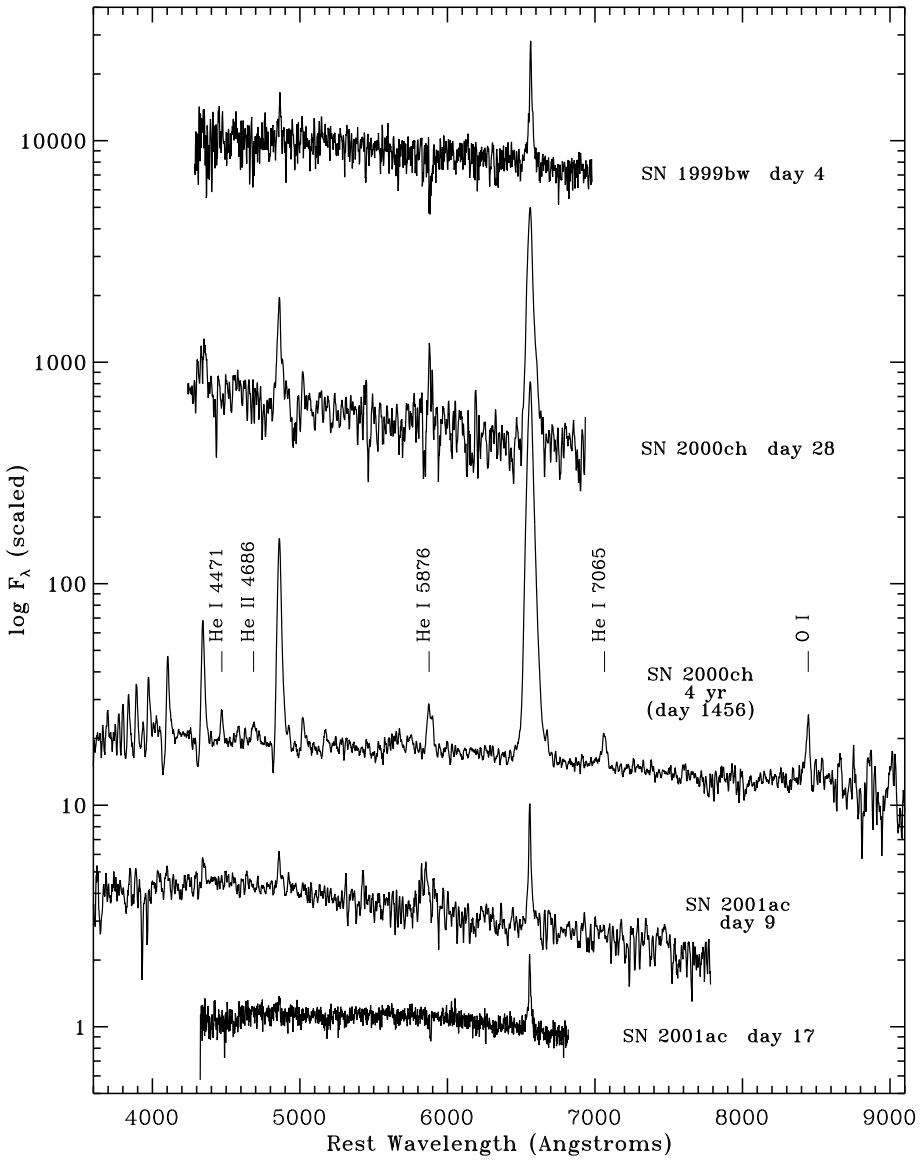

Figure 2. Spectra of SN impostors obtained with the Lick 3m reflector (see Table 6). The day 28 spectrum of SN 2000ch was published previously by Wagner et al. (2004), but the others are previously unpublished. SN 1999bw on day 4 is a fairly noisy spectrum dominated by Balmer lines. The late-time spectrum of SN 2000ch obtained about 4 yr after discovery shows interesting changes from the earlier spectrum and covers a wider wavelength range. The two spectra of SN 2001ac on days 9 and 17 show interesting evolution of the spectrum over a short time, where the broad He I λ5876 line disappears and the Balmer lines fade.

images as taken with the R band (Li et al. 2003). Template images are constructed for each field by choosing the best monitoring data and then stacking them. For photometric calibration, we use the red magnitudes for the stars in the SN fields in the USNO B1 catalog (Monet et al. 2003). Although the accuracy of this calibration is only $\sim$0.2$-$0.3 mag for an individual star, there are usually more than 10 stars available in each field, so the uncertainty due to calibration is < 0.1 mag. The data are then reduced in a similar fashion as the KAIT photometry pipeline. The final photometry of the objects are listed in Tables 1$-$5 and the apparent light curves are shown in Figure 1.

SN 1999bw: Unfortunately, SN 1999bw was not extensively observed by KAIT, and the luminosity appears relatively constant over the $\sim$10 days when it was observed. The apparent $B-V$ color at the time of discovery is $\sim$0.8 mag, suggesting either that the eruption was redder than a normal LBV, or that it suffered significant circumstellar reddening.

SN 2001ac: Our KAIT $BVRI$ photometry of SN 2001ac covers about one month after discovery, and seems consistent with a relatively fast and steady decline (within uncertainty), fading by $\sim$1–1.8 mag (in various filters) in 30 days. This suggests that it may have been discovered after the time of peak luminosity. The apparent $B-V$ color evolves only mildly during this time, from $\lesssim$0.2 to $\sim$0.6 mag toward the end of the observed epoch. The increasing relative strength of the R-band compared to the others at late times

may result from the very strong Hα seen in the spectrum (see below).

SN 2002bu: The bright eruption of SN 2002bu was well observed by KAIT. We started observing it photometrically about 5 days before maximum light, and followed it for almost 100 d thereafter when it had faded by about 3 mag. The light curve of SN 2002bu shows an initial 10–20 day rounded peak, followed by a "hump" (i.e., almost a plateau) with a subsequent slower rate of decline; qualitatively, this decline with a change in decay rate resembles that of SN 1997bs (Van Dyk et al. 2000). The apparent color reddens with time, from $B-V \approx 0.45$ mag at peak, to $\sim$0.8 mag at late times (Figure 1), similar to the color evolution of SN 2008S (Smith et al. 2009a). The color evolution is substantially different from a normal SN II-P, never getting as red as a SN II-P and apparently becoming slightly blue again as the object fades.

SN 2003gm: We obtained only two unfiltered KAIT measurements of SN 2003gm, including the discovery and one image 6 days later. Both were 17.0$\pm$0.1 mag; the limited light curve is not shown.

SN 2006bv: We obtained three unfiltered measurements of SN 2006bv with KAIT, as listed in Table 4 and shown in Figure 1, where it has been shifted by -1 mag for clarity of display. The peak occurred a few to 20 days after discovery. Unfortunately, no late-time measurements are available, and we were not able to secure spectra of the eruption.

U2773-OT: We presented KAIT unfiltered photometry of this 2009 transient in UGC 2773 (U2773-OT hereafter) in Smith et al. (2010a), but the transient has remained bright and has even continued its slow rise in the year since then. Table 5 gives additional unfiltered KAIT photometry for this source, continuing after the last data point in the previous paper. See Smith et al. (2010a) for further details.

2.2 Previously Unpublished Spectra

All spectra were reduced using standard techniques (e.g., Foley et al. 2003). Routine CCD processing and spectrum extraction were completed with the Image Reduction and Analysis Facility (IRAF), and the data were extracted with the optimal algorithm of Horne (1986). We obtained the wavelength scale from low-order polynomial fits to calibration-lamp spectra. Small wavelength shifts were then applied to the data after cross-correlating a template sky to the night-sky lines that were extracted with the SN. Using our own reduction routines, we fit spectrophotometric standard-star spectra to the data in order to flux calibrate our spectra and to remove telluric lines (Wade & Horne 1988; Matheson et al. 2000). Most observations were aligned along the parallactic angle to reduce differential light losses (Filippenko 1982). Information regarding both our photometric and spectroscopic data (such as observing conditions, instrument, reducer, etc.) was obtained from our SN database (SNDB). The SNDB uses the popular open-source software stack known as LAMP: the Linux operating system, the Apache webserver, the MySQL relational database management system, and the PHP server-side scripting language (for further details, see Silverman et al. 2010).

SN 1999bw: We were only able to obtain one spectrum of SN 1999bw shortly after discovery on day 4, and unfortunately the spectrum is rather noisy. It shows the strong narrow Balmer emission lines characteristic of LBVs. The Hα line has a Lorentzian shape with a FWHM $\approx$ 630 km s^{-1}, but the broad wings extend to roughly $\pm$3000 km s^{-1} in our data. This may be due to electron scattering, but may also suggest that some of the mass is moving rather fast, similar to SN 2009ip (Smith et al. 2010a) and η Car (Smith 2008). No P Cygni absorption is seen at this low resolution in Hα. Aside from Hβ, no other emission features are seen in this wavelength range, but Na I D absorption is present.

SN 2000ch: The light curve and spectra of SN 2000ch were already discussed in detail by Wagner et al. (2004). However, we obtained an additional high signal-to-noise, late-time spectrum after that paper was published. The new spectrum of SN 2000ch in Figure 2 was obtained roughly 4 yr after discovery, on 2004 April 26 using the Lick 3m reflector. Even at this late time, the spectrum still shows relatively broad (FWHM $\approx$ 1,500 km s^{-1}) strong Balmer emission lines as well as prominent triplet He I lines and even He II λ4686. O I λ8446 is also seen. The Balmer lines have strengthened relative to the continuum, with about twice the equivalent width compared to day 28. In the higher quality spectrum we can now see clear P Cyg absorption features in the higher Balmer lines. This 2004 spectrum is now quite valuable, because Pastorello et al. (2010) just recently reported the discovery of multiple subsequent eruptions of the same star that produced SN 2000ch, but much later in 2008 and 2009. According to their photometry, our new spectrum showing a very strong Hα line with an emission equivalent width of 461 Å was obtained at relative quiescence about halfway between the 2000 and 2008 eruptions. It suggests that the wind speed during quiescence is similar to that during the eruptive states. Most of the same spectral features (i.e. He I emission lines, etc), are also seen in spectra of the subsequent outbursts.

SN 2001ac: The visual spectrum of SN 2001ac has a blue continuum and narrow Balmer emission lines typical of LBVs. The spectra are rather noisy, so we cannot comment on many details. One interesting aspect is that over a relatively short time period of about a week, between days 9 and 17, the prominent and broad emission feature at around 5800 Å disappears. This could be a blueshifted emission line of He I λ5876 from some hot and fast ejecta seen at early times, but this is speculative with such a noisy spectrum. After this broad emission fades, the spectrum closely resembles that of SN 1999bw. Like many LBVs, SN 2001ac's Hα line shows a composite profile, with a narrow core that can be approximated with a Gaussian FWHM $\approx$ 287 km s^{-1} on day 9, but also with a broader base that can be fit with a Gaussian with FWHM $\approx$ 1505 km s^{-1} and extending to roughly $\pm$1500 km s^{-1} at the continuum level. The emission equivalent width on day 9 is 46 Å. The day 17 Hα profile is very similar, although Balmer lines weaken and Hβ disappears with time. By comparison with previous events, this probably indicates a relatively slow outflow speed of around 290 km s^{-1} for the bulk of the ejecta or wind, whereas the broader base may be due to electron scattering wings. It is of course difficult to rule out the presence of unseen fast material, however.

SN 2002bu: Our spectral coverage of SN 2002bu is much better than the previous cases, with 5 epochs over the first $\sim$100 days when we also have photometry. Figure 3 shows all 5 spectra, where we repeat our first spectrum (day 11) in

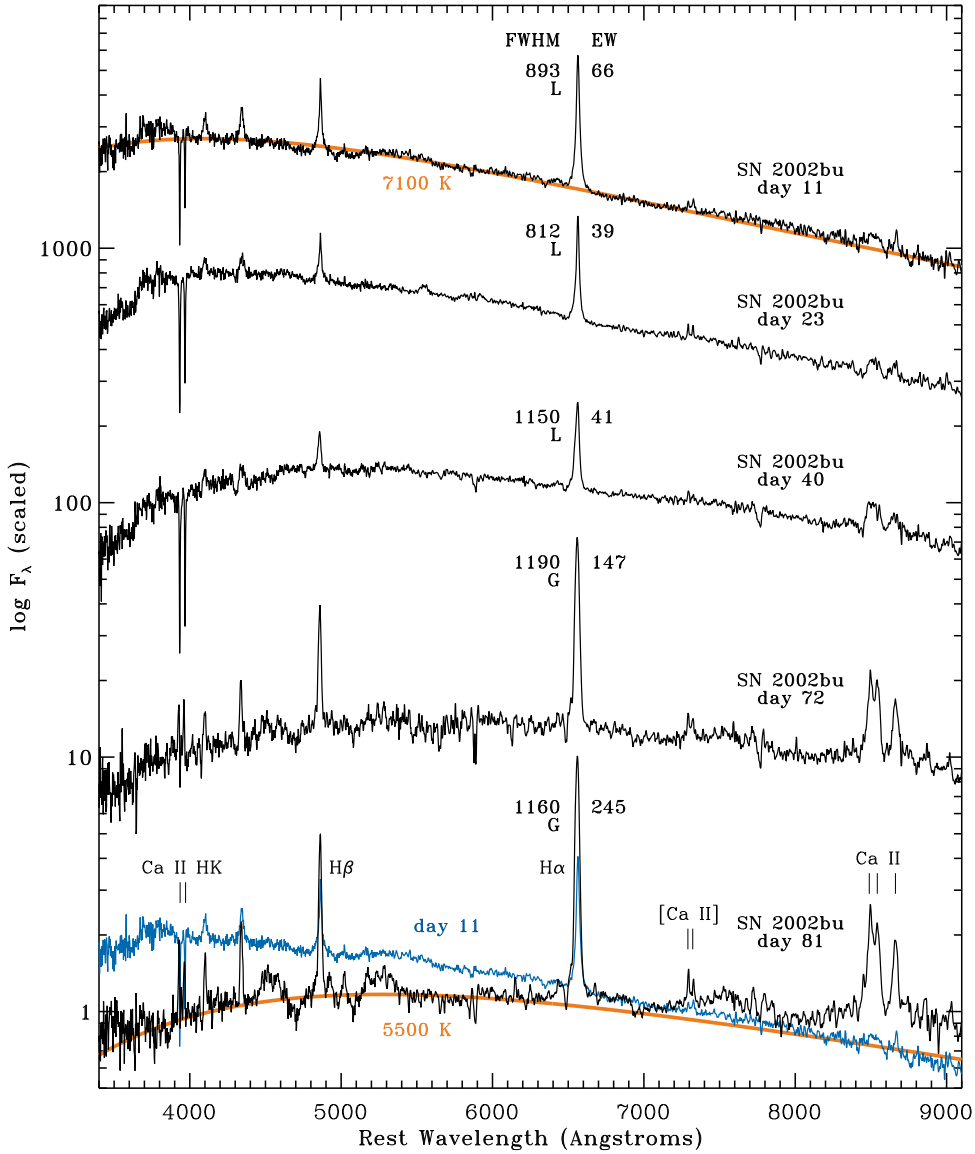

Figure 3. Previously unpublished Lick/3m spectra of SN 2002bu on days 11, 23, 40, 72, and 81. The continuum shape gets redder with time, and the Balmer emission line equivalent widths get stronger as the continuum fades. The FWHM (plus either "G" for Gaussian or "L" for Lorentzian) and equivalent width of Hα are listed aside the emission line for each epoch. The spectrum transitions from a "hot" LBV at early times to a "cool" LBV at late times, with the red [Ca II] doublet and the IR Ca II triplet strengthening, while Ca II H and K go from absorption to emission. The blue tracing at the bottom is the day 11 spectrum plotted over the last day 81 spectrum to emphasize the changes in continuum shape and line intensities. The orange curves show blackbodies. All epochs have been dereddened by the same value of $E(B-V) = 0.012$ mag (i.e. correcting for Galactic reddening, but not any additional reddening that may be local, so the blackbody temperatures shown are lower limits).

blue at the bottom for direct comparison with the late time (day 81) spectrum.

The most remarkable aspect of SN 2002bu's spectrum is its evolution over time. As the transient fades during the first ∼80 days, the continuum gets substantially redder, while emission lines from the [Ca II] doublet and the Ca II IR triplet strengthen relative to the continuum. Ca II H and K transition from strong absorption features at early times to narrow emission features at late times, and a more complex absorption spectrum is evident in the last two epochs on days 72 and 81. Additionally, the Hα line profile (Figure 4) shows a change from a Lorentzian profile for the first three epochs, similar to SN 2009ip (Smith et al. 2010a), to a more Gaussian profile with an asymmetric shape. The red wing of Hα appears to weaken at late times, perhaps indicating the blueshift of lines that results when new dust formation blocks emission from receding parts of the ejecta or CSM interaction region as seen in some SNe IIn (see, e.g., Smith et al. 2009b). Given the dusty shells resolved around Galactic LBVs like η Car, dust formation in an eruptive event would not be surprising, although direct evidence for it has been scant so far. In the last spectrum on day 81, the continuum

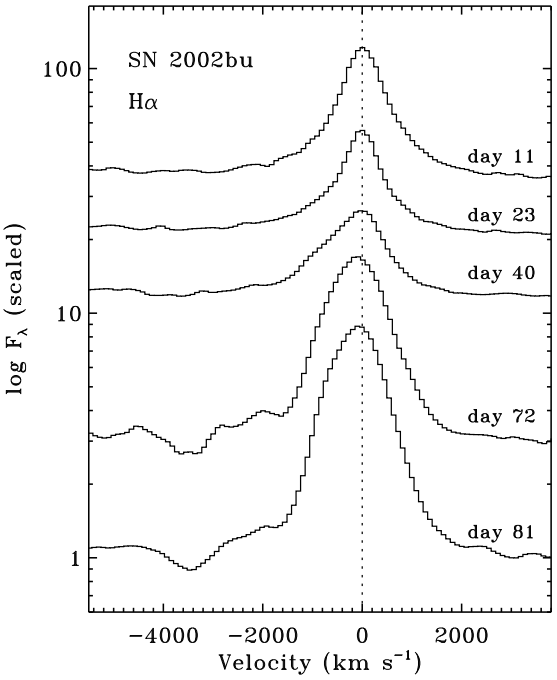

Figure 4. Kast/Lick-3m spectra of the Hα line velocity profile in SN 2002bu on days 11, 23, 40, 72, and 81.

cannot be fit with a single blackbody. At $\lambda < 7000$ Å it appears well fit by a 5500 K blackbody, but in this case the excess emission at longer wavelengths implies an IR excess, perhaps due to hot dust emission. The IR excess could be caused by newly formed dust or an IR echo (or both; Fox et al. 2010; Smith et al. 2009b), but the formation of new dust is consistent with the Hα line profile evolution.

Overall, the observed spectral changes signify a transition from a spectrum that at early times resembles hot SN impostors with smooth continua and strong Balmer lines like SN 1997bs and SN 2009ip, to one that at late times looks cooler and develops the strong [Ca II] lines seen in SN 2008S and NGC 300-OT. Smith et al. (2010a) discussed the dichotomy of these "hot" and "cool" spectra in various LBVs, but here *in SN 2002bu we see them both in the same object over time.* A transition such as this could be quite common among LBVs, since so far, few SN impostors have good spectral coverage as the objects fade during a major eruption. For example, there is only one spectrum at day 2 available for SN 1997bs (Van Dyk et al. 2000), to which the spectra of SN impostors are often compared. This provides yet another link in observed properties between LBVs and the unusual transients with obscured progenitors, SN 2008S and NGC 300-OT (see Smith et al. 2010a for further discussion of this link). A more inclusive comparison of the spectra of several LBVs is provided later in the paper.

The detailed evolution of the Hα line in SN 2002bu is interesting (Figure 4). From day 11 to 23 the line gets slightly narrower, and weakens relative to the continuum, showing a Lorentzian profile at both epochs. The day 40 profile is transitional; it has about the same relative strength as day 23, but is now somewhat broader and slightly asymmetric, with a devloping hump on its blue side. By the last two epochs, substantial changes are apparent; the line now has a more Gaussian profile shape and is broader with a FWHM of roughly 1200 km s^{-1}, and it seems to be more asymmetric or blueshifted. It is intriguing that this progressive blueshift might be evidence for dust formation, as noted above. Hα also seems to have developed blueshfted P Cygni absorption features at -3500 km s^{-1} in the last two epochs, similar to SN 2009ip (Smith et al. 2010a), although these might also be due to some other absorption feature. Hβ also seems to develop stronger broad blueshifted absorption, but it is at a different velocity. Higher resolution spectra of this transient would have been quite valuable.

SN 2010dn: We present early-time spectra of SN 2010dn in Figure 5. Moderate-resolution spectra obtained with the Kast spectrograph at Lick observatory on days 9 and 19 after discovery are shown in Figure 5a, where they are compared to the very similar spectrum of SN 2008S from Smith et al. (2009a) that was obtained with the same instrument. Both objects show strong narrow [Ca II] and Ca II emission, in addition to the Balmer emission lines. The overall continuum shape and the weak spectral features in the blue are also remarkably similar in both objects. In fact, spectroscopically, SN 2010dn is a near twin of both SN 2008S and N300-OT. A 6900 K blackbody function is shown in orange for comparison to the blue continuum shape of SN 2010dn on day 9. On days 9 and 19, we measure Hα emission equivalent widths of 31.5 and 26.7 Å (±2 Å), respectively, in the Lick spectra.

We also obtained a high-resolution spectrum of SN 2010dn on day 12 after discovery using the DEIMOS spectrograph at Keck, shown in Figure 5b. This was limited in wavelength coverage to the red spectrum showing Hα and the [Ca II] doublet. Velocity profiles of Hα and [Ca II] λ7291 from the DEIMOS spectrum are shown in Figure 6. Most of the Hα flux can be accounted for with a broad Lorentzian profile with FWHM $\approx$ 860 km s^{-1}, as shown in Figure 6a, but there is also excess emission from a narrow component on top of this profile. Qualitatively, the mostly Lorentzian profile with a small contribution from very narrow emission closely resembles that of the Type IIn SNe 1998S and 2006gy at early times (Chugai 2001; Smith et al. 2010b), which was thought to be indicative of diffusion of radiation through an opaque circumstellar envelope or slow wind. In the day 12 spectrum taken with DEIMOS, we measure an Hα equivalent width of 38.6 Å (±2 Å).

Superposed on this intermediate-width Lorentzian profile is a much narrower Hα line. The narrow component of Hα has the same profile as the narrow emission seen in the pair of [Ca II] lines, shown in Figure 6b; the [Ca II] lines show the narrow profile better because they are free from the underlying broad profile. These narrow components have FWHM values of roughly 110–120 km s^{-1}, but they are asymmetric with a very steep drop on the blue side of the line. The red wing has a Lorentzian shape that would imply FWHM = 155 km s^{-1} if it were symmetric, so perhaps this is a better indicator of the expansion speed of the circumstellar gas emitting these narrow components. These narrow [Ca II] profiles are qualitatively identical to those of the same lines in N300-OT, which also showed asymmetric profiles with a Lorentzian red wing and a steep cutoff on the blue side, with very similar widths of 140–190 km s^{-1} at early times (Berger et al. 2009). Similar profiles were seen in other lines such as [O I] $\lambda\lambda$6300,6364 in N300-OT as well (Berger et al. 2009),

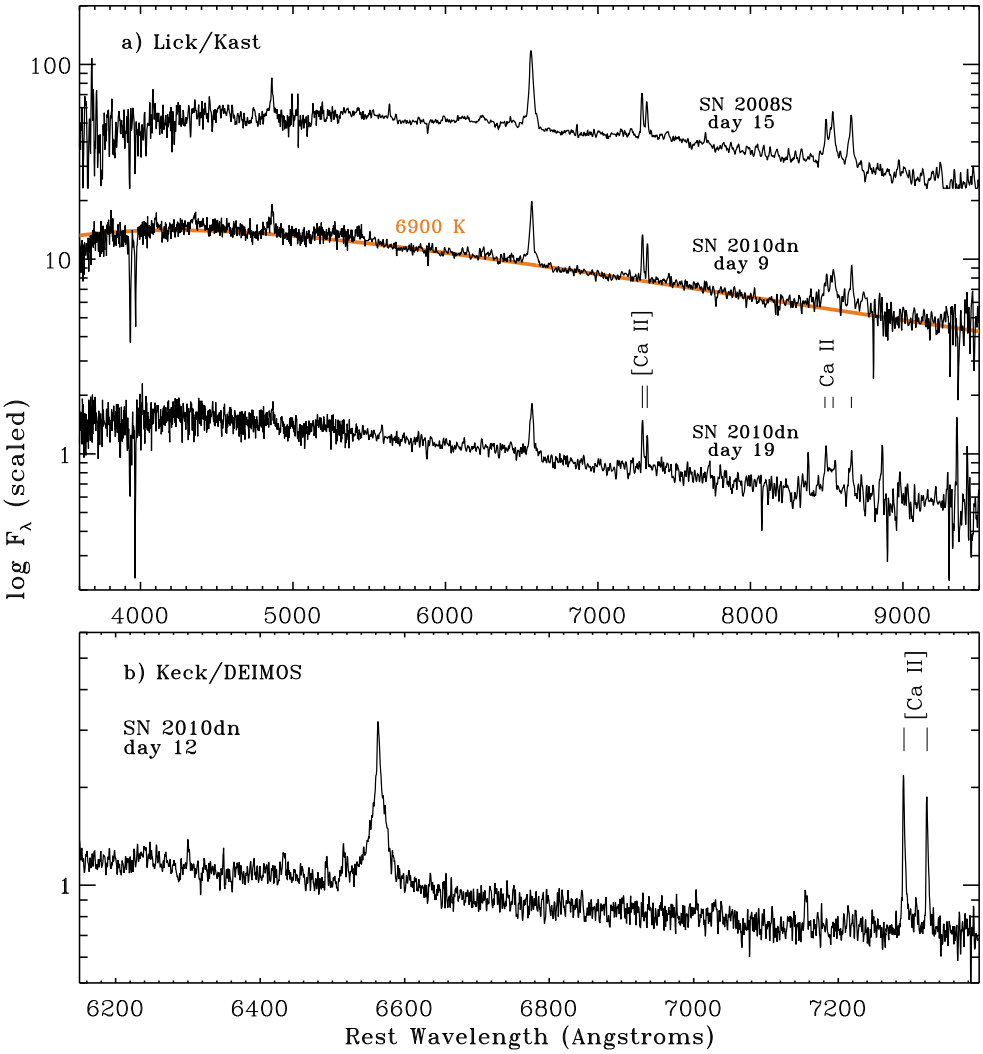

Figure 5. (top) Lick/3m spectra of SN 2010dn obtained on days 9 and 19, compared to a spectrum of SN 2008S from Smith et al. (2009a). (bottom) Keck/DEIMOS spectrum on day 12. The bright lines are Hα and the [Ca II] doublet, while the fainter narrow lines are moslty Fe II.

and we see the same profile in the narrow component of Hα in SN 2010dn, so we infer that the shape is not the result of some peculiar excitation/ionization effect unique to Ca II.

So far, N300-OT and SN 2010dn are the only SN impostors with comparable high-resolution spectra available for these [Ca II] lines, so their nearly identical asymmetric profiles are rather intriguing. The shape of these asymmetric *forbidden* lines has not been explained, but suggests either an intrinsically aymmetric distribution of emitting gas oriented the same way in both objects, or dust obscuration of the blue wing with a particular geometry.

3 COMPARATIVE RESULTS

3.1 Comments on Individual Events

Here we briefly list relevant observational material for suspected members of the class of SN impostors or giant LBV eruptions, collected from the literature for the purposes of this discussion (see Table 7). When published analyses exist, we refer to those papers and adopt the same assumptions except where noted. For new observational material, our data were collected as part of the Lick Observatory Supernova Search (LOSS), as noted above. In most cases below, we adopt distance moduli from the NASA Extragalactic database[4] and we take line-of-sight Galactic extinction values of $E(B-V)$ from Schlegel et al. (1998). Two of the transients listed below were discovered recently. We list them here and provide some initial details for completeness, but cannot yet comment on their late-time behavior since they are still being studied.

P Cygni: Although famous for its namesake line-profile shape, P Cygni is also notable as the *first* LBV, and for being only the third variable star discovered — after Tycho's SN and Mira. (It was of course not referred to as an LBV at the time, but was called a nova.) Despite the excitement it

[4] `http://nedwww.ipac.caltech.edu/`

Table 7. A List of SN impostors considered here

Transient	Host Gal.	Date	mag (peak)	R.A./Dec. (J2000)	Discoverer	Refs.[a]
P Cygni	MW	1600-55	2.8	20 17 47.20 +38 01 58.5	Blaeu	[1]
η Car	MW	1837-60	-1.0	10 45 03.59 –59 41 04.3	Herschel	[1]
SN 1954J	NGC 2403	1954	16.5	07 36 55.36 +65 37 52.1	Tammann, Sandage	[2]
SN 1961V	NGC 1058	1961	12.5	02 43 36.42 +37 20 43.6	Wild	[3,4]
HD 5980	SMC	1993-94	8.8	00 59 26.57 –72 09 53.9	Barbá & Niemala	[5]
V1	NGC 2366	1994-?	17.4	07 28 43.37 +69 11 23.9	Drissen et al.	[6]
SN 1997bs	NGC 3627	1997 04 15	17.0	11 20 14.25 +12 58 19.6	LOSS	[7]
SN 1999bw	NGC 3198	1999 04 20	17.8	10 19 46.81 +45 31 35.0	LOSS	this work
SN 2000ch	NGC 3432	2000 05 03	17.4	10 52 41.40 +36 40 08.5	LOSS	[8]
SN 2001ac	NGC 3504	2001 03 12	18.2	11 03 15.37 +27 58 29.5	LOSS	this work
SN 2002bu	NGC 4242	2002 03 28	15.5	12 17 37.18 +45 38 47.4	Puckett, Gauthier	this work
SN 2002kg	NGC 2403	2002 10 26	19.0	07 37 01.83 +65 34 29.3	LOSS	[9,10]
SN 2003gm	NGC 5334	2003 07 06	17.0	13 52 51.72 –01 06 39.2	LOSS	[9]
2005-OT	NGC 4656	2005 03 21	18.0	12 43 45.84 +32 06 15.0	Rich	...
SN 2006bv	UGC 7848	2006 04 28	17.8	12 41 01.55 +63 31 11.6	Sehgal, Gagliano, Puckett	this work
SN 2006fp	UGC 12182	2006 09 17	17.7	22 45 41.13 +73 09 47.8	Puckett, Gagliano	...
SN 2007sv	UGC 5979	2007 12 20	17.4	10 52 40.05 +67 59 14.2	Duszanowicz	...
SN 2008S	NGC 6946	2008 02 01	17.6	20 34 45.35 +60 05 57.8	Arbour	[11]
2008-OT	NGC 300	2008 05 14	16.2	00 54 34.16 –37 38 28.6	Monard	[12,13]
SN 2009ip	NGC 7259	2009 08 26	17.9	22 23 08.26 –28 56 52.4	Maza, Pignata et al.	[14]
2009-OT	UGC 2773	2009 08 18	18.0	03 32 07.24 +47 47 39.6	Boles	[14]
2010da	NGC 300	2010 05 23	16.0	00 55 04.86 –37 41 43.7	Monard	[15,16]
2010dn	NGC 3184	2010 05 31	17.1	10 18 19.89 +41 26 28.8	Itagaki	this work

[a] Primary references for sources of light curves and early spectral analysis: [1] Smith & Frew (2010); [2] Tammann & Sandage (1968); [3] Zwicky (1964); [4] Bertola (1963,1965); [5] Jones & Sterken 1997; [6] Petit et al. (2006); [7] Van Dyk et al. (2002); [8] Wagner et al. (2004); [9] Maund et al. (2006); [10] Van Dyk et al. (2006); [11] Smith et al. (2009a); [12] Bond et al. (2009); [13] Berger et al. (2009); [14] Smith et al. (2010a); [15] Bond (2010); [16] Chornock et al. (2010). The comment "this work" refers to new data published in the present paper for the first time.

generated at the time, there are only sparse observations of its 1600-1665 A.D. eruption, with only a handful of surviving reports during the main light curve peak that lasted ∼10 yr (see Figure 7; from Smith & Frew 2010, in prep.). These historical observations are valuable for recording the long timescale variability of P Cygni, but the sparse sampling suggests that if there had been short timescale variation as exhibited by many other LBV eruptions around peak, then it could easily have been missed. Thus, a brief unobserved peak could have been more luminous than the several-year sustained peak of the eruption, which had an absolute magnitude of roughly –11 mag (according to Lamers & de Groot 1992). Most of these observations were made with the newly invented telescope, and a typical value for the uncertainty of these observations is ±0.2–0.3 mag, although the quality of observations may vary considerbly from one epoch to another (see Smith & Frew 2010). These are visual (i.e., unfiltered) observations, converted approximately to modern V-band based on the likely color of LBV outbursts, although this is uncertain and depends on reddening and the strength of Hα. The spectrum during outburst was not recorded, of course. P Cygni also suffered a second major outburst in 1655 (dashed in Figure 7) that reached a peak almost as luminous as the first, with an absolute magnitude of roughly –10.5. After this second outburst, P Cygni faded and remained faint for several decades, but then brightened suddenly around 1700. It has been relatively tame and brightening very slowly since then. From modern observations of its shell nebula, we can infer that the dominant expansion speed of the 1600 A.D. eruption was about 136 km s^{-1} (Smith & Hartigan 2006).

Eta Carinae: The complex light curve of η Car has a long history of discussion that will not be repeated here (see Frew 2004). A very recent study by Smith & Frew (2010) recovered many new historical observations from the 19th century and uncovered some mistakes in earlier works going back to Herschel's original reports. The new light curve of Smith & Frew (2010) looks substantially different in detail from previously published and often reproduced light curves of η Car (e.g., Innes 1903; see Frew 2004 for a thorough discussion of the historical data), and the Smith & Frew light curve is used here (Figures 7 and 8). The star suffered two shorter-duration bursts in 1838 (−13.5 mag) and 1843 (−13.8 mag), which preceded a final rise at the end of 1844 (−14.0 mag), from which the star declined slowly for more than 10 yr afterward. Again, we do not know what the spectrum looked like during the 1840s eruption, but reports of its red or "ruddy" color probably indicate strong Hα emission. Following another smaller eruption in ∼1890, the star is apparently still slowly recovering from the upheaval of its 19th century eruptions (e.g., Smith et al. 2003a; Davidson et al. 2005). The 1890 eruption was probably much more luminous than it looked, since the star is thought to have been buried in ∼4 mag of visual extinction at that time (Humphreys et al. 1999). The light curve of the 1890 event is also shown in Figure 7, with a correction for this extinction applied. Based on the kinematics of the bipolar Homunculus nebula, the polar expansion speed for the bulk of the matter ejected in the major eruption was 650 km s^{-1}, dropping to values as low as 40 km s^{-1} at the pinched equatorial waist (Smith 2006). However, deep spectroscopy of the surroundings outside the Homunculus reveal that the 19th century eruption also ejected a small amount of extremely fast material moving at ∼5000 km s^{-1}, probably requiring a strong shock wave during the event (Smith 2008). A smaller bipolar nebula called the Little Homunculus is growing inside the larger one (Ishibashi et al. 2003), and its kinematics suggest that it was ejected in the smaller 1890 event (Smith 2005). Both the kinematics of the Little Homunculus and historical spectra obtained during the 1890 event suggest an ejection

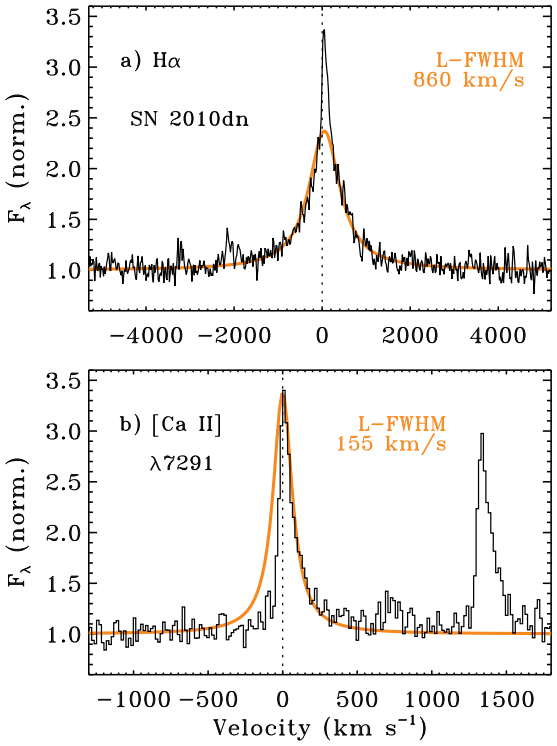

Figure 6. Velocity profiles (a) of Hα and (b) of [Ca II] λ7291 from the day 12 Keck/DEIMOS spectrum of SN 2010dn. [Ca II] λ7323 can also be seen at the right. Symmetric Lorentzian profiles with FWHM = 860 and 155 km s^{-1}, resepctively, are shown for comparison in orange.

speed of around 200 km s^{-1} (Smith 2005; Whitney 1952; Walborn & Liller 1977).

SN 1954J/V12: This LBV outburst in NGC 2403 was well observed photometrically by Tammann & Sandage (1968), although no spectra of the outburst are available. The massive star was clearly an irregular blue variable star (V12) for a decade before the peak of its giant eruption in 1954, and the star apparently survived the event as a faint reddened star (Smith et al. 2001; Van Dyk et al. 2005). A spectrum obtained by Van Dyk et al. (2005) in November 2002 revealed a narrow Hα profile suggesting an expansion speed of ∼700 km s^{-1}, although the expansion speed during the peak of the eruption is not known since spectra during the event are not available (in the case of η Car, however, it is reassuring that the present-day wind speed is similar to that of the Homunculus nebula; Smith 2006). As with the case of P Cygni, a brief peak in the light curve with a brighter maximum might have been missed due to a relatively long gap in the observations just before the recorded peak (Tammann & Sandage 1968).

SN 1961V: Of all the "SN impostors", SN 1961V is one of the most controversial, due to its very high luminosity ($M_{\rm pg}$ at peak was almost −18 mag) that blurs any clear distinction between real core-collapse SNe IIn and LBV-like eruptions, if it is indeed an LBV. Whether or not the surviving star is detected is key, but this question has advocates on both sides (Van Dyk et al. 2002; Chu et al. 2004; Filippenko et al. 1995; Goodrich et al. 1989). Because this source is so controversial and so much brighter than the rest of the SN impostors, we feel that it needs special consideration and we discuss it in more detail in §4.4. The light curve shown in Figure 8 is compiled from Zwicky (1964), Bertola (1963, 1965), and Bertola & Arp (1970). Zwicky (1964) estimated ejection speeds of 3700 km s^{-1} from the width of Hα in spectra obtained during the main eruption.

HD 5980: This remarkable WR+LBV eclipsing binary is the most luminous star in the Small Magellanic Cloud (SMC). It had already been an interesting object of study for decades as a massive eclipsing binary of two WN stars (one is actually a WNH star; see Smith & Conti 2008), where one star had a somewhat variable spectral type changing from WN to O7. It then surprised astronomers when it suffered a giant LBV eruption around 1993-1994, at which time the primary star brightened and changed its spectral type from a WN star to a H-rich B supergiant (Bateson, Gilmore, & Jones 1994; Barbá & Niemala 1994; Barbá et al. 1995). A substantial literature has built up about this star, and Koenigsberger (2004) has provided a recent review of the spectral and photometric properties of the binary and its outburst. In Figure 7 we use a smoothed version of the visual light curve (i.e. ignoring measurements during eclipses) adapted from Jones & Sterken (1997), which is shown here for reference. After two main peaks during the main outburst that lasted almost one year, the star has apparently taken about a decade to settle back to its pre-outburst state; a recent study by Koenigsberger et al. (2010) finds variability over several decades in historical data from the mid-20th century. It is noteworthy that the B1.5 Ia+ spectal type of the erupting star in 1994 implies a significantly hotter temperature than the canonical ∼8,000 K F-type supergiant expected in LBV eruptions. This turns out to be the case for a number of SN impostors, including V1 (Drissen et al. 2001), SN 2000ch, and SN 2009ip (Smith et al. 2010a); we will return to these "hot" LBV eruptions later. The wind speed of the erupting component of the binary system was estimated as 600 km s^{-1} (Koenigsberger et al. 1998).

V1 in NGC 2366: This source has been discussed in detail in a series of papers by Drissen and collaborators (Drissen et al. 1997, 2001; Petit, Drissen, & Crowther 2006). It is located in the giant starbursting H II region NGC 2363 within the dwarf irregular galaxy NGC 2366. Its eruption began when the star brightened rapidly in 1994, and it seems to have stayed at near-maximum ever since (see Figure 7). Interestingly, while the visual magnitude remained roughly constant at M_V of about -10.2 mag during this time, the UV flux actually brightened and the temperature indicated by spectral analysis increased (Petit et al. 2006). As with HD 5980, this once again contradicts the traditional view of pseudo photospheres in LBV eruptions having an F-type supergiant spectrum at maximum light. V1 has been subject to detailed modeling of its optical and UV spectrum, which can be matched by a stellar wind with $\dot{M} \approx 5 \times 10^{-4} M_{\odot}$ yr^{-1} and an average wind terminal speed of 300 km s^{-1} (Petit et al. 2006). Unlike some other LBV eruptions, the spectrum is not consistent with that of an explosion, but is consistent with a strong supergiant wind. This provides compelling evidence that in some cases, LBV eruptions are indeed wind driven while in others they seem to be partly explosive.

SN 1997bs: This SN of questionable integrity in M66 was the first "SN" discovered by the LOSS, but subsequent

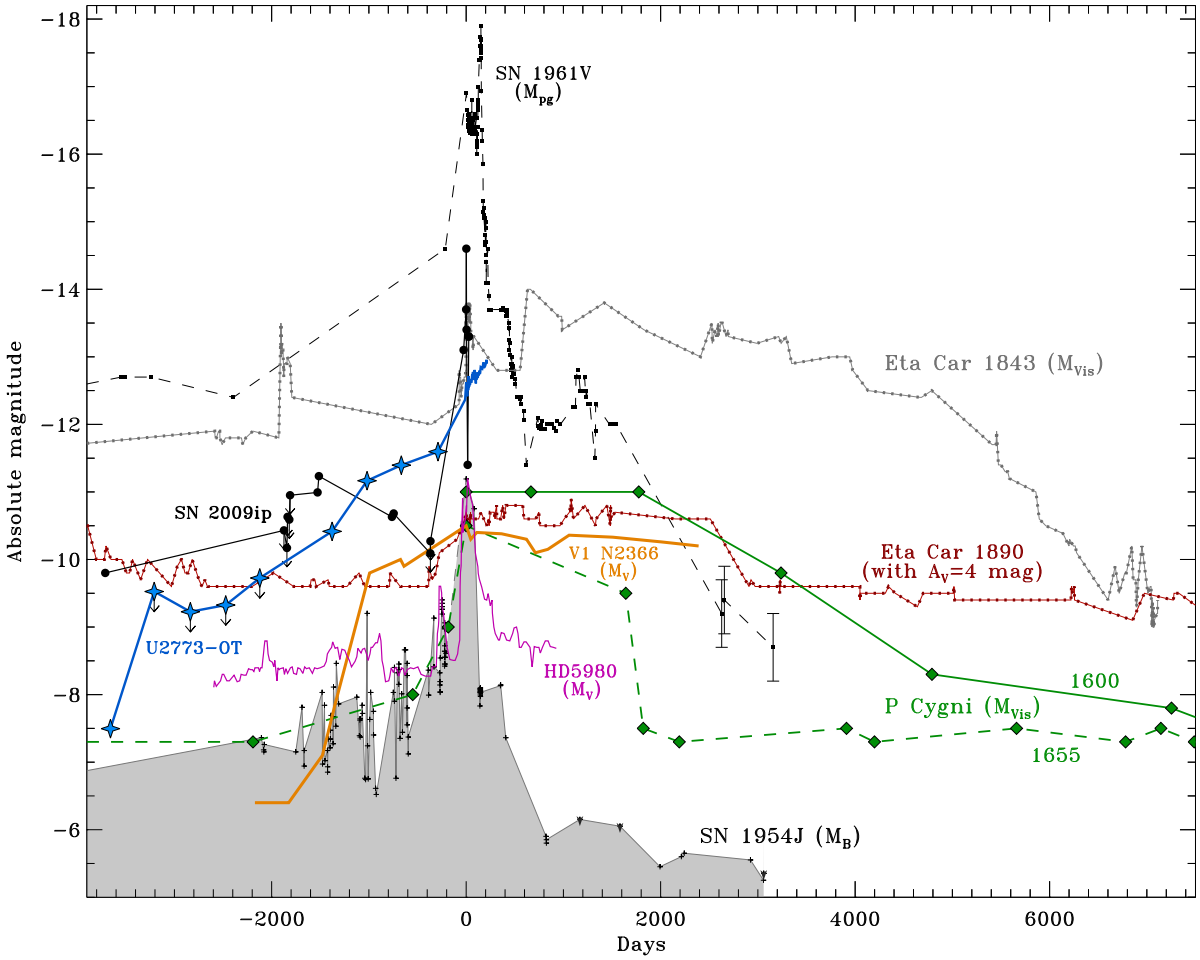

Figure 7. Long timescale LBV light curves, adapted from Smith et al. (2010a). Absolute-magnitude light curves of LBV eruptions for cases where information is available over long (i.e. decade) timescales, including observations before the main eruptions. We show the historical 19th century Great Eruption of η Carinae from Smith & Frew (2010; grey) as well as the 1890 outburst corrected for 4 mag of visual extinction (brown). We also show P Cygni's pair of eruptions in 1600 (green diamonds; solid) and 1655 A.D. (green diamonds; dashed) (see Smith & Frew 2010 and references therein). The eruption of SN 1954J (V12 in NGC 2403; Tammann & Sandage 1968) is shown as a gray shaded plot. The absolute magnitude of SN 1961V corrected for A_B=0.26 mag is shown with small filled squares, compiled from photometry in Zwicky (1964), Bertola (1963,1965), and Bertola & Arp (1970). The thick orange curve is the LBV eruption of V1 in NGC 2366 (Drissen et al. 2001; Petit et al. 2006), although shifted to an arbitrary date. The magenta curve is for the eruption of HD 5890 in the SMC during 1993-1994 (from Jones & Sterken 1997). We also show the decade-long pre-eruption light curves from the recent transients SN 2009ip (black filled circles) and U2773-OT (blue stars) from Smith et al. (2010a). Unfiltered visual magnitudes are shown for η Car and P Cyg, B magnitude for SN 1954J, photographic (approximately B-band) for SN 1961V, V magnitudes for V1 and HD 5980, and unfiltered (approximately R-band) for SN 2009ip and U2773-OT. Although these are different filters, our multi-band photometry of SN 2002bu shows that the V and R-band lightcurves are almost identical in shape.

analysis revealed that it was most likely not a genuine core-collapse event (Van Dyk et al. 2000). The V and R-band light curves and optical spectra we use here were discussed extensively by Van Dyk et al. (2000), shown in Figure 8. The progenitor was identified in pre-discovery images as a luminous star with $M_V \approx -8.1$ mag, and Van Dyk et al. (2000) conjectured that the star may have survived. Li et al. (2002) did not detect the star in late-time follow-up images obtained with *HST*, suggesting that the star may have disappeared or perhaps that it may have been deeply enshrouded in dust. Van Dyk et al. measured a FWHM of 765 km s^{-1} from Hα in spectra obtained on day 2 after discovery, and noted Lorentzian line wings extending to $\pm$3,000 km s^{-1}.

SN 1999bw: We discovered SN 1999bw in NGC 3198 on KAIT images taken as part of the LOSS on 1999 Apr. 20.2 UT (Li et al. 1999), and the first spectrum revealed that it was similar to SN 1997bs (Filippenko et al. 1999). As noted earlier, Hα in our day 4 spectrum can be approximated by a Lorentzian profile with a FWHM of $\sim$630 km s^{-1}, with a broader base with FWZI of roughly 3000 km s^{-1}. Sugerman & Meixner (2004) reported the detection of SN 1999bw in archival infrared data obtained in 2004 with the *Spitzer Space Telescope*, but no detailed follow-up study has been performed. A single spectrum of SN 1999bw was published by Matheson (2005). We obtained limited $BVRI$ and unfiltered photometry of SN 1999bw with KAIT, as listed in Table 1. We obtained a spectrum at Lick during the initial

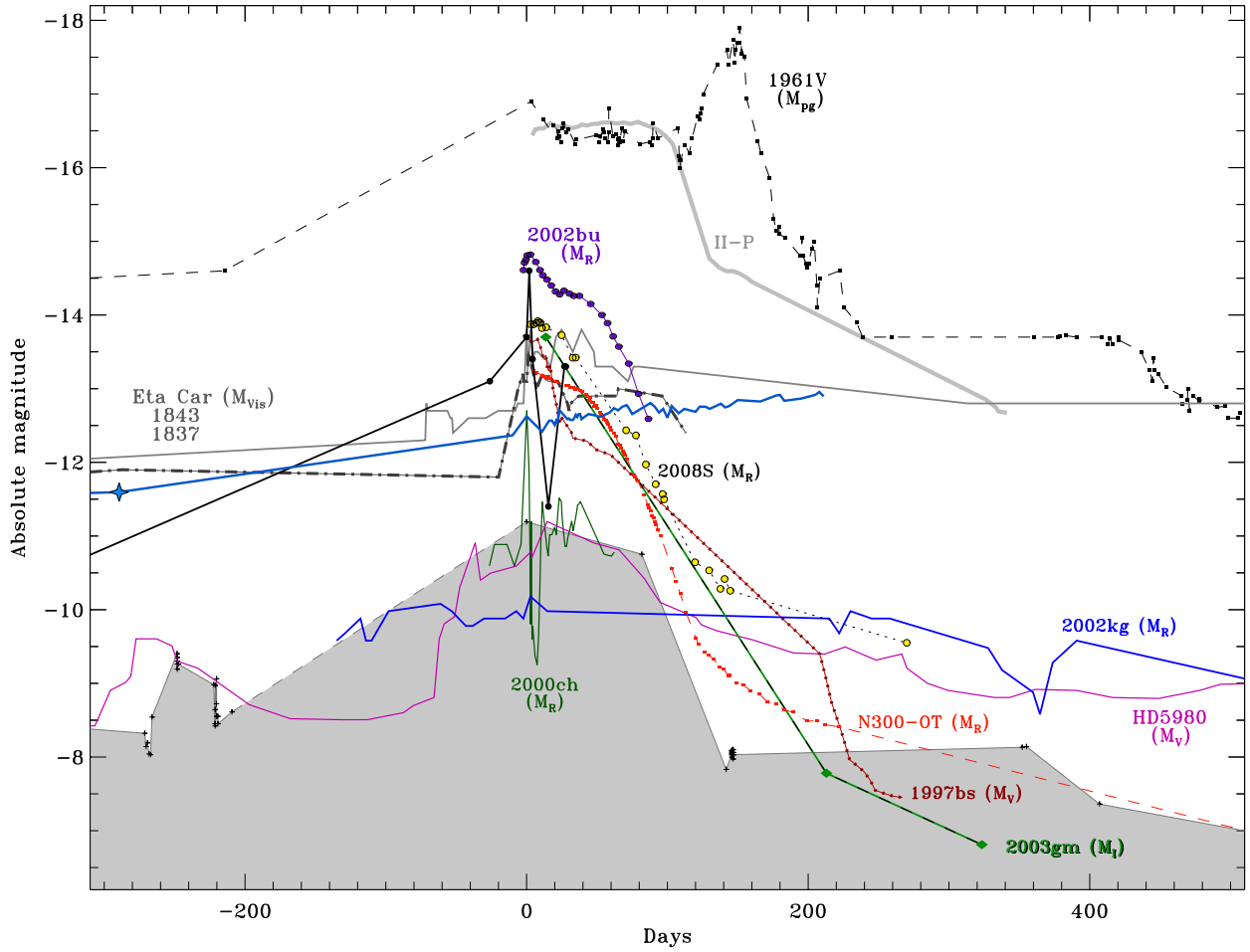

Figure 8. Similar to Figure 7, but zooming in on the time around peak brightness for several eruptive transients. In addition to the light curves repeated from Figure 7, we add the V-band light curve of SN 1997bs (Van Dyk et al. 2000; brown dotted), the R-band light curves of SN 2000ch (Wagner et al. 2004; green), SN 2002bu (this work; purple dots), SN 2002kg (Van Dyk et al. 2006; blue), SN 2008S (Smith et al. 2009a; yellow dots), and NGC 300-OT (Bond et al. 2009; red squares and dashed line), and the I-band light curve of SN 2003gm (Maund et al. 2006; green/black dashed line). For comparison with a normal Type II-P event, we also show the R-band light curve of SN 1999em (Leonard et al. 2002; thick gray curve). We show both the 1837 (solid gray) and 1843 (dot-dashed darker gray) precursor eruptions of η Car (Smith & Frew 2010).

peak, listed in Table 6 and shown in Figure 2. We adopt $m - M = 30.42$ mag for the host galaxy NGC 3198, and $E(B-V) = 0.012$. This suggests that SN 1999bw had a peak absolute R magnitude of about -12.65, intermediate between those of P Cygni and η Carinae.

SN 2000ch (LBV1 in NGC 3432): Observations of SN 2000ch were discussed in detail by Wagner et al. (2004; see also Van Dyk 2005), showing that it had a spectrum similar to that of SN 1997bs with a smooth continuum and bright Balmer emission lines. Its light curve was quite different, however, with a sharp rise and dip over a timescale of $\sim$5 days, superposed on a relatively constant plateau. The peak absolute R magnitude was -12.8, and the plateau at roughly -10.6 mag may have been either the quiescent state of a very luminous star or a prolonged S Dor-like eruption. The R light curve from Wagner et al. (2004) is shown in Figure 8. We obtained additional spectra at Lick, as listed in Table 6 and shown in Figure 2. The spectrum during outburst (day 28) has a strong Hα line with a Lorentzian profile shape and a FWHM of 1400 km s^{-1}. The line is somewhat asymmetric, with a blue wing extending to -2500 km s^{-1} and the red wing reaching $+4300$ km s^{-1}. In our late-time spectrum from 2004 discussed above, the Hα line width was similar with FWHM $\approx$ 1500 km s^{-1}.

As this paper was in the final stages of preparation, Pastorello et al. (2010) presented additional data showing that the same LBV star that erupted as SN 2000ch also suffered three additional eruptions in 2008 and 2009. Perhaps this object should be called "LBV1" in NGC 3432. Like the 2000 transient, these later eruptions were erratic and fast variations with peak R-band absolute magnitudes of -12.1 to -12.7. LBV1 showed rapid dips and recovery on timescales of a few days, similar to SN 2009ip, but repeatedly over several years. These recurring eruptions are not reproduced in Figure 8, but this interesting object is discussed thoroughly by Pastorello et al. (2010). Pastorello et al. (2010) drew comparisons between LBV1 and the binary HD 5980, suggesting similar binary encounters as a possible

mechnism, among other, behind the rapid and erratic variability. The erratic variability with multiple fast peaks and dips is qualitatively similar to the wild pre-1954 variability of SN 1954J/V12. If this comparison is appropriate, then the erratic variability may signify a growing instability, and we should not be surprised if LBV1 culminates with a more major eruption in the next decade or so. In any case, we should keep an eye on this star!

SN 2001ac: We discovered SN 2001ac on KAIT images taken on 2001 Mar. 12.4 and 13.3 UT (Beckmann & Li 2001) as part of the LOSS. A spectrum obtained by Matheson et al. (2001) was similar to those of SNe 1997bs and 1999bw, with a blue continuum and strong Balmer emission lines. No detailed analysis of SN 2001ac has been published; we presented limited $BVRI$ and unfiltered KAIT photometry (Table 2) and spectra near maximum light (Table 6, Figure 2). We adopt $m - M = 32.22$ mag and $E(B-V) = 0.027$ mag for the host galaxy NGC 3504, suggesting a peak absolute R magnitude of roughly -14.1 mag, comparable to that of η Car. As noted earlier, from our spectrum on day 9, the Hα line profile has a composite shape that can be fit with a Gaussian core FWHM of 287 km s^{-1} and broader Gaussian wings with FWHM of 1505 km s^{-1}.

SN 2002bu: Located in NGC 4242, SN 2002bu was discovered by Pucket & Gauthier (2002) on 2002 Mar. 28.26 UT. The progenitor was not detected to limiting red magnitudes of 20.5-21.0 mag. Preliminary reports of the spectrum indicated that it resembled a Type IIn or an LBV, with strong and narrow Balmer emission lines and a flat continuum (Ayani & Kawabata 2002). We obtained extensive $BVRI$ photometry with KAIT (see Table 3) as well as a series of spectra from Lick (Table 6, Figure 3). We adopt $m - M = 29.71$ mag and $E(B-V) = 0.012$ mag for NGC 4242. This suggests a peak absolute R magnitude of roughly -15, which places it among the brightest examples of the known SN impostors. The multi-color light curves and spectral evolution are described in some detail above. From spectra on day 11, Hα exhibits a Lorentzian profile with FWHM of 893 km s^{-1} and wings that extend to $\pm$2500 km s^{-1}. The temporal evolution of the spectrum was discussed above.

SN 2002kg/V37: The progenitor of this transient in the nearby spiral galaxy NGC 2403 (also host to V12/SN 1954J) was first identified by Van Dyk (2005) as Variable 37 from Tammann & Sandage (1968), a bright blue irregular variable like the Hubble-Sandage variables (i.e., a classical LBV). Observations of the increased brightness that was dubbed SN 2002kg have been discussed in detail by Maund et al. (2006) and Van Dyk et al. (2006). Its absolute peak V magnitude during outburst[5] was roughly -10 mag, making it one of the faintest of the recognized SN impostors, and the total brightening compared to its progenitor was only about 2 mag. We show the KAIT R-band light curve from Van Dyk et al. (2006) in Figure 8. Although SN 2002kg is usually discussed with the other SN impostors that are attributed to giant LBV eruptions like η Car, it seems plausible that SN 2002kg was not really a giant LBV eruption, but rather, a normal S Dor phase of a massive LBV star. This is based on its relatively modest increase in brightness that may be consistent with a change in bolometric *correction* only. The difference between these two is that a giant LBV eruption is defined as an increase in bolometric *luminosity*, whereas it is thought that the bolometric luminosity remains roughly constant in a normal S Dor phase (see Humphreys et al. 1999). Van Dyk estimated $M_{bol} = -9.8$ mag for the progenitor star, which is consistent with the observed peak absolute visual magnitude. The outburst SN 2002kg was very similar in magnitude to the previous eruptions experienced by V37 around 1920 and 1930 (Tammann & Sandage 1968). Weis & Bomans (2005) also associated SN 2002kg with V37, and claimed that the surviving star was detected again several years after the outburst. Both Maund et al. (2006) and Van Dyk et al. (2006) presented spectra of SN 2002kg, showing strong narrow Balmer emission lines with a narrow component having widths of 330–370 km s^{-1} and broader wings with widths of 1500–1900 km s^{-1}, consistent with electron scattering wings. P Cygni absorption features in Balmer lines also suggest expansion speeds of roughly 350 km s^{-1}. The spectra revealed strong narrow [N II] $\lambda\lambda$6548,6583 emission, similar to other LBVs and probably indicating the presence of a massive circumstellar nebula.

SN 2003gm: This transient source in NGC 5334 was also analyzed in detail by Maund et al. (2006). Unfortunately, photometric data are sparse and the available spectra are rather noisy. We show the I-band light curve from Maund et al. (2006) in Figure 8 (green/black). There are only 3 photometric I-band points, but as noted by Maund et al. (2006), the absolute peak magnitude and the decay rate appear very similar to SN 1997bs. The peak M_I was about –13.7, and the M_R and M_V values are probably similar to within $\pm$0.8 mag. We obtained unfiltered KAIT photometry on days 0 (discovery) and day 6, both of which were 17.0$\pm$0.1 mag. Early time spectra of SN 2003gm are similar to SN 2000ch, with Hα having a rather narrow width of only $\sim$131 km s^{-1}, but with broader wings having a width of 1472 km s^{-1} (Maund et al. 2006). Maund et al. estimated the metallicity of the host galaxy as 0.7 $Z_{\odot}$. Like SN 2002kg, the progenitor star was identified as a luminous star in pre-explosion data, and Maund et al. (2006) estimated $M_V \approx -7.5$ mag for the progenitor, indicating that the star brightened by more than 5 magnitudes during its giant LBV eruption.

N4656-OT (2005): This optical transient source in NGC 4656 was discovered by Rich (2005) with an unfiltered magnitude of 18.0 mag on 2005 Mar. 21 and 22 UT (the transient was also visible in unfiltered images taken a few days earlier at 18.5 and 18.3 mag; Yamaoka 2005). Elias-Rosa et al. (2005) reported that a spectrum of this transient had a blue continuum with strong narrow Balmer emission lines having widths of 730 km s^{-1}, but with no broad base as seen in normal SNe IIn, suggesting that it was an LBV-like event similar to SN 1997bs and not a SN. The spectrum also showed narrow Ca II H and K absorption. Unfortunately, we did not obtain additional data on this transient, and no other comprehensive analysis has been published to date. Adopting m–M = 28.69 mag (5.47 Mpc; from Tully et al. 2009) and $A_R = 0.035$ (Schlegel et al. 1998), the peak absolute unfiltered ($\sim R$-band) magnitude is -10.73 mag at the time

[5] There is some inconsistency in the literature about the peak absolute magnitude of SN 2002kg. At different places in their paper, Maund et al. (2006) quote M_V values of –9, –9.6, and –10.4 mag. Van Dyk et al. (2006) quote $M_V = -9.8$ mag in their text.

of discovery. If indeed N4656-OT is a giant LBV eruption, this makes it one of the less luminous examples, comparable to SN 1954J or HD 5980. No information is available about its progenitor star.

SN 2006bv: Occurring in UGC 7848, SN 2006bv was discovered by Sehgal et al. (2006) on 2006 Apr. 28.36 UT in unfiltered images with a magnitude of 17.8. A spectrum obtained 2 days later showed a smooth blue continuum and very narrow Balmer emission lines with FWHM of 400 km s^{-1} (Blondin et al. 2006). Immler & Pooley (2006) presented optical and UV photometry obtained a few days later and an upper limit to the X-ray flux, and concluded that it was fading rapidly. We secured some limited photometric measurements of SN 2006bv (Table 4), but we were unable to obtain spectra (this makes it difficult for us to confirm from an independent analysis that this is indeed an LBV and not a faint SN). We adopt $m - M = 33.0$ mag and $E(B-V) = 0.015$ mag for UGC 7848, suggesting a peak absolute unfiltered ($\sim R$) magnitude of roughly -15.2. This places SN 2006bv among the most luminous of the SN impostors, comparable to SN 2002bu.

SN 2006fp: This object was discovered on 2006 Sep. 17 UT by Puckett & Gagliano (2006) with an unfiltered magnitude of 17.7, while images obtained the following night had a slightly brighter magnitude of 17.6. The progenitor was not detected a year earlier to a limiting magnitude of 19.6. Spectra obtained by Blondin et al. (2006) revealed a reddened continuum with strong Balmer emission lines with very narrow widths of 300 km s^{-1}, but with a slightly broader base of around 1000 km s^{-1} (FWHM). The spectrum was most similar to previous SN impostors SN 1999bw and SN 2001ac, and Blondin et al. noted that the peak absolute magnitude corresponding to the discovery magnitude was roughly –14 mag, similar to other luminous LBV giant eruptions. Since the object was reddened, however, the true absolute magnitude at peak was more luminous. No comprehensive study of this object has been presented, and we did not secure additional photometry or spectroscopy. Adopting $m - M = 32.0$ mag for UGC 12182, and correcting also for a rather large line-of-sight Galactic extinction $A_R = 1.168$ mag (Schlegel et al. 1998) implies that the peak unfiltered absolute magnitude (approximately R-band) was about –15.47 mag. This makes SN 2006fp among the most luminous giant LBV eruptions at its peak.

SN 2007sv: Located in UGC 5979, SN 2007sv was discovered by Duszanowicz (2007) on 2007 Dec 20.9 UT with an unfiltered magnitude of 17.4. Low-resolution spectra obtained by Haratyunyan et al. (2007) show a blue continuum and narrow (FWHM < 1000 km s^{-1}) Balmer emission lines. No comprehensive study of this object has been presented, and we did not obtain additional photometry or spectroscopy. Adopting $m - M = 31.57$ mag (20.6 Mpc) and a small Galactic reddening of $A_R = 0.046$, we find that the absolute magnitude of SN 2007sv at discovery was roughly -14.2 mag, comparable to several other luminous giant LBV eruptions.

SN 2008S: This optical transient has been discussed extensively in the recent literature, with comprehensive photometric and spectroscopic datasets published by Smith et al. (2009a) and Botticella et al. (2009). The progenitor was very faint at optical wavelengths, but interestingly, was detected as a bright IR source in pre-discovery archival *Spitzer* data (Prieto 2008; Prieto et al. 2008; Thompson et al. 2009). Its optical spectrum had bright [Ca II] and Ca II emission lines and bright narrow Balmer emission lines, with a spectrum very similar to the yellow hypergiant IRC+10420 (Smith et al. 2009a). Its peak R-band absolute magnitude was -13.9 mag, and the light curve from Smith et al. (2009a) is shown in Figure 8. Smith et al. (2009a) noted expansion speeds of about 1000 km s^{-1} near the time of peak luminosity, dropping to about 550 km s^{-1} after a few months.

N300-OT (2008): This transient was a near twin of SN 2008S in most ways, including the obscured nature of its progenitor (Prieto 2008; Prieto et al. 2008; Thompson et al. 2008). Comprehensive analyses of the optical photometry and spectra were presented by Bond et al. (2009) and Berger et al. (2009). Its peak M_R was -13.3 mag. Berger et al. inferred an expansion speed of 560 km s^{-1} from the widths of emission lines, whereas Bond et al. (2009) suggested a slower speed of only 75 km s^{-1} based on the separation of the double peaks in emission lines. To be consistent with expansion speeds inferred from line widths in other objects, we adopt FWHM = 560 km s^{-1} as the representative expansion speed in the discussion below.

SN 2009ip: This SN impostor is the first in modern times to be discovered with precursor LBV-like eruptive variability in the decade leading up to its peak brightness, and its photometry and spectra were first analyzed in detail by Smith et al. (2010a). A subsequent analysis of similar spectra by Foley et al. (2010) confirmed the conclusions of Smith et al. (2010a). The unfiltered light curve presented by Smith et al. (2010a) is shown in both Figures 7 and 8. Smith et al. (2010a) inferred expansion speeds of roughly 600 km s^{-1} from Hα line widths, but also noted faster material at 3,000–5,000 km s^{-1} seen in broad P Cygni absorption features of lines like He I λ5876. This is the first time we have seen conclusive evidence for a second component with such high speeds reminiscent of the blast wave around η Car (in most other LBVs, the presence of broad emission wings can be explained by electron scattering and does not necessarily implicate faster moving ejecta). Days before submission of this paper, Drake et al. (2010) reported another subsequent outburst of SN 2009ip, apparently satisfying the expectation of Smith et al. (2010a) that "we should not be surprised if the eruption continues."

U2773-OT (2009): As for SN 2009ip, Smith et al. (2010a) discovered that U2773-OT was also an LBV that exhibited eruptive variability in the decade leading up to its discovery. Its spectra were different, however, with narrower lines and a cooler spectrum, more closely resembling that of a cool S Dor phase. A subsequent analysis of similar spectra by Foley et al. (2010) supported these conclusions. We adopt the unfiltered light curve and optical spectra presented by Smith et al. (2010a), although we also update the light curve with new photometric observations obtained with KAIT (see Table 5 and Figure 8). Spectra of this transient indicated expansion speeds of order 350 km s^{-1} (Smith et al. 2010a; Foley et al. 2010).

SN 2010da: This transient occured in NGC 300, following 2 yr after the well-studied and obscured optical transient in the same galaxy, and was also discovered by Monard (Monard 2010). A comprehensive study has not yet been published for this very recent source, but based on initial reports (Khan et al. 2010b; Brown 2010; Elias-Rosa et al.

2010; Chornock & Berger 2010; Berger & Chornock 2010; Immler et al. 2010; Bond 2010), this object appears consistent with an LBV giant eruption or SN impostor similar to SN 1997bs in some respects. Its progenitor was relatively faint at visual wavelengths but was apparently enshrouded in dust based on the bright IR source at the same position (Khan et al. 2010a, 2010b). Another preliminary analysis by Laskar et al. (2010) found pre-eruption variability analogous to U2773-OT and SN 2009ip (Smith et al. 2010a), but detected in the near-IR. At discovery, it had an apparent R magnitude of roughly 16.0 (Monard 2010), suggesting an absolute R magnitude of -13.5, similar to other LBV eruptions and almost identical to the 2008 transient in NGC 300. Further detailed study of this object is currently underway by several groups.

SN 2010dn: This recent transient was discovered by K. Itagaki (see Nakano 2010) in the nearby galaxy NGC 3184, and the initial spectrum taken two days after discovery showed narrow Balmer emission lines and a blue continuum similar to some LBVs, plus visible emission of [Ca II] and Ca II (Vinko et al. 2010). We adopt $m - M = 30.4$ mag (a distance of roughly 12 Mpc) and $E(B-V) = 0.017$ mag for NGC 3184, although the presence of [Ca II] emission suggests a dusty circumstellar environment (Smith et al. 2009a, 2010a; Prieto et al. 2008) so the true reddening may be higher. On day 2, SN 2010dn had an unfiltered magnitude of 17.1 (Nakano 2010), corresponding to a peak absolute magnitude of roughly -13.3. This is similar to N300-OT.

We presented the first published spectra of SN 2010dn in Figures 5 and 6, and we noted that the overall character of the spectrum was almost identical to those of SN 2008S and N300-OT, with strong narrow [Ca II] lines, intermediate-width emission from the Ca II IR triplet and Balmer lines, and a similar continuum suggesting a temperature around 7000 K. In our high-resolution Keck/DEIMOS spectrum on day 11, the Hα line had a FWHM of 900 km s^{-1}, which is similar to SN 2008S, but it displayed a mostly Lorentzian line profile shape unlike its close cousins. Atop the Lorentzian Hα profile, it also had a weak additional narrow component, perhaps indicating that it has additional dense slow CSM irradiated by the transient. The asymmetric profiles of the [Ca II] lines are qualitatively identical to those of N300-OT (Berger et al. 2009). According to Berger (2010), non-detection of the progenitor in archival *HST* images obtained $\sim$9 yr before discovery implies a V-band (F555W) absolute magnitude fainter than -6.3 mag. Based on the [Ca II] emission lines and associations with dusty environments (Smith et al. 2009a, 2010; Prieto et al. 2008), however, it is possible that the progenitor could potentially be intrinsically more luminous than this. Study of this transient is still underway at the time of writing.

3.2 Light Curve Morphology

The light curves of SN impostors in Figures 7 and 8 exhibit a wide variety in both peak luminosity, duration, and light curve shape. As we discuss later, light curve behavior is not necessarily correlated with their spectral properties, nor does the duration of the event seem to scale with the mass ejected. Some events show extremely complex and rapid rises and dips in absolute magnitude, sometimes multiple times, whereas other events exhibit a simple 10-yr plateau or single 100 d exponential decay. There does not seem to be any simple way in which the light curve properties scale, probably because there are a number of different physical parameters that can vary in each system: the progenitor mass and luminosity, the ejected mass and velocity, different input radiative and kinetic energy budgets, possible binary encounters, etc. Without knowing the physical mechanism(s) at work, it seems difficult to derive clearly meaningful information from the light curves alone, especially without the benefit of photometric observations in multiple filters.

3.3 Color and Temperature Evolution

Not much is known about the color evolution of SN impostors, and the question is mired by the possible presence of severe CSM dust and reddening. There is a relatively poor observational record of the UV characteristics during SN impostor outbursts.

It is becoming clear, however, that some long-held paradigms are certainly wrong. The common wisdom has been that LBV eruptions should always be seen at relatively cool temperatures of no cooler than $\sim$7500 K with an F-supergiant like spectrum (e.g., Humphreys & Davidson 1994; Davidson 1987), and that they therefore have small or zero bolometric correction at their peak. The reasoning behind this expectation is that LBVs develop opaque winds during their eruptions, with pseudo-photospheres that always tend toward these temperatures because of the opacity in the wind (see Davidson 1987).

This picture does apply to the cool states of normal S Doradus episodes of LBVs (Humphreys & Davidson 1994; Smith et al. 2004), but it apparently is not always the case in giant eruptions. Some giant eruption events do inded fit the bill, of course, with apparent temperatures of $\sim$7000 K and F supergiant-like spectra (e.g., U2773-OT, SN 2002bu, SN 2010dn, etc.). Other SN impostors such as SN 2009ip clearly do not fit this expectation, however. Detailed UV and optical spectroscopy of V1 in NGC 2366, for example (Petit et al. 2006), showed a much hotter temperture during its eruption, and revealed that the temperature and bolometric luminosity actually increased with time while the optical photometry showed a plateau. Also, SN 2009ip and other events showed hotter temperatures and a spectrum unlike an F supergiant.

In this older view, one would expect the coolest temperatures to coincide with peak luminosity when the pseudo photosphere is the largest, and that the effective photosphere would either stay at constant temperature or even get hotter as the eruption subsides, causing the mass-loss rate and opacity to drop. Instead, in some cases where information is available, we see much warmer temperatures of 12,000 K or more at peak, with the temperture then getting cooler as the object fades.

Substantial redward evolution with time may be expected from an explosion that suffers adiabatic cooling as the photosphere recedes through ejecta, as in a Type II-P event. Figure 1 shows that the redward color evolution of SN impostors is different from a normal SN II-P, never becoming as red. The more subtle drop in the characteristic emitting temperature with time is similar to a Type IIn SN powered by CSM interaction (e.g., Smith et al. 2010b), where the apparent temperature drops with time because

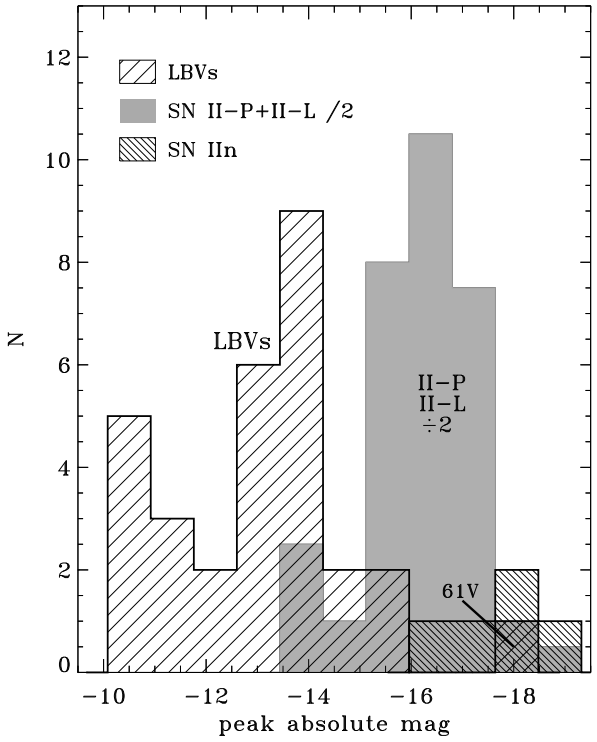

Figure 9. Histogram of the peak absolute magnitudes (mostly R, but some are V; from Table 8) for giant LBV eruptions. These are compared to the absolute R magnitudes of the KAIT sample (Li et al. 2010) of 52 normal SNe II-P and 10 SNe II-L (added together and divided by 2; shaded gray), and 5 SNe IIn. Notice SN 1961V to the lower right as the only LBV overlapping with SNe IIn.

the blast wave decelerates as it sweeps up large amounts of mass (van Marle et al. 2010). Dust formation in these events may also cause increased extinction and reddening, and may therefore have a strong influence on the apparent color with time. Further investigation of the color evolution of SN impostors, including both UV and IR observations, are sorely needed.

3.4 Peak Absolute Magnitudes

A key parameter for any transient source is its peak absolute visual magnitude. In the case of LBV giant eruptions, this is critical for evaluating the extent to which the star exceeded its own Eddington limit. Unfortunately, we do not have photometry in the same filters for each source, so we must compare R and unfiltered magnitudes (generally about the same) to V-band or unfiltered visual magnitudes for historical sources like η Car an P Cygni. For sources where both V and R are available, the difference is typically not more than a few tenths of a magnitude, and the qualitative shapes of the light curves in different filters are similar (e.g., SN 2002bu; Figure 1). Absolute peak magnitudes and the corresponding filters are listed in Table 8.

Figure 9 shows a histogram of peak absolute magnitudes for SN impostors (hatched), compared to the distribution of peak R magnitudes for normal SNe II-P and II-L (shaded gray) and SNe IIn (narrow hatched), taken form the KAIT sample (Li et al. 2010). LBV eruptions clearly form a separate population that is distinct from SNe. While the SNe II-P and II-L favor peak absolute magnitudes of roughly -16.5 ± 1.5, the LBVs are skewed to lower luminosity.

There appears to be one clear outlier among the LBVs in Figure 9, and that is the well-known event SN 1961V with a peak absolute magnitude of -17.8. SN 1961V is an unusual case, and later in this paper we consider the question of whether it is really an LBV eruption or something else — perhaps a genuine SN IIn resulting from core collapse, but preceded by an LBV eruption (see below). SN 1961V is well within the range observed for SNe IIn (Figure 9).

Excluding SN 1961V, all the LBV eruptions span a range of absolute magnitudes from about -10 to -16. There is some overlap with the low-luminosity tail of the SNe II-P distribution; we note that objects like SN 2005cs, SN 2001dc, and SN 1999br (see Pastorello et al. 2007a) are included in this sample. As noted by Smith et al. (2009a), the color evolution and spectral properties of these low-luminosity SNe II-P are quite distinct from SN impostors. (The highly reddened SN 2002hh is also included in the SN II-P sample of Figure 9, and its true absolute magnitude is more luminous than its apparent value because of local extinction.)

The distribution of LBV peak magnitudes in Figure 9 hints that there may be two subgroups — a more luminous class with peak magnitudes clustered around -14 ± 1.5, and a less luminous group with peaks of -10 to -11.5 mag. Since the SN impostors in this sample were discovered with widely differing search parameters (it includes historical objects in our galaxy as well as some discoveries by amatueres and by systematic surveys like LOSS), we cannot test the statistical significance of these two luminosity classes. SN impostors are faint compared to true SNe, and it is thus likely that their discoveries are highly imcomplete in most SN searches. This is particularly true for the less luminous group (-10 to -11.5 mag), so the true luminosity function of the impostors may look quite different from what is displayed in Figure 9. For example, in a volume-limited sample, there could be more -10 to -11.5 mag impostors than the more luminous examples. This is an area where future discoveries of SN impostors will be highly beneficial. Is it really two groups, or is it a continuous distribution of luminosities? How low does the distribution of SN impostor peak luminosities go? For the purposes of discussion in this paper, we tentativey refer to these as relatively low- and high-luminosity events, while being mindful that there may not be a true physical separation.

In any case, there is a practical problem with identifying eruptive peak magnitudes of roughly -10 or fainter, which is that we enter the territory of quiescent absolute bolometric magnitudes for very luminous stars. Namely, at the low end of this distribution, incomplete observational data will make it difficult to reliably distinguish genuine LBV giant eruptions (increase in bolometric luminosity) from the more common S Dor-type excursions. Recall that in an S Dor excursion, the star is supposed to brighten at visual wavelengths because of a change in apparent temperature and radius, but not necessarily luminosity, which in turn alters the bolometric correction, so either UV data or detailed atmospheric models become necessary. However, recent studies of S Dor excursions may hint that the traditional view of

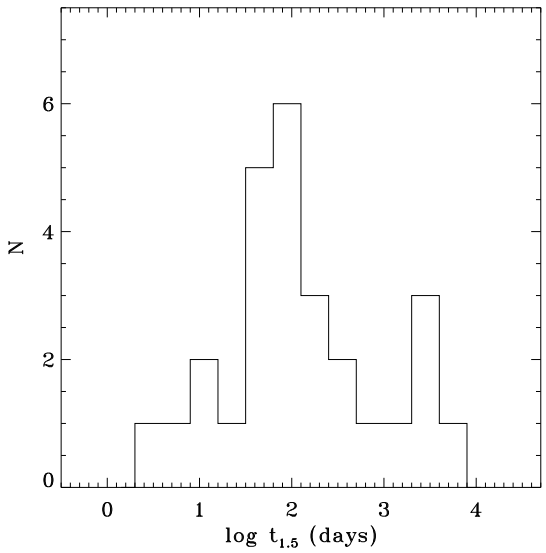

Figure 10. Histogram of the logarithm of values of $t_{1.5}$ listed in Table 8.

constant luminosity may need to be modified as well (e.g., Groh et al. 2009), making the situation more murky.

At first glance, it may be tempting to naively group relatively low and high luminosity eruptions into different subclasses, but this would be too oversimplified and not necessarily helpful. In several cases we have well-studied LBVs where the star suffers multiple eruptions, qualifying for the low- or high-luminosity category *in subsequent eruptions of the same star*. Instead, Figure 9 should be taken as a demonstration of the rather wide diversity of the eruptive phenomenon in general. A theory that attempts to explain the mechanism of the eruptions should strive to reproduce this diversity.

3.5 Characteristic Rise and Fall Timescales

The rise timescales are poorly constrained for most SN impostors, because they are most often discovered around the time of peak luminosity due to the smaller telescopes used for most transient searches, while larger telescopes are used mainly for followup observations. Adequate information about fainter progenitors is therefore rare, limited to cases with good archival data. This situation is, of course, improving with time as high-quality archives become more populated with observations, and with transient searches conducted with larger telescopes.

Discovery near peak implies a rather sudden onset for the brightening of some SN impostors, and hence, a fast rise timescale comparable to SNe. We do see examples, however, of very slow rise times as well, as in the case of U2773-OT, which rose steadily for at least 5 years, and is in fact still rising. This, as well as precursor eruptions and variability seen in some objects like η Car, V12/SN 1954J, and SN 2009ip, points toward a significant "preparatory" phase in SN impostors. This is physically meaningful because it signals a growing instability, rather than a sudden event. This echoes the fact that LBV eruptions are apparently sometimes a preparatory phase for the eventual core-collapse SN, at least in the case of luminous SNe IIn (e.g., Smith et al. 2007, 2008, 2010b; Gal-Yam & Leonard 2009; Foley et al. 2007; Pastorello et al. 2007).

Timescales for SN impostors to fade from maximum are much better characterized than their rise times. In SNe, the rate of decline provides information about the ejecta mass (i.e., the diffusion time) and energy source (i.e., radioactive decay rates). In SN impostors, the direct meaning of the decline rate is not immediately clear, but characterizing the distribution of relative rates at which SN impostors fade may eventually help distinguish between models.

For comparison among the sample of sources, we define a timescale, $t_{1.5}$, as the time in days for a transient to fade by roughly 1.5 magnitudes from its peak. This is either the time beginning at discovery or peak visual luminosity, depending on the available information. Some cases require exceptions, such as the brief precursor eruptions of η Car in 1838 and 1843, when observations are imcomplete and we are not sure if the source actually faded by a full 1.5 mag. In cases such as this, the value of $t_{1.5}$ is approximate, and represents the time over which the star appeared to be fading back to its quiescent level. The resulting values of $t_{1.5}$ are listed in Table 8, and a historgram of the values is plotted in Figure 10. Cases where more than one value of $t_{1.5}$ is listed in Table 8 correspond to more than one major outburst observed from the same source. Since this is not a complete sample with uniform coverage for each source, the histogram in Figure 10 is meant to convey the range of timescales observed, rather than a statistically significant distribution. Figure 10 does not show the typical timescales for SNe II-P, which is always close to 100 days.

SN impostors span a wide range of fading timescales, clearly peaked at durations around $\sim 10^2$ days. There are also examples that fade quickly in only a few days, and several cases that last for a decade. An important point that distinguishes SN impostors from true SNe is that the fading timescale does not necessarily tell us anything about the amount of mass ejected. Both η Car and P Cygni had durations of $\sim$10 yr for their major eruptions, but from measurements of their nebulae we know that η Car ejected more than 10 $M_\odot$ (Smith et al. 2003b), whereas P Cygni only ejected about 0.1 $M_\odot$ (Smith & Hartigan 2006). Furthermore, η Car also showed two brief events of $\sim$100 days duration, when it is possible that much of the mass may have been ejected (Smith & Frew 2010), and it had another decade-long outburst in the 1890s when only 0.1–0.2 $M_\odot$ was ejected (Smith 2005). Unfortunately, measuring the mass for extragalactic SN impostors, where circumstellar nebulae are not resolved, is impossible without a detailed understanding of the physical mechanism and the radiative transport involved in the outbursts. The sustained energy source of the decade-long eruptions is therefore unclear, but it is probably not caused by diffusion from an extremely large mass of ejecta.

The very fast declines correspond to obvious sharp dips in the light curves, in many cases corresponding to drops in magnitude to the quiescent progenitor's luminosity or even fainter. Notable cases of these sharp dips are SN 2009ip (Smith et al. 2010a), SN 2000ch (or LBV1 in NGC 3432; Wagner et al. 2004; Pastorello et al. 2010), SN 2002kg (Van Dyk et al. 2006; Maund et al. 2006). The cause of these is unclear, but Smith et al. (2010a) have hypothesized that they may correspond to sudden ejections of massive shells

Table 8. A collection of observed parameters for SN impostors

Transient	M(peak) (mag/filt.)	$t_{1.5}$ (days)	V_{exp} (km s^{-1})	EW(Hα) (Å)	Multi-peak (Y/N)	Sharp Dip (Y/N)	M(prog.) (mag/filt.)
P Cygni	-11,-10.5/Vis.	1800,3600	136	...	Y	N	-9.7/Vis
η Car	-13.5,-13.8,-14,-10.8/Vis.	110,200,4400,3000	200,650,5000	...	Y	Y	-12/Vis
SN 1954J	-11.3/B	100	700	...	Y	Y	-7.5/B
SN 1961V	-17.8/pg	∼200	3700	...	Y	N	-12.4/pg
HD 5980	-11.1/V	200	600	...	Y	N	-8.1/V
V1	-10.5/V	>2000	300	...	N	N	...
SN 1997bs	-13.8/V	45	765	119	N	Y	-8.1/V
SN 1999bw	-12.65/R	>10	630	53.7	N	N	...
SN 2000ch	-12.8,-12.7,-12.3,-12.1/R	2,25,50,8	1400	461	Y	Y	-10.6/R
SN 2001ac	-14.0/R	∼50	287	46.4	N	N	...
SN 2002bu	-14.97/R	70	893	66	N	N	...
SN 2002kg	-10.4/R	365,∼600	350	39	Y	Y	-8.2
SN 2003gm	-14.4/I	∼65	131	...	N	N	-7.5
NGC 4656-OT	-10.7/u.f.(R)	?	730	...	N	N	...
SN 2006bv	-15.24/u.f.(R)	>40	400	...	N	N	>-13.5
SN 2006fp	-15.6/u.f.(R)	?	300	...	N	N	>-13.6
SN 2007sv	-14.25/u.f.(R)	?	<1000	...	N	N	>-11.7
SN 2008S	-13.9/R	75	1100	53.7	N	N	-6.5/IR
NGC 300-OT	-13.2/R	80	560	...	N	N	-7.5/IR
SN 2009ip	-14.5/u.f.(R)	7,>40	600,5000	214	Y	Y	-9.8/R
UGC 2773-OT	-13?/u.f.(R)	>400	350	33	N	N	-7.8/R
SN 2010da	-13.5/R	?	660	...	?	?	...
SN 2010dn	-13.3/R	?	155,860	...	?	?	>-6.3/V

of material, which expand quickly and cool while remaining opaque. After the shell finally becomes optically thin, the emergent luminosity may return to its previous level. This is of course just a working hypothesis; detailed radiative transfer calculations that include sudden massive shell ejections would be valuable.

Several objects show evidence for multiple peaks or multiple separate eruptions. This is discussed further below, but it is also relevant to mention here that repeated eruptions in the same source can often have different timescales. The delay time or dormant time between these multiple outbursts may also be highly relevant, perhaps indicating a recovery timescale or orbital timescale in the case of binary encounters. Due to incomplete archival information, it is of course very difficult to constrain the possible occurance of previous eruptions in objects where precursors have not been documented.

3.6 Expansion Speeds and Line Profiles

While the ejecta mass is difficult to estimate from observations of SN impostors, their spectra are extremely valuable for providing direct estimates of the expansion speeds during an eruption. Aside from studying the kinematics of spatially resolved circumstellar nebulae in the nearest examples, which may have been decelerated through interaction with pre-existing CSM, direct spectra of outbursts are the only way to understand the kinematics of the ejection. The speed of ejection provides important clues to the nature of the star, because in some scenarios one expects the expansion speed to be related to the star's escape velocity (i.e., RSG stars have very slow winds of ∼20 km s^{-1}, LBVs and blue supergiants have speeds of a few hundred km s^{-1}, and compact WR stars typically have fast winds of more than 1000 km s^{-1}). The observed expansion speed and its change with time through the outburst are also critical for understanding the physics of the eruptive event (explosive blast wave or sustained wind). Understanding the distribution of SN impostor expansion speeds is also relevant for understanding the pre-SN evolution of SNe IIn, where narrow lines from the pre-shock CSM can be observed.

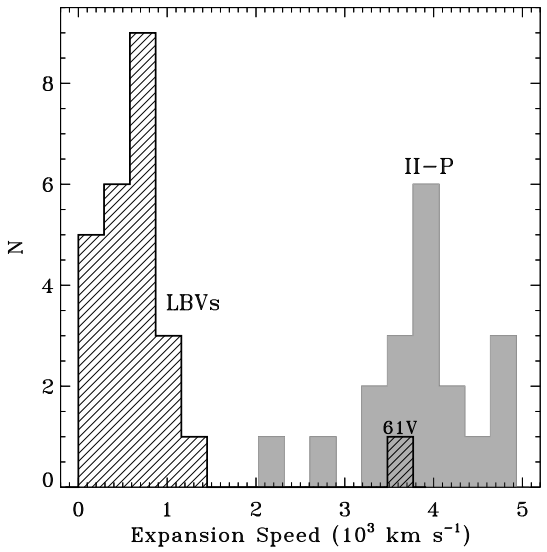

Figure 11. Histogram of the expansion speeds for LBV eruptions, measured by the FWHM of Hα in most cases when spectra are available during the eruption, or from the expansion speed of the resulting nebulae in the cases of P Cygni and η Car (see Table 8). Expansion speeds for the KAIT sample of SNe II-P is shown for comparison, measured from Fe II lines in the middle of the plateau (see Poznanski et al. 2009). True core-collapse SNe IIn apparently fill the gap between LBVs and SNe II-P, with typical line widths of 1000–4000 km s^{-1}.

To assess the distribution of expansion speeds for our sample of SN impostors, we generally took the FWHM value of the Hα emission line, either measured directly in our spectra or quoted from the literature, as the primary indicator of the expansion speed for the bulk of the material

in the ejecta/wind of SN impostors. However, this was supplemented with other information. For η Car and P Cygni, values of $V_{\rm exp}$ were inferred from the kinematics of their expanding nebulae (Smith 2005, 2006, 2008; Smith & Hartigan 2006), and even this is incomplete (e.g., we only listed the polar expansion speed for the Homunculus nebula of 650 km s^{-1}, while a latitude-dependent range of speeds is seen down to 40 km s^{-1} at the equator; Smith 2006). Also, in cases such as SN 2009ip, fast speeds of ∼5000 are seen in absorption only, in He I and Balmer lines (Smith et al. 2010a; Foley et al. 2010). The adopted values of $V_{\rm exp}$ are listed in Table 8 and the distribution is shown in Figure 11.

The dominant outflow speeds in SN impostors span a wide range from around 100 km s^{-1} up to somewhat more than 1000 km s^{-1}, with a peak in the distribution around 600-800 km s^{-1} (Figure 11). Note that in Figure 11 we are aiming for the dominant outflow speed, so we did not include the fast material moving at ∼5000 km s^{-1} around η Car or SN 2009ip, because in both cases this fast material is thought to constitute a very small fraction of the total mass (Smith 2008; Smith et al. 2010a). Contrast this with the case of SN 1961V, which showed an Hα FWHM of 3700 km s^{-1} in spectra taken during the peak of the eruption (Zwicky 1964). The observed expansion speed in Hα is one of several ways in which SN 1961V is a clear outlier among the SN impostors, and in fact, we argue later that SN 1961V is not a SN impostor at all, but is instead a true core-collapse SN. From Figure 11, one can see that the expansion speed of SN 1961V is much closer to the range of speeds seen in SNe II-P than to the SN impostors. It is also worth noting that there is little overlap between speeds in SNe II-P and SN impostors; the KAIT sample of SNe II-P in Figure 11 from Poznanski et al. (2009) includes faint and low-energy SNe II-P such as SN 2005cs. Speeds observed in the intermediate components of Hα in SNe IIn occupy the intermediate zone between SN impostors and SN II-P, with typical speeds of 1000–4000 km s^{-1}.

In addition to the FWHM values for Hα, SN impostors also show remarkable diversity in the detailed shapes of their line profiles. As described above, one can see lines dominated by a Lorenztian shape, a Gaussian shape, or a combination with a narrow Gaussian core and Lorentzian wings. In several cases (e.g., SN 2002bu discussed earlier) one sees a transition from a Lorentzian line shape at early times to a Gaussian shape in the same object, which is also seen in SNe IIn (Smith et al. 2008, 2010b). This diversity is not understood, but is likely related to the changing optical depth of the wind or ejecta, since electron scattering through dense material will produce Lorentzian shapes. Lorentzian profiles are more noticable in SN impostors than in core-collapse SNe because the intrinsic line width is narrower, making the scattering wings out to a few 10^3 km s^{-1} easier to see.[6] Perhaps detailed radiative transfer modeling of these evolving line shapes will lead to an understanding of the density of the winds and ejecta, and hence, the mass ejected in a given event. SN impostors also show a range of asymmetry in their line profiles, with some very symmetric emission lines and some with strong blueshifted absorption (some rare cases even show *redshifted* absorption at high resolution; Berger et al. 2009). This may depend on either different viewing geometry from one object to the next or different optical depths and ionization levels in the winds.

[6] For this reason, SN observers may be unfamiliar with Lorentzian line wings, and consequently, some observers have fit individual broad components to the line wings and erroneously inferred the presence of very fast moving gas.

3.7 Spectral Morphology

Figure 12 displays a gallery of visual-wavelength spectra of a number of SN impostors, collected from our database and from the literature (see the caption for Figure 12 for references). We have attempted to gather spectra as close to maximum light as possible, but complete coverage of SN impositors is not always available, and so we see a distrubition of times after peak or discovery. The spectrum can evolve with time, as illustrated in cases such as SN 2002bu, so some caution is needed to interpret Figure 12. Readers are referred to individual papers to examine the spectral evolution of each object; this is too large a topic to describe here. Nevertheless, it is clear that we do *not* see consistent spectral evolution in all objects. While some transients like SN 2002bu evolve from characteristically "hot" to "cool" with time, there are other examples which are cool at early times or examples that remain hot at late times. Thus, the diversity in spectral characteristics shown in Figure 12 is real and is likely representative of the class.

All the SN impostors share the common property of strong Balmer line emission with relatively narrow lines compared to SNe (this is, in fact, one of the criteria used to classify them as a SN impostor, in addition to their relatively faint absolute magnitudes). Beyond that, there seems to be a wide range of qualitative properties that can be attributed to the characteristic temperature of the emitting photospheres or pseudo-photospheres. Smith et al. (2010a) have discussed the dichotomy of relatively "hot" LBVs like SN 2009ip and relatively "cool" objects like U2773-OT, while both are characteristic of LBVs. In Figure 12 we have attempted to organize the spectra very roughly with the hotter objects on the top half and the characteristically cooler objects toward the bottom. The "hot" objects are characterized by smoother and steeper blue continua, stronger and broader Balmer lines, relatively weak absorption, and less complex spectra in general. The "cool" objects tend to have redder continua, weaker and narrower Balmer lines, strong [Ca II] and Ca II emission, deeper P Cygni absorption features, and in some cases stronger absorption spectra similar to F-type supergiants (U2773-OT is the best case of this) or to yellow hypergiants like IRC+10420 (see Smith et al. 2009a). As noted earlier, there are intermediate objects, and there are some that transition from reatively hot to cool as time passes. We do not see any trend that the hotter objects are necessarily more luminous, although they do tend to have stronger and somewhat broader Balmer lines. It is interesting that the narrow [Ca II] emission that was so remarkable in SN 2008S and N300-OT is actually present to varying degrees in many of the SN impostors. Smith et al. (2010a) have discussed the [Ca II] and Ca II lines in more detail, while Smith et al. (2010a) and Prieto et al. (2009) have suggested that these lines may be related to the presence of pre-existing circumstellar dust.

Few of the objects are hot enough to exhibit He I emis-

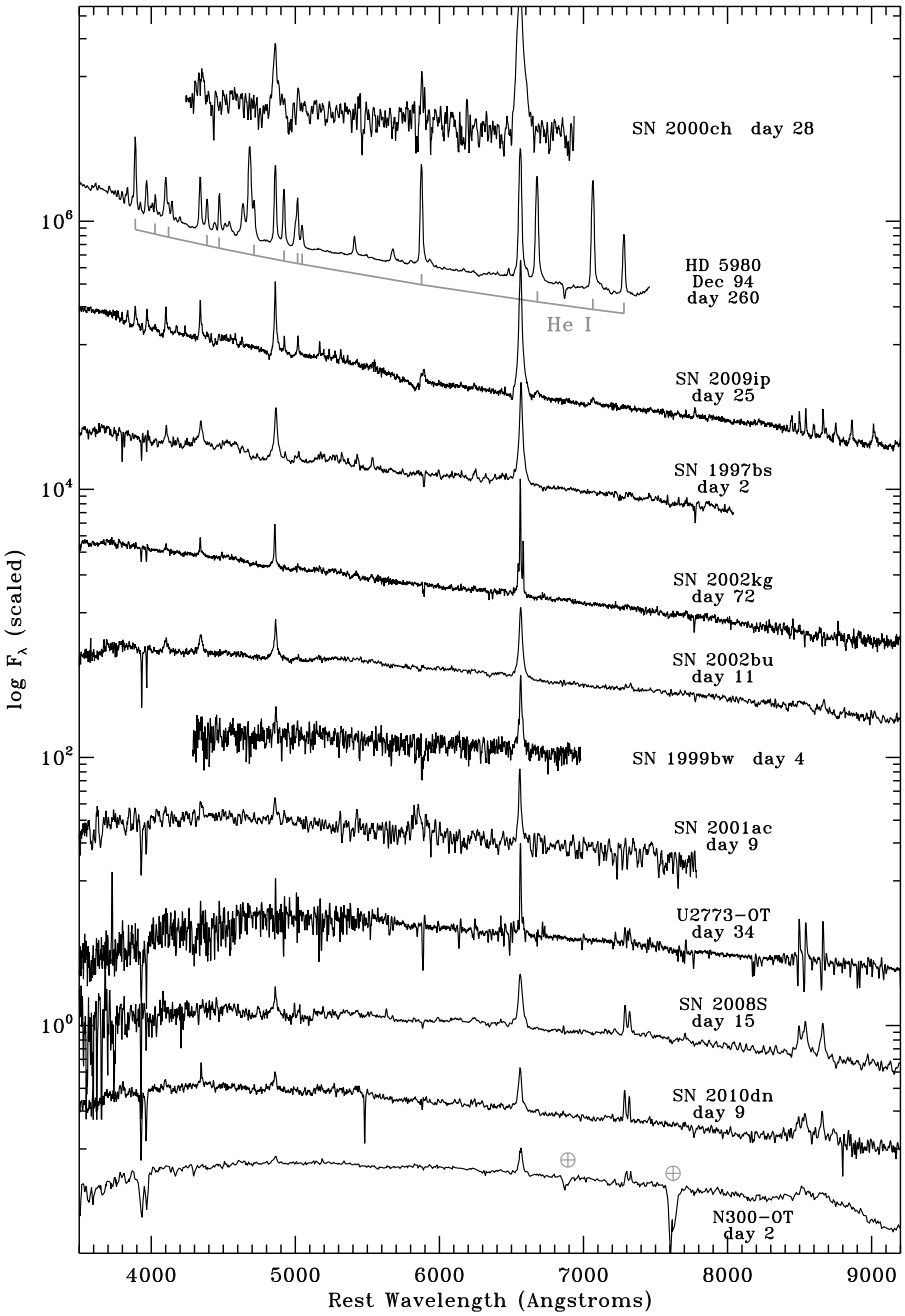

Figure 12. A comparison of most of the known SN impostors near their time of maximum light. The spectrum of SN 2008S is from Smith et al. (2009a), and the spectra of UGC 2773-OT and SN 2009ip are from Smith et al. (2010a). NGC 300-OT is a low-resolution spectrum taken from Bond et al. (2009), which is not corrected for telluric absorption (major telluric bands are marked). Most of the remaining spectra are from our own spectral database, although the spectra of SN 2002kg (Van Dyk et al. 2006) and SN 1997bs (Van Dyk et al. 2000) were previously published. We also show the spectrum of HD 5980 a few months after the peak of its LBV eruption on Dec. 31 1994; this is an *HST*/STIS spectrum from Koenigsberger et al. (1998), and the locations of numerous He I lines are indicated.

sion lines, which is generally quite weak if present, and often fades quickly with time. HD 5980 is peculiar in this sense, because it has extremely strong He I and He II emission lines (see Figure 12). In this case, however, we know that the eruptive star in the HD 5980 eclipsing binary system has a very luminous and hot WR companion star, which may strongly influence the observed spectrum during outburst. SN 2009ip, SN 2000ch, and one early epoch of SN 2001ac also show evidence for weaker He I emission.

3.8 Correlations in observed properties?

This sub-section could be made very brief by simply stating that there are no obvious correlations among various observed properties of SN impostors. We do not, for exam-

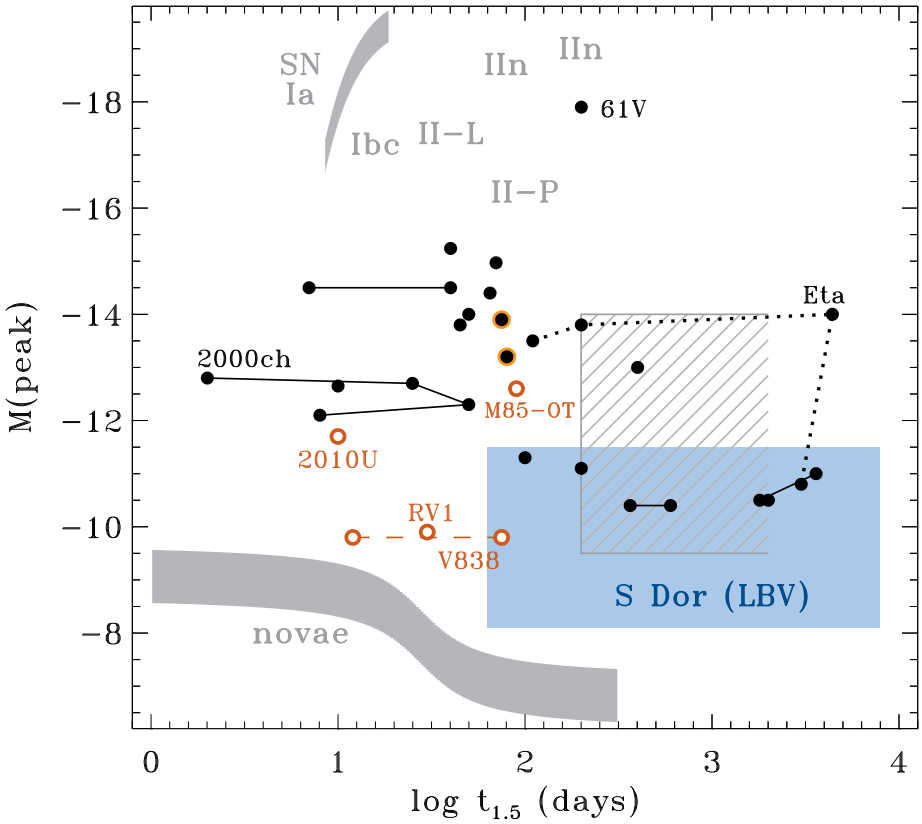

Figure 13. Peak absolute magnitude as a function of the characteristic fading timescale, $t_{1.5}$, defined in §3.5. SN impostors from Table 8 are shown as solid black points. The two of these that are outlined in orange are the notable and often debated cases of SN 2008S and N300-OT, which do not stand out among the population of SN impostors. SN impostor outbursts for which more than one eruption has been documented in the same source are connected by solid or dashed black lines. For comparison in gray, we also show the peak luminosity vs. $t_{1.5}$ relations for for novae (adapted from Della Valle & Livio 1995), SNe Ia (adapted from Phillips et al. 1999), and very rough locations for SNe II-P, II-L, and IIn on this plot (note that SNe IIn occupy a large area above the plot as well, due to very luminous examples). Locations of the intermediate-luminosity transients discussed in §4.5, which are reputed to be something different from SN impostors, are plotted in red (again, two peaks of the V838 Mon eruption are connected by a dashed line). The hatched gray box shows the range of parameter space that has been attributed to LBVs in the past (e.g., Kulkarni et al. 2007), but this is clearly incomplete and only captures a few of the SN impostors. The solid light blue box corresponds to normal S Doradus-type outbursts of LBVs (thought to exhibit no substantial increase of bolometric luminosity), which partly overlaps with giant eruptions of LBVs where the bolometric luminosity does increase. Confidently distinguishing between the two cases requires knowledge of the star's quiescent luminosity. We caution that the left side of the plot at moderate luminosities might be highly incomplete for LBVs, due to selection effects.

ple, see any trend between luminosity and expansion speed, since both fast and realtively slow expansion speeds are seen among both luminous and relatively faint SN impostors. Although the description of spectral morphology is more qualitative, we also see no trend that SN impostors with characteristically "hot" spectra are more luminous, or vice versa. Instead, the main lesson seems to be that LBVs/SN impostors are highly diverse, occupying a range of parameters without obvious correlations.

As an example, consider the plot shown in Figure 13, which relates the duration of a transient event to its peak luminosity, as is commonly done for transient sources. This is adapted from a similar plot shown by Kulkarni et al. (2007) and others, although here we have expressed the duration in terms of a somewhat different quantity, $t_{1.5}$. SNe Ia and novae obey clear relations described elsewhere, and core-collapse SNe tend to be fairly localized (except for SNe IIn). However, the eruptions of LBVs or SN impostors essentially fill the entire range of the so-called "gap" in Figure 13 between SNe and novae, covering timescales from a day to decades, and ranging over two orders of magnitude in peak luminosity. As noted elsewhere in this paper, we even have cases where the same star suffered multiple eruptions that appear in very different places in Figure 13 (these cases are connected by solid or dashed lines). Although there is no obvious "main sequence" along which LBVs reside in Figure 13, there does seem to be a concentration around $t_{1.5} \approx 50 - 100$ days and M(peak) $\simeq -14$ mag. This common location for SN impostors includes the well-studied and often debated events SN 2008S and N300-OT. The transient M85-OT also appears to reside comfortably among the most common types of SN impostors, and is not exceptional in this regard.

As a starting point, then, it may be prudent for theory to focus on possible physical mechanisms that can lead to $\lesssim$100 day events with peak luminosities of $2{\times}10^7$ $L_\odot$,

and to then explore variations in physical parameters that extend this parameter space. The wide observed diversity may be attributed to a huge range in possible physical parameters, such as ejected mass, explosion energy, progenitor mass and luminosity, Eddington factor, etc., which can obviously affect quantities like the relevant thermal or diffusion timescales, and the photospheric radius with time during a transient. The few cases where we have detailed estimates of ejected mass and energy already exhibit differences of orders of magnitude.

Some of the observed diversity may also depend strongly on previous recent mass-loss history. For example, the amount of local dust extinction around the progenitor, and by extension the presence of strong [Ca II] emission lines, IR excess, or perhaps absorption lines in the spectrum, may depend on how recently the star suffered a previous outburst that created a dense and dusty CSM. The same progenitor star might look extremely different depending on how much time has elapsed since the last eruption, and how much mass was ejected in that event. A hypothetical eruption of η Carinae that is identical to its 1890 event could look very different if it were to occur a few hundred years from now when the Homunculus nebula has largely dispersed. Thus, the observed diversity in spectra and color of transient events may not necessarily be tied to diverse physical properties of the outbursts themselves. There is no clear reason to expect the previous mass-loss history to be correlated with other observed properties, of course.

To make matters worse, it is well established that the eruptive mass loss of LBV eruptions can be strongly nonspherical, and so observed properties may depend on viewing angle. For example, the outflow speed that one would derive from spectra of η Carinae would appear to be $\sim$650 km s^{-1} if it were viewed from a latitude near the pole, but one would infer a much slower outflow speed of 40–100 km s^{-1} if an observer happened to be looking from a low latitude projected along the equator (see Smith 2006). This may well play a role in some of the diversity in outflow speed of SN impostors in Figure 11. Similarly, the amount of line-of-sight extinction toward a source may be very latitude dependent if it arises in the local circumstellar environment. If a progenitor star were surrounded by a dusty torus such as those commonly thought to reside around supergiant B[e] stars, for example, an observer situated near the equator might deduce that the progenitor was completely obscured and enshrouded. (A cautionary note is that this same observer would then *underestimate* the star's bolometric luminosity by a factor of 5-10 if that estimate were based on the measured IR luminosity.) We might expect something like 10% of SN impostors to be viewed from low latitudes, so perhaps a few cases of heavily obscured progenitors is not so surprising. Again, there is no expectation that viewing angle will correlate with any other observed property, except perhaps extinction.

4 DISCUSSION

4.1 Progenitor Star Diversity

One of the most important clues to the nature of SN impostors is the initial mass and evolutionary stage of the progenitor star in its quiescent state before the outburst. Unfortunately, this information is rarely available and hard to come by, and detection bias for progenitors tends to favor cases where the progenitor star is relatively luminous. An added difficulty is that, in the absence of eclipsing binaries like HD 5980, it is of course always difficult to measure the star's mass, which depends on evolutionary models, assumed reddening, uncertain bolometric corrections, assumed inclination and geometry of obscuring material, etc.

It has been well-established that the instability we associate with LBVs occupies a large range of initial mass, from the most massive stars that may exist down to about 20-25 $M_{\odot}$ (Smith et al. 2004). It is therefore no surprise that several of the SN impostors appear to have very luminous progenitor stars within this range (e.g., SN 2009ip, SN 1997bs, η Car, P Cygni, HD 5980, etc.). A few examples seem to have progenitor stars around the lower bound of this mass range at $\sim$20 $M_{\odot}$ (U2773-OT, V12/SN 1954J, V1 in NGC 2366), while there is suggestive evidence that the $\sim$18–20 $M_{\odot}$ progenitor of SN 1987A may have experienced an LBV-like episode in its pre-SN evolution (Smith 2007).

However, the recent discovery of the relatively faint obscured progenitors of objects like SN 2008S and N300-OT was a surprise, and seems to extended this range of initial masses well below 20 $M_{\odot}$. Given the slope of the initial mass function, we may expect to see more of these events in coming years, hopefully with identifiable progenitor stars. An extremely interesting open question raised by SN 2008S and N300-OT is just how low in initial mass stars may experience extreme LBV-like eruptions. Does the eruptive phenomenon extend even below the lower limit for core-collapse SNe at $\sim$8 $M_{\odot}$, and if so, are sudden energetic bursts important for the formation of some planetary nebulae? Thompson et al. (2009) have touched upon this issue, but more examples and better constraints in the progenitor stars are needed. This is discussed further below.

The recent recognition that eruptions similar to LBVs may occur in moderately massive stars with initial masses below 20 $M_{\odot}$ has rather profound consequences. While the ultimate trigger and physical mechanism for LBV giant eruptions remains unknown, it has generally been accepted that the eruptive behavior is the consequence of these stars approaching or exceeding the classical Eddington limit. If the progenitor stars of SN 2008S and N300-OT really did have initial masses well below 20 $M_{\odot}$, this is surprising and informative, since *stars in this mass range will never approach the classical Eddington limit in the normal course of their evolution*. The most massive stars with initial masses above 60 $M_{\odot}$ will naturally and unavoidably be driven to a super-Eddington state in their post-main-sequence evolution, while stars with initial masses of 25–40 $M_{\odot}$ may approach the Eddington limit in a post-RSG phase, after they have shed significant mass and thereby raised their L/M ratio. Stars below 20 $M_{\odot}$, however, have relatively tame luminosities and do not have mass-loss rates high enough to bring their L/M ratios to such dangerous levels. Thus, while more massive stars can easily exceed the Eddington limit temporarily with small adjustments in opacity or stellar structure, lower mass stars require a substantial input of extra energy to bring them to the exceptional peak luminosities observed and to successfully eject large amounts of mass. While η Car was about 5 times the Eddington luminosity at the peak of its giant eruption, the SN impostors

SN 2008S and N300-OT that reached a similar peak luminosity had Eddington factors of more like 40–80 (see Smith et al. 2009; Bond et al. 2009).

4.2 Pre-Outburst Variability (or not) and Multiple Eruptions

Very few of the eruptive transients discussed here have information about the pre-outburst progenitor star. When this information is available, though, it is extremely valuable. While progenitor detections are hard to come by, multi-epoch progenitor detections are even more rare.

Nevertheless, based on improving archival data, the observational case is building that several SN impostors experience a phase of growing instability that can precede the most dramatic brightening (usually associated with the time of discovery) by a few years or decades. A classic example of this is η Carinae, which showed a slowly increasing visual magnitude for a century before its mid-19th century eruption, but then – more remarkably – showed several very brief precursor brightening events before the main extended bright phase of its eruption (see Smith & Frew 2010). V12/SN 1954J is another key historical example, which showed very peculiar and erratic variabiltiy for 5–10 yrs before its giant eruption. More recent examples include SN 2009ip and U2773-OT, which showed slow ∼5 yr episodes preceding their eruptions (Smith et al. 2010a). SN 2000ch has shown multiple recurrances of brief brightening episodes (Pastorello et al. 2010), and SN 2009ip has now exhibited another eruption ∼1 yr later (Drake et al. 2010). HD 5980 exhibited some minor brightening episodes before its major eruption, and of course P Cygni suffered a second eruption 55 years after the beginning of its first major eruption (Smith & Frew 2010). At the very least, the presence of multiple recurring outbursts is a strong indication that the stars survive these events, and that the underlying physical mechanism is not a terminal event such as a core collapse, an electron capture SN, or a failed SN. This is discussed more below.

A critical point is that if these stars can experience multiple outbursts on relatively short timescales, then *there is no gaurantee that a given transient event is the first one experienced by that star.* A given progenitor may be in a state where it is still recovering from a previous recent burst, which may have been an extremely disruptive event, while any dusty CSM surrounding that progenitor may have been ejected in a very recent but undocumented previous eruption.

Thus, one must be cautious in interpreting the significance of a given progenitor's observed properties – especially if it is based on a single epoch or a brief range of time. This is perhaps an area where much longer time baselines from plate archives may be of substantial benefit. The luminosity one infers from an observation of a progenitor is not necessarily the *quiescent* bolometric luminosity of the star or the normal state of that star, and may therefore cause erroneous estimates of that star's initial mass. Furthermore, if the progenitor was heavily obscured, one must be careful in making direct comparisons to classes of stars that are always heavily enshrouded, like OH/IR stars or AGB stars, because the obscuring dust may have a very different origin in a recent eruption. Thus, initial masses and evolutionary states derived from progenitor observations must be taken with a grain of salt. Ideally, one would like to combine information about the progenitor with estimates of the ages of surrounding stars, as Gogarten et al. (2009) did for N300-OT. More studies of this type may help advance the field significantly.

4.3 Outburst Diversity: Explosions or Winds?

All massive stars in the local universe have considerable radiation-driven stellar winds, and these winds become a dominant and defining characteristic for evolved supergiants and hypergiants. Namely, the strong emission lines that define WR stars, LBVs, blue supergiants, and yellow hypergiants are caused by their extended and often partially opaque stellar winds. Given the similarity between the spectra of SN impostors and those of Galactic LBVs and hypergiants, it is natural to conclude that extreme winds are also the key physical mechanism in SN impostors. Detailed modeling of the spectra for a few events, like V1 in NGC 2366 (Petit et al. 2006) has demonstrated this.

However, some recent clues also suggest that hydrodynamic expulsion of the stellar envelope may be at work in some eruptions. This was suspected based on the ratio of kinetic to radiated energy in η Carinae (Smith et al. 2003b), and the presence of an energetic blast wave was later confirmed by the discovery of extremely fast ejecta surrounding this star (Smith 2008). Similar fast material has now also been seen in SN 2009ip (Smith et al. 2010a; Foley et al. 2010). Thus, these strong blast waves imply that dynamic explosions are an important ingredient in at least some LBV giant eruptions, in addition to extremely strong winds. While the total mass lost in an event may be the same for an extreme but temporary wind as compared to an explosion, the corresponding implication for the underlying physical mechanism is quite important. An explosion implies a severe restructuring of the star on a dynamical timescale, requiring a deep deposition of energy inside the star, and the radiative transient we see is an after-effect. In the case of a wind, the implication is that the luminosity of the star has increased, and that increase in luminosity causes mass to be lifted from the surface of the star in quasi-steady-state. Given the complex light curves of some SN impostors, it is easy to imagine a hybrid situation where an initial shock heats the envelope, and the resulting increase in radiative luminosity drives a strong wind. Furthermore, one can imagine that a range of energy deposition could lead to a large diversity of observed phenomena ranging from enhanced winds to explosions, as explored by Dessart et al. (2009). In other words, it seems possible that the diversity in winds and explosive phenomena might be different manifestations of the same basic energy deposition.

With the possibility of explosive mechanisms for the origin of SN impostors also comes the possbility that their luminosity might be enhanced or even dominated by interaction of the blast wave with dense CSM, as in traditional SNe IIn, but with lower-energy shock waves. This hypothesis has not been explored much in models for the spectra of SN impostors, but seems quite promising given the remarkable spectral similarities between SN impostors and SNe IIn (see Smith et al. 2010a; Foley et al. 2010).

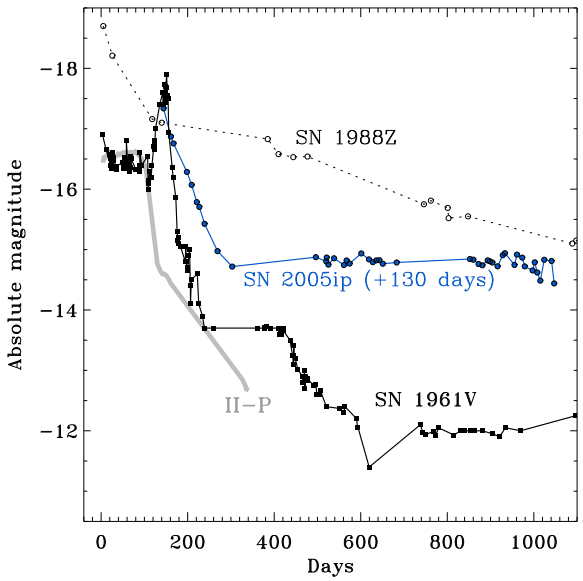

Figure 14. Same as Figure 8, but comparing the light curve of SN 1961V to that of a normal SN II-P and two examples of well-studied SNe IIn. The light curves of SN 1999em (II-P), SN 2005ip (IIn), and SN 1988Z (IIn) are the same as they appear in Figure 1 of Smith et al. (2009b), except that the light curve of SN 2005ip is shifted by +130 days for reasons discussed in the text.

4.4 SN 1961V: LBV mega-eruption or a true core-collapse SN IIn?

In light of the distribution of LBV eruption properties, a close re-examination of SN 1961V is worthwhile, since it is the prototype of Zwicky's original Type V class of SNe, it has colored much interpretation of the SN impostors because of some similarity to η Carinae, and it is a rare case where the progenitor star was identified in the decades before the event. Goodrich et al. (1989) first made the case that SN 1961V was not actually a core-collapse SN, but was instead an exaggerated η Carinae-like outburst; this was based on the detection of intermediate-width (2000 km s^{-1}) Hα emission at the expected position of the SN in a ground-based spectrum taken 25 yr after the peak of the eruption. Filippenko et al. (1995) tentatively identified a red source seen in early *Hubble Space Telecope* (*HST*) images, suggesting that this may be the dusty source predicted by Goodrich et al. Later imaging studies with the refurbished *HST* disagreed on which source was coincident with SN 1961V (Van Dyk et al. 2002; Chu et al. 2004). Despite this disagreement about which star is the survivor, SN 1961V is usually regarded as a prototype of the SN impostors because it was well studied and was the original "Type V" supernova. It is ironic, then, that our present comparison finds SN 1961V to be an extreme outlier among the class of SN impostors in every measurable way. This begs the obvious question: *Was SN 1961V really an impostor?*

After considering the distribution of properties among LBVs and SNe IIn, the answer seems to be "Probably not." The original motivation for linking SN 1961V to η Car was the relatively narrow width of its emission lines compared to SNe II-P, plus its slow and unusual light curve evolution. However, these and essentially all of its observed properties are consistent with the class of true SN IIn, where the narrow lines and extra luminosity are thought to arise from core-collapse explosions interacting with dense CSM. The Type IIn class was not yet recognized at the time of the outburst (leading to Zwicky's suggestion of a new Type V), but there has been much progress in understanding the properties of SNe IIn in recent years.

Based on photographic spectra taken during the peak of the outburst, Zwicky (1964) inferred an expansion speed of 3700 km s^{-1} from the width of Hα, while Branch and Greenstein (1971) estimated $V_{\rm exp} \simeq 2000$ km s^{-1} based mainly on calculated fits to Fe II and similar lines in a series of spectra taken at different times during the event. Goodrich et al. (1989) estimated 2100 km s^{-1} from Hα in the very late-time spectra. Humphreys & Davidson (1994) contended that such narrow lines meant that SN 1961V was "definitely" not an ordinary SN and more closely resembled η Car. However, the conjecture that SN 1961V was not a true SN based on its narrow lines is not valid. Most *bona-fide* SNe IIn have line widths of 1000–4000 km s^{-1} (e.g., Chugai et al. 2004; Smith et al. 2008, 2009b, 2010b; Filippenko 1997); even some of the most luminous SNe known have lines as narrow as 1000 km s^{-1} (Smith et al. 2008, 2010b; Prieto et al. 2007). Looking at Figure 11, the expansion speed inferred from line widths in SN 1961V is clearly more in-line with normal SNe than with the rest of the LBV eruptions.

The light curve of SN 1961V – while complex and quite unusual – also does not provide a very compelling case that it was not a true SN. Figure 14 compares the light curve of SN 1961V to that of a normal SN II-P and to those of two well-studied SNe IIn: SN 1988Z and SN 2005ip.[7] The long decay time for SN 1961V is easily accounted for by continued CSM interaction at late times; both SN 2005ip and SN 1988Z were more luminous for a longer time. SN 1961V is thus intermediate between these classic SNe IIn and a normal SN II-P (i.e., at no time is it less luminous than a normal SN II-P), making it a somewhat less extreme version of CSM interaction than SN 2005ip. The absolute magnitude of the brightest peak in SN 1961V's light curve was almost identical to that of SN 2005ip. The rather stark interruptions in its decline (interpreted as late "plateaus" by Humphreys et al. 1999) also find clear precedent in SN 2005ip, whose light curve declined rapidly until day 160 when it abruptly hit a floor and remained at the same luminosity (or even rose slightly) for years afterward (Smith et al. 2009b).

Still, the light curve of SN 1961V is admittedly a bit

[7] Here we find that the peak absolute magnitude was almost −18 mag. Humphreys & Davidson (1994) chose to adopt the closest of published distances to NGC 1058 ($m - M$=28.6 mag; 5.3 Mpc), making the peak magnitude −16.4, which is still brighter than any other SN impostor and comparable to normal SNe II-P. Most estimates, however, favor a larger distance and therefore a higher luminosity for SN 1961V. The expanding photosphere method applied to SN 1969L gives $m - M$=30.13−30.25 mag for NGC 1058 (Schmidt et al. 1992; 1994), whereas the Hubble flow distance (assuming H_0 = 73.0 km s^{-1} Mpc^{-1}) gives $m - M$=29.77 mag. We therefore adopt $m - M$=30.0 mag, and also correct the light curve for a Galactic extinction value of A_B=0.27 mag (the B-band extinction is probably most appropriate for the photographc magnitudes in the light curve), making the peak absolute magnitude roughly −17.8, far exceeding any other SN impostor.

unusual compared to most SNe IIn. The key property that makes it seem unique is that it shows an initial luminous plateau at −16.5 mag for ∼105 days, followed by a second more extreme peak reaching almost −18 mag before declining rapidly thereafter. This can potentially be understood as a superposition of a normal SN II-P plateau (like SN 1999em) followed by a late-time addition of luminosity from enhanced CSM interaction, as seen in a SN IIn like SN 2005ip. This superposition is shown schematically in Figure 14 with the light curve of SN 2005ip (Smith et al. 2009b) shifted by +130 days for comparison. The only requirement here, from the CSM-interaction point of view, is that the CSM shell had an inner cavity of lower density than the main shell, so that the time when the blast wave struck the densest part of the CSM shell was delayed by 120-130 days. A delayed turn-on of the CSM interaction luminosity is understandable with a thin dense shell at a large radius (e.g., van Marle et al. 2010). A late turn-on even has clear observational precedent among SNe IIn: an extreme case is the recent SN IIn 2008iy, which started with a luminosity comparable to a SN II-P, but continued to rise slowly for ∼400 days (Miller et al. 2010).

With a SN blast wave expansion speed of ∼4000 km s^{-1} (adopting Zwicky's estimated speed from spectra during the event), the shock would have struck the shell after day ∼105 when the rise to the bright peak began if the shell had a radius of $\gtrsim$250 AU. This is entirely plausible given the observed shells around known LBVs and the shells inferred around other SNe IIn. If that LBV shell had initially been ejected at a few hundred km s^{-1} (also typical of LBVs) it would imply that the shell had been ejected within ∼5 yr before the final SN explosion. Indeed, $\lesssim$1 yr prior to the beginning of the main peak, SN 1961V was already in a precursor outburst state with an absolute magnitude of −14.5 (see Figure 8), which is quite similar to η Car and other LBV eruptions. This provides a self-consistent picture, where SN 1961V suffered a precursor LBV outburst that was followed within a few years by a true core-collapse SN IIn.

While somewhat complicated, this scenario fits in well with current ideas about SNe IIn, and it is appealing because it no longer requires the progenitor to have been an astoundingly massive $\gtrsim$240 $M_{\odot}$ star that is substantially more massive than any known in the local universe. If the high pre-maximum luminosity is attributed to an LBV-like outburst rather than the quiescent star, and if the peak outburst was a genuine core-collapse SN explosion, then conjectures that the progenitor was incredibly massive (up to 2000 $M_{\odot}$; Utrobin 1984, Goodrich et al. 1989; Humphreys & Davidson 1994) are clearly erroneous. It also relieves the difficulty of trying to account for the tremendous energy budget of SN 1961V with a non-terminal event.

If this surmize is true, then it is the first definitive detection of a precursor LBV outburst prior to a SN IIn, further strengthening the LBV/SN IIn connection. This builds upon earlier results of the precursor LBV-like outburst before the unusual Type Ibn event SN 2006jc (Pastorello et al. 2007b; Foley et al. 2007), as well as the detected progenitor of the SN IIn 2005gl that was inferred to be an LBV-like star (Gal-Yam & Leonard 2009). In fact, it remains possible that the progenitor identified as a possible LBV by Gal-Yam & Leonard (2009) could have been in an eruptive state at the time the pre-discovery archival data were obtained, although this is uncertain. A decade before SN 1961V, the progenitor was observed at a bolometric magnitude of about −12.4, similar to the quiescent bolometric luminosity of η Carinae. Like Goodrich et al. (1989), we infer that this is likely to be the quiecent bolometric luminosity of the progenitor star, making it comparable to the most luminous stars known. Since the progenitor resided in a giant H II region similar to the Carina Nebula, this appears reasonable.

In this continued CSM-interaction context, the undulations in the late time decay of SN 1961V are also easily explained by simply assuming that the expanding blast wave overtook a series of additional shells at larger radii, causing a small and temporary enhancement in the luminosity. SN 1988Z, SN 2005ip, and other SNe IIn demonstrate that this is achievable. The luminosity of a SN IIn can turn on or off at any time, depending on the density of material it is running into. If the CSM environment was dusty, some of this late-time luminosity may also be attributable to a reflected light echo (remember that the SN 1961V historical light curve is in photographic magnitudes, which favor blue wavelengths). As noted earlier, putative detections of the surviving star in recent times have been controversial, so proof of the SN IIn hypothesis remains elusive based on modern data. Even if the a source is detacted at the correct position, however, it may still be fueled by weak CSM interaction at late times, or it may be another star in the crowded star cluster. For example, Li et al. (2002) detected the SN IIn 1995N many years after explosion, while SN 1988Z still remains luminous. The conjecture by Chu et al. (2004) that the Hα source identified in their data (object 7) "cannot be the SN or its remnant because of the absence of forbidden lines" is incorrect if the late-time luminosity is powered by CSM interaction rather than by the radioactive decay tail. Stockdale et al. (2001) detected a non-thermal radio continuum source at the position of SN 1961V, and Chu et al. (2004) showed that this radio source is coincident with the only strong Hα emission-line star in the cluster. The radio and narrow Hα emission are certainly consistent, in principle, with the strong continued CSM interaction that one may expect in the SN IIn hypothesis. Furthermore, the presence of dust inferred from strong IR emission in the late time data of SN 1961V is also consistent with the SN IIn hypothesis, as a strong IR excess from new dust formation and from an IR echo were both seen in SN 2005ip (Smith et al. 2009b; Fox et al. 2010).

We conclude, therefore, that the peak of SN 1961V was probably not a SN impostor after all, but a *bona-fide* SN IIn caused by a core-collapse event. We suggest that the initial peak for the first ∼105 d was akin the plateau of a normal SN II-P (this does not exclude the possibility of narrow lines from CSM interaction being present at that time), while the so-called "super outburst" when SN 1961V reached $M_{\rm pg} \approx -18$ mag and then faded rapidly may have been powered by CSM interaction as in a SN IIn like SN 2005ip. In this scenario, the essential difference between SN 1961V and a conventional SN IIn is that the CSM interaction was *delayed*, probably because the CSM shell was at a large radius with an interior cavity. In future studies, readers are therefore advised to disregard the fact that SN 1961V was included in figures in this paper comparing the light curves and other properties of LBV eruptions, at least to the extent that these plots are taken as indicative of LBVs.

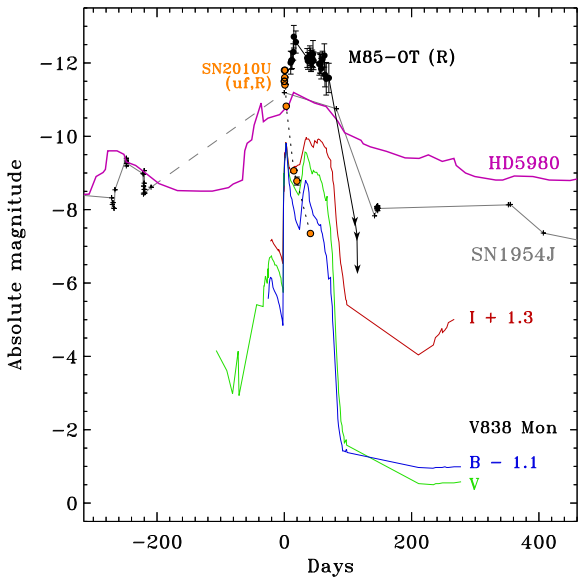

Figure 15. Absolute magnitude light curves of the transients V838 Mon and M85-OT, along with the LBVs V12/SN 1954J and HD 5980 for comparison. V12 and HD 5890 are the same as in previous figures in this paper. The B, V, and I-band light curves (blue, green, and red, respectively) of V838 Mon are from Sparks et al. (2008), while the R-band light curve of M85-OT is from Kulkarni et al. (2007). The combined unfiltered and R-band light curve of SN 2010U is also shown as orange dots and a dotted black line, from Humphreys et al. (2010; and references therein).

4.5 Other Intermediate-Luminosity Transients

While the distinction between LBV eruptions and true core-collapse SNe may be more clear after considering the distribution of LBV eruption properties, the bottom end of the LBV distribution remains nebulous. Drawing a clear dividing line between true LBV giant eruptions and "normal" S Doradus eruptions is not as easy as previously suggested (e.g. Humphreys & Davidson 1994), since the notion that S Doradus eruptions always occur at constant bolometric luminosity has not withstood rigorous analysis (Groh et al. 2009), and the conjecture that these eruptions should always have atmospheres with temperatures around 8000 K is also incorrect. For example, it is unclear if the eruptions of HD 5980 and SN 2002kg do indeed qualify as giant LBV eruptions, since it is not clear that they experienced a substantial increase in bolometric luminosity, and the total amount of mass and energy lost were not much in excess of their quiescent states. Of course, defining a transient as a giant LBV eruption or S Dor outburst at the lower end of SN impostor luminosities (see Figure 13) also requires reliable knowledge of the progenitor's luminosity — in order to decide of the bolometric luminosity has indeed increased — which is often not available. (For the SN impostors with relatively high peak luminosities above −13 mag, this is not a problem because no stars have a quiescent luminosity this high, and so the bolometric luminosity must have increased substantially.)

Furthermore, the bottom end of the luminosity distribution for SN impostors also overlaps with transients that may not really be LBV eruptions, and might not even be associated with massive stars. Thompson et al. (2009) have proposed a new sub-class of transients where the progenitor star was heavily obscured and had relatively low bolometric luminosities, exhibiting [Ca II] emission in addition to narrow Balmer emission lines. This was inspired largely by the discovery and detailed observations of SN 2008S and N300-OT, discussed extensively above. However, whether these transients constitute an entirely new class of outbursts, or if they instead represent an extension of LBV-like eruptions to lower masses than previously thought (i.e. below 20–25 $M_{\odot}$) is controversial (see Smith et al. 2010a for a recent summary of the debate; see also Thompson et al. 2009; Smith et al. 2009; Prieto et al. 2010). The source of the disagreement is that all of the properties attributed to this putatively new class of objects are already observed among known LBVs. Obscuring dust shells are certainly common among known LBVs, while we have demonstrated here (Figure 12) that the presence of [Ca II] emission is seen in many of the SN impostors to varying degrees, although it had not been emphasized in discussions before 2008, and these lines are seen in hypergiants with very strong winds like IRC+10420 (Smith et al. 2009).

Recently, Prieto et al. (2009) presented a mid-IR spectrum of N300-OT that contained an emission feature reminiscent of the polycyclic aromatic hydrocrbon (PAH) features seen in some proto-planetary nebulae, and they interpreted this as indicative that the progenitor of N300-OT was a carbon-rich super-AGB star. However, the presence of PAH emission features does not necessarily constitute C-rich chemistry.[8] Moreover, prominent PAH features have been seen in the mid-IR spectra of known LBVs such as HD 168625 (e.g., Umana et al. 2010), which has a luminosity corresponding to an initial mass of about 25 $M_{\odot}$. One cannot rely on the inference of amorphous carbon grains as necessarily indicative of carbon-rich gas chemistry either, since carbon grains form at much higher temperatures than silicates, and the conditions for rapid dust formation in ejected shells may be very different from the conditions in RSG/AGB winds. The presence of PAH features in a SN impostor spectrum, or the presence of carbon grains, is therefore not necessarily indicative of a carbon-rich AGB star.

Alternatively, it is quite possible that the reason the progenitor stars of SN 2008S and N300-OT were obscured (and possibly why they had low luminosities) is because the stars suffered a previous recent outburst that had not been documented. LBVs are known to suffer multiple successive eruptions (see §4.2). The most distinguishing property of the SN 2008S and N300-OT progenitors was their relatively low luminosity, implying initial masses lower than 20 $M_{\odot}$. Although the observed IR luminosities (which are really minimum luminosities) are consistent with some models for the most extreme super-AGB stars, studies of the star formation history of N300-OT's environment favor a more massive progenitor star of 12-25 $M_{\odot}$ (Gogarten et al. 2009).

Thus, it is difficult to reliably classify SN 2008S and N300-OT as a wholely new and separate type of transient

[8] PAH emission features are seen in proto-planetary nebulae and H II regions mainly because there is sufficient near-UV radiation to excite them, not because the gas is highly carbon-enriched.

(note that they reside in the most common location for SN impostors in Figure 13). Until we actually identify the underlying physical mechanism of the outbursts (see §4.6), this difference is rather semantic, depending on whether one prefers to see them as an extension of eruptive phenomena in more massive stars or a different class of eruptions occurring in stars below 20 $M_{\odot}$. (In either case, they are extremey interesting, and may be more common than SN impostors from more massive progenitors simply because of the slope of the initial mass function.) For these reasons, we have included SN 2008S and N300-OT among the other SN impostors, but perhaps the debate will continue for decades until the stars recover from the outbursts and reveal themselves or until they finally explode as core collapse SNe.

Nevertheless, it appears that some recent transients are pushing the bottom end of the envelope that encompasses LBVs, the strongest evidence of which is their relatively low-luminosity progenitors and stellar environments. The physical mechanism of all these outbursts remains elusive. The following transients share some overlap with LBVs, but do bear some perceived differences well. We note them in a separate section here because previous authors interpreted them as something other than LBVs.

V838 Mon: The best studied of this group of unusual transients is V838 Mon, which erupted at a distance of ∼6 kpc in our Galaxy in 2002, and has since produced a spectacular light echo in its circumstellar reflection nebula (Sparks et al. 2008; Bond et al. 2003). The transient had a peak absolute V magnitude of −9.8, and studies of its associated cluster of B-type stars implies an age of $\lesssim$25 Myr and an initial mass of $\gtrsim$8 $M_{\odot}$ if the transient is an evolved star (Afsar & Bond 2007). The complex, multi-peaked BVI light curve from Sparks et al. (2008) is shown in Figure 15. From this, we determine values of $t_{1.5}$ of roughly 12 and 75 days for the main and secondary peaks.

Figure 16 shows a visual spectrum of V838 Mon from our spectral database, obtained with Kast/Lick on 2002 Feb. 11, about 5 days after the main B and V-band peak in the light curve. This spectrum is representative of the early bright stages of the transient, whereas the spectrum evolved significantly at late times, becoming much redder and displaying deep molecular absorption features (e.g., Bond et al. 2003). We find it quite remarkable that the spectrum of V838 Mon near maximum light is nearly a carbon-copy of the visual-wavelength spectrum of U2773-OT, which had a more luminous LBV progenitor star and a more luminous and longer-lasting eruption than V838 Mon. The only substantive difference between the spectra of V838 Mon and U2773-OT is that the narrow absorption lines in U2773-OT are somewhat stronger than in V838 Mon.

M85-OT: We discovered M85-OT during the normal course of the LOSS in January 2006. Kulkarni et al. (2007) presented the first detailed study of this object, and drew attention to its faint progenitor star and the transient's apparent differences compared to novae, SNe, and LBVs. Alternatively, Pastorello et al. (2007a) argued that it could be a very faint core-collapse SN. The absolute R-band light curve of M85-OT from Kulkarni et al. (2007) is shown in Figure 15. Kulkarni et al. suggested that the peak luminosity and decay rate of this transient occupied a "gap" between novae and SNe in luminosity, but faster than LBVs. As we have seen in this paper, however, LBV eruptions occupy a larger range of characteristic fading times than previously recognized, from a day to a decade, and the light curve of M85-OT with a peak absolute magnitude of almost −13 and a decay time of 80–100 days fits well within the paramter space occupied by known LBV giant eruptions (Figure 13). M85-OT also appeared somewhat redder than LBVs, suggesting a temperature of roughly 5000 K (Kulkarni et al. 2007), but this depends on the assumed extinction and reddening. Note that these authors estimated an upper limit to the extinction based on the observed Balmer decrement, assuming that it should follow the standard Case B low-density recombination value. However, Balmer line ratios in dense winds and ejecta do not always follow standard recombination values, so the reddening could be higher. Indeed, Prieto et al. (2008b) later showed that M85-OT had a large IR excess, suggesting a very dense dusty CSM. This means that the apparent temperature of M85-OT may have been warmer than 5000 K, and that its peak magnitude was probably more luminous. It also means that the progenitor could have been substantially more luminous than Kulkarni et al.'s upper limit to the absolute g magnitude of the progenitor star of > -4.1 mag. While this would still be fainter than the most luminous LBVs, it approaches the values inferred for N300-OT and SN 2008S.

In Figure 16, we show the Keck/LRIS spectrum of M85-OT from Kulkarni et al. (2007). We show it corrected for the value of $E(B-V)$=0.14 mag adopted by those authors (black spectrum), as well as a higher reddening correction of $E(B-V)$=0.7 mag (gray spectrum). With this higher reddening, the continuum can be approximated by a temperature around 6500 K, except for wavelegnths below 4500 Å where line blanketing may be important (this is also the case for fits involving cooler temperatures and lower reddening correction). The point of this comparison is that a larger value for the extinction and reddening is plausible, which could mean that the transient and its progenitor were more luminous (for a reddening of 0.7 mag, as shown here, the peak absolute visual magnitude would have been around −14.5, for example). The spectrum of M85-OT closely resembles that of N300-OT, also shown in Figure 16 for comparison. Both transients have weak emission from the Ca II IR triplet, weak narrow Hα, and fairly strong Ca II HK absorption, implying that at the times when the spectra were taken, the emitting photospheres probably had similar temperatures. In that case, the higher reddening correction we have shown here would also bring the continuum shapes into better agreement.

After considering the distribution of properties of LBV eruptions described in this paper, as well as a comparison between the spectrum of M85-OT and N300-OT, it is much less clear based on the properties of the outburst alone that M85-OT is something altogether different from other SN impostors, especially if it is shifted upward by 0.5–1 mag in Figure 13 due to a higher reddening value. The strongest case for a different type of souce comes from its local environment that implies an initial mass around 7 $M_{\odot}$ or less (Ofek et al. 2008), which is similar to V838 Mon and lower than SN 2008S and N300-OT.

SN 2010U: Nakano (2010) discovered SN 2010U in NGC 4212, with an unfiltered magnitude of 16.0 on 2010 Feb. 5.6 UT. The peak unfiltered magnitude was 15.9, and the progenitor was undetected at a limit of 18.0 mag. At

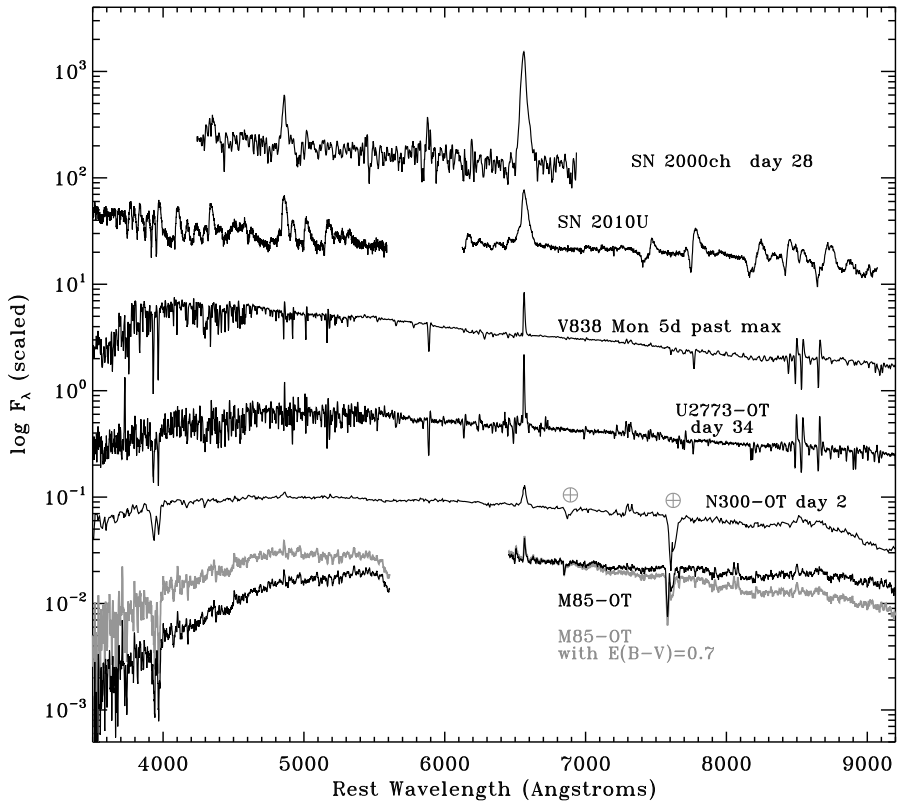

Figure 16. Spectra from our database of a few of the intermediate-luminosity transients discussed in §4.5, compared to SN impostors shown earlier in Figure 12. The spectrum of SN 2010U was taken on 2010 Feb. 7 with Keck/LRIS, and corresponds to day 2 after discovery. We obtained the spectrum of V838 Mon with Lick/KAST on 2002 Feb. 11, about 5 days after the brightest peak in the B and V light curves (see Figure 15). The observed flux has been corrected for $E(B-V)$=0.87 mag, following Munari et al. (2005). The spectrum of M85-OT is the Keck/LRIS pectrum from Kulkarni et al. (2007); here we show it corrected for $E(B-V) = 0.14$ mag (black), as in that paper, as well as what it would look like corrected for a larger value of $E(B-V)$=0.7 mag (gray) for comparison. The comparison spectra of SN 2000ch, UGC 2773-OT, and N300-OT are the same as in Figure 12.

a distance of 3.3 Mpc for NGC 4212, the corresponding peak absolute magnitude is roughly −11.7 mag (not corrected for reddening). A spectrum obtained 2 days later by Mario, Vinko, & Wheeler (2010) showed a blue continuum with strong narrow Balmer emission lines with P Cyg absorption features indicating outflow speeds of order 900 km s^{-1}, similar to many SN impostors. Humphreys et al. (2010) recently suggested that this source is not an LBV eruption, but is instead a luminous nova. The light curve is shown in Figure 15 for comparison. It does fade faster than some LBVs like HD 5980 and V12 (shown here), but the rapid fading is comparable to or even slower than brief events in SN 2009ip (Smith et al. 2010a) and SN 2000ch (Wagner et al. 2004; Pastorello et al. 2010). Its peak luminosity is closer to SN impostors than to novae (Figure 13).

We obtained one spectrum of SN 2010U on 2010 Feb. 7 using Keck/LRIS, and the resulting spectrum is shown in Figure 16. This date corresponds to 2 days after discovery and about 1 day after maximum light (i.e., well before the transient faded significantly). Among our sample of SN impostors, SN 2010U most closely resembles the spectrum of SN 2000ch (also shown in Figure 16). It is interesting, then, that the fast decay and peak absolute magnitude of SN 2010U are also very similar to those of SN 2000ch, which is a confirmed LBV showing additional multiple eruptions many years later (Pastorello et al. 2010). It would be very interesting to continue observing SN 2010U, to see if it follows suit. Based on the similarity in both light curves and spectra between SN 2010U and SN 2000ch, the claim that SN 2010U is a luminous nova and not an LBV-like eruption becomes less secure; the observed properties of the transient seem more consistent with LBVs than with novae. As noted by Humphreys et al. (2010), however, the upper limits for the progenitor star and its surrounding population seem to argue that it had an initial mass $\lesssim 5\ M_\odot$ in this case. This provides another case where eruptions that closely resemble LBVs seem to occur in lower-mass stars as well.

M31 RV1: Rich et al. (1989) discovered a luminous red variable star in M31, which rose to a bolometric absolute magnitude of −9.8 in September 1988. In the I-band it then faded about 3 mag in 43 days, and had been 5 mag fainter in pre-discovery images. It did not fade nearly as much in the K band after discovery, suggesting that the bolometric luminosity did not necessarily change much, and that either dust obscuration increased or the object cooled after the outburst. The nature of this transient is unclear, but it showed the absorption-line spectrum of an M0 supergiant plus narrow Balmer line emission. IR data are not available before discovery, so one cannot exclude the possibility that the progenitor was heavily obscured. Kulkarni et al. (2007)

compared it to M85-OT, although that source was more luminous and faded more slowly, and M85-OT showed the Ca II IR triplet and other features in emission and did not exhibit the TiO and other absorption bands characteristic of a cool M supergiant. In terms of its absolute magnitude and strong evolution to the red as it faded, M31 RV1 was more like V838 Mon than M85-OT, although it is not known to have had a complex multi-peaked light curve like V838 Mon. Recently, Shara et al. (2010) examined archival *HST* images obtained 10 years after the transient event and suggested that a detected source is consistent with an old nova rather than a merger event, but continued study of the remnant object is needed.

PTF10fqs: This is an apparently red-colored transient located in outer parts of a spiral arm of M99, with peak absolute visual magnitude of about −11, expansion speeds of around 800 km s^{-1}, and a spectrum very similar to V838 Mon as well as SN impostors SN 2008S and N300-OT (Kasliwal et al. 2010). Overall, the outburst of PTF10fqs appeared extremely similar to other SN impostors on the faint end of the distribution. As with M85-OT, visual upper limits to its progenitor would imply a star less massive than about 8 $M_{\odot}$ if there were no local extinction. However, based on the red color of the transient and the presence of [Ca II] emission in its spectrum, the progenitor may have been heavily obscured like SN 2008S and N300-OT, but unfortunately, upper limits in the mid-IR are well *above* the IR luminosities for the progenitors of SN 2008S and N300-OT, so a more massive star cannot be ruled out for PTF10fqs.

The initial masses for these objects are uncertain, but at least one can be confident that they are not among the most luminous stars known. Stellar ages for the local environments of both V838 Mon and M85-OT are consistent with initial masses curiously close to the dividing line between core-collapse SNe and massive white dwarfs at around 8 $M_{\odot}$. For PTF10fqs a more massive star cannot be ruled out because of uncertainty in the pre-outburst extinction, but it may be in this range as well. The progenitor of SN 2010U was proposed to be somewhat lower at about 5 $M_{\odot}$. One obvious possible suggestion for these transients is that they may arise from electron-capture SNe, expected to occur at initial masses around 8–10 $M_{\odot}$. This possibility was suggested for SN 2008S and N300-OT as well (Thompson et al. 2009; Botticella et al. 2009); mounting evidence argues against this interpretation for these particular sources, but it remains a possibility for the other objects.

Other potential explanations include a wide variety of failed core-collapse SNe (e.g., Fryer et al. 2009; Moriya et al. 2010), the explosive birth of a massive white dwarf initiating the planetary nebula (PN) phase (Thompson et al. 2009), or stellar mergers and other tidal encounters (see below). The possibility that the PN phase might be initiated by a sudden explosive or eruptive event is extremely interesting from the point of view of understanding the late evolution of intermediate-mass stars and the dynamics of PNe, but well beyond the scope of our present paper and in need of further theoretical investigation. If true, there is potentially a great deal of synergy between studies of the transient sources and the associated nebulae in the mass ranges above and below 8 $M_{\odot}$. Stellar mergers and tidal encounters represent another attrative explanation for these transients and other SN impostors, since there is no clear obstacle to binary encounters above or below ∼8 $M_{\odot}$.

In summary, we find that based on criteria such as absolute magnitude, rate of fading, light curve shape, or even color and spectra, it is difficult to reliably distinguish LBV eruptions from non-LBVs (if indeed the objects discussed in this section are a distinct set of events). The only reliable way to establish a difference is based on having good information (and indeed, when one considers the possibility that they may be obscured at visual wavelengths by CSM dust, we must also include deep IR data) about their faint progenitor stars or their progenitor environment. Such information is rarely available except for nearby objects. Without such detailed information, claims of new types of transients may be unsubstantiated or highly speculative. This is a sobering fact to keep in mind as we embark on an era of more intensive transient studies.

Caveat: An interesting twist involves binary evolution, which should not be overlooked. We have emphasized that estimates of a progenitor star's initial mass based on studies of the surrounding stars (e.g., Gogarten et al. 2010) provide some of our most important contraints on the nature of the progenitor stars. One potential pitfall, however, is the following: A star with an initial mass below 8 $M_{\odot}$ may accrete a substantial amount of mass from its companion, raising it to more than 12 $M_{\odot}$, and changing its evolutionary fate and perhaps leading to the types of eruptions encountered in initially more massive stars. Similarly, a secondary star with initial mass of, say, 12–15 $M_{\odot}$ may gain enough mass to raise its luminosity and make it behave like a 20–25 $M_{\odot}$ star, and so on. The point is that even in cases where we have good constraints on the surrounding stellar population, the progenitor star may actually have been more massive than we are led to believe. This complexity is somewhat unsettling.

4.6 What is the underlying mechanism?

After more than a half-century of research since the Hubble-Sandage variables were identified (Hubble & Sandage 1953), the underlying cause and trigger of LBV giant eruptions remains unexplained. This makes it very difficult to say whether a given observed non-SN transient event is or is not an LBV, and this is exacerbated by the huge diversity in observed LBV properties demonstrated in this paper. Some LBVs are highly obscured by their own ejected dust shells (some are even *completely* obscured for decades) while others show no sign of dust whatsoever; some LBV giant eruptions involve $\gtrsim 10^{50}$ erg explosions and 10–20 $M_{\odot}$ of ejected mass, while others have only 10^{47} ergs and 0.01 $M_{\odot}$; and so on. As described in the previous section, there is considerable overlap with transients that are purported to be non-LBVs.

As with the case of distinguishing between SNe Ia and all other types of SNe, some clue of the physical mechanism is needed before we can reliably differentiate LBV giant eruptions from other transient events arising in moderately massive and intermediate-mass stars. Unfortunately, we do not yet have a clear working hypothesis for the physical mechanism behind LBV eruptions, so one hopes that observational clues can help narrow the field. Among the most important observational clues are the ejection speed of material launched from the star, as well as the total mass

and energy budget. As discussed in §4.3, the outflow velocities observed in most sources are a few 10^2 up to a little more than 10^3 km s^{-1}, and these are suggestive of either strong supergiant winds or CSM interaction, whereas some sources (e.g., η Car and SN 2009ip) show evidence for a small mass of much faster material moving at $\sim$5000 km s^{-1} (Smith 2008; Smith et al. 2010a; Foley et al. 2010), probably requiring the presence of a leading blast wave as well. Whether or not impulsive or explosive acceleration of the envelopes is at work in all SN impostors is uncertain, but shock waves clearly are at work in a few of them, and so any successful theory must incorporate this. The total mass and energy budgets are harder to evaluate. Nearby examples with resolved nebulae from past outbursts allow us to measure the mass of ejecta directly, and here we see a huge range from 0.01 to more than 10 $M_\odot$ ejected in a single event. Unfortunately, the mass ejected in distant SN impostors is poorly constrained.

We can, however, estimate the total escaping radiated energy budget for each, which is given roughly by $E_{\rm rad} = \zeta t_{1.5} L_{\rm peak}$, where ζ is factor of order unity that depends on the exact shape of the light curve. $L_{\rm peak}$ is the luminosity corresponding to the inferred peak absolute bolometric magnitude corrected for extinction. From Table 8, then, one can deduce a huge range in values of $E_{\rm rad}$ from $\sim 2\times10^{49}$ ergs (η Car), down to $\lesssim 10^{46}$ ergs. *Caveat:* we must remember a lesson from nearby examples such as η Car, however, where the kinetic energy budget of more than 10^{50} erg greatly outweighs the escaping radiative energy budget of $\sim 10^{49}$ ergs.

An interesting timescale to consider is the "buildup" or "recovery" timescale for the radiated energy budget, which is the time the star would require to supply $E_{\rm rad}$ in its quiescent state, given by

$$t_{\rm rad} = E_{\rm rad}/L_* = t_{1.5}\frac{\zeta L_{\rm peak}}{L_*}$$

where L_* is the quiescent pre-outburst bolometric luminosity of the progenitor star. This is relevant in a type of model where the output core luminosity of the star is constant over a long timescale compared to the event, and where the extra radiated energy is presumed to be the result of thermal energy being stored in the star's enveloped and then released suddenly by some mechanism. It is also relevant for the time it takes the star to re-establish thermal and radiative equilibrium after a disruptive event. Here too we see a wide range of values, with $t_{\rm rad} \approx 40$ years for η Car, $\sim$1.1 yr for SN 2009ip, and 32 yr for SN 2008S. If one can establish that $t_{\rm rad}$ is considerably longer than any observed timescale of variability in the progenitor, then it is likely that an additional energy reservoir is required (the need for extra energy obviously increases if one makes an allowance for kinetic energy as mentioned above). It also seems likely that $t_{\rm rad}$ may be related to the amount of mass ejected from the star or the amount of envelope mass involved in the adjustment of the star, although this is based only on the vague notion that the Kelvin-Hemholz timescale for the ejected mass plays a critical role. These considerations, while not conclusive, may be kept in mind when thinking about various models mentioned below.

Investigating and evaluating theoretical possibilities is far beyond the scope of this paper, but here we list some hypothetical mechanisms, as well as their pros and cons from the perspective of explaining the observed phenomena associated with SN impostors.

Continuum-driven super-Eddington winds? In addition to η Carinae, all of the luminous SN impostors clearly exceed the classical (i.e., electron-scattering) Eddington limit during the brightest phases of their outbursts. In the case of η Car, the star apparently exceeded the classical Eddington limit by a factor of Γ=5 for more than a decade. Other SN impostors that appear to have lower progenitor masses but similar peak luminosities can achieve much more extreme values of Γ=40 to 80. Regardless of the origin of this super-Eddington (SE) luminosity, it is unavoidable that such sustained high luminosities will in fact drive a strong wind from the star (unless of course the emerging radiation is from an already-successful hydrodynamic explosion). A few examples that have been studied in detail (e.g., V1 in NGC 2366; U2773-OT) are clearly consistent with wind-like spectra rather than explosions, so models of SE winds are certainly applicable to at least *some* of the SN impostors. Much of the work on the properties of SE so far has been conducted by Owocki and collaborators (Owocki et al. 2004; van Marle et al. 2008, 2009; Shaviv 2000). These studies on continuum-driven SE winds assume a strong increase in luminosity as a precondition for the models, concentrating primarily on the physics of driving mass from the surface of the star in quasi-steady-state. These models do not, however, address the deeper question of what triggers the required increase in bolometric luminosity, or what the ultimate energy source is.

Runaway Pulsations? Following early work on the pulsational instability of massive stars (Ledoux 1941; Schwarzschild & Härm 1959; Appenzeller 1970), there is an expectation that the outer envelopes of massive stars should be quite unstable. Can runaway pulsational instability give rise to sudden mass ejections and luminous transients like SN impostors? Stothers & Chin (1993) proposed that an ionization-induced dynamical instability in their models of very massive stars could lead to violent outbursts such as that experienced by η Carinae, but Glatzel & Kiriakidis (1998) criticized this model because the adiabatic approximation is not valid for the envelopes of these stars, and their non-adiabatic models could not reproduce the instability except at very low temperatures. Non-linear growth of non-adiabatic *strange mode* pulsations, however, may occur in the envelopes of luminous stars where the thermal timescale is short and comparable to the dynamical timescale (e.g., Glatzel et al. 1999; Glatzel & Kiriakidis 1993; Kiriakidis et al. 1993; Gautschy & Saio 1995, 1996). Non-linear growth of strange-mode pulsations is expected in very luminous stars, but may also occur in less massive stars such as AGB stars (Gautschy & Saio 1995, 1996); thus, the full range of initial mass over which these pulsations are effective at triggering instability is uncertain, but potentially interesting for SN impostors and related transients. Strange-mode instabilties depend on the iron opacity bump and occur primarily in the outer envelope of standard stellar evolution models (containing less than 1% of the stellar mass); they therefore lead only to relatively minor increases in luminosity (a few tenths of a magnitude) and perhaps somewhat enhanced wind mass loss. It has therefore been challenging to explain the major outbursts characteristic of SN impostors with the strange-mode instability. (Stange mode pulsations may help trigger

the normal S Doradus variations of LBVs, however, and can potentially account for their observed microvariations.) Further work is needed to determine if similar instabilities might occur deeper in the star, if they are to explain the ejection of several $M_{\odot}$ and 10^{49}–10^{50} ergs, as in a major outburst like η Carinae. For example, Young (2005) has described alternative stellar evolution models that include the effects of wave-driven mixing and rotation in the core evolution, and find that these stars are more extended, and that they therefore have the iron opacity bump deeper in the star. With the critical opacity bump in deeper layers, more mass and thermal energy are above the potentially unstable region, and Young (2005) hypothesizes that this stellar structure might give rise to more energetic and massive eruptions like SN impostors.

Runaway mass loss and the Geyser model? Much of the observed phenomenology of LBV eruptions is reminiscent of geophysical geysers or volcanoes (see Humphreys & Davidson 1994). As described above, LBVs sometimes are seen to exhibit growing instability leading up to a large eruption. The occurance of multiple shells in some cases suggests that eruptions may be followed by a more quiescent recovery time before the instability builds again. This has led to the suggestion of a geyser-like model for LBV giant eruptions (Maeder 1992), where very luminous stars reach cool temperatures in their post-main-sequence evolution, allowing a recombination front (akin to a boiling front in a geyser) to proceed into the star, thereby initiating a rise in mass loss because of the change in opacity. This increased mass loss continues until the star contracts to warmer temperatures, when the cycle begins again. The simplicity of such a thermal engine is appealing, although more detailed calculations are needed to study the hydrodynamic response of a star in these conditions. It seems unlikely that this mechanism can explain the extreme amounts of mass ejected in brief energetic events, the sharp increases in bolometric luminosity, or the explosive property of some eruptions. Another potential drawback of this mechanism is that it will only occur in very luminous stars near the classical Eddington limit, and so cannot explain the full diversity of SN impostor eruptions, some of which apparently occur at relatively modest initial masses below 20 $M_{\odot}$. It is nevertheless an interesting possibility for eruptions in the most luminous stars.

Pulsational pair-instability ejections? Heger & Woosley (2002) have described a type of severe mass-loss event known as pulsational pair-instability (PPI) ejections, when a very massive star can eject of order 10 $M_{\odot}$ in an explosive but non-terminal event. This is the same pair-formation instability that leads to a pair-instability SN (PISN; Barkat et al. 1967; Rakavy & Shaviv 1967; Bond et al. 1984; Heger & Woosley 2002), but it occurs in a mass range below that of successful PISNe, where the explosive burning is not enough to completely unbind the star, resulting in a $\sim 10^{50}$ erg ejection of the outer envelope only. Woosley et al. (2007) and Smith et al. (2007, 2010b) have mentioned the PPI as an attractive explanation for the precursor LBV-like mass ejections that precede some very luminous SNe IIn like SN 2006gy. Smith et al. (2010b) has emphasized that expectations for PPI ejections match properties of some giant LBV eruptions in every *observable* way (large mass ejected, H-rich envelopes, total energy of $\sim 10^{50}$ erg, etc.), but also noted several problems with attributing PPI events as a general explanation for all LBV giant eruptions. First, the PPI occurs during final burning phases and is expected to transpire in the few years to decades immediately before core collapse. However, many LBVs have massive shells with dynamical ages of 10^3 – 10^4 yr, indicating that they have survived for millenia after the giant eruption that ejected their shells.[9] Second, the PPI is only predicted to occur for the most massive stars with initial masses above $\sim$95 $M_{\odot}$, and usually only at low metallicity,[10] whereas LBVs are know to arise from stars with initial masses as low as 20–25 $M_{\odot}$ (Smith et al. 2004). Recent observations of low-luminosity progenitors may extend this mass range even lower, to within 10–20 $M_{\odot}$, as described above. These lower-mass LBVs will never encounter the PPI, so the PPI can only provide a possible explanation for the most extreme LBV giant eruptions in the most luminous stars like η Car, not the full range of the observed LBV-like eruption phenomenon.

Other shell-burning explosions? What about other types of explosive burning events, analogous to the PPI, but not necessarily restricted to the late-phase O or Si burning? This may relax the requirements for the very high core temperatures needed for the PPI, and hence, may relax the restrictions on initial masses that experience explosive buring instabilities. This is an old idea, first suggested (somewhat ironically) as a possibility for SN 1961V by Branch & Greenstein (1971), and revisited several times since then (Guzik et al. 1999, 2005; Smith et al. 2003a; Smith 2008; Smith & Owocki 2006; Dessart et al. 2009). Substantive models for such an event do not yet exist, but should be pursued. Hypothetically, one can imagine that the energy source could be nuclear fusion of a small amount of material, if oscillations (i.e. non-radial g-modes, unsteady convection, external perturbations, etc.) in the lower envelope mix fresh H-rich fuel into deeper and hotter layers of the star, triggering explosive burning. Initial simulations suggest that boundary layers within the star may be susceptible to dynamic disturbances (Meakin & Arnett 2007; Guzik et al. 1999, 2005). Even a few percent of a solar mass of burnt H, for example, or a few tenths of a solar mass in silicon burning, would be sufficient to provide the extra energy inferred for giant LBV eruptions. Different amounts of energy deposited at different depths within the star could conceivably account for the wide diversity in observed properties of SN impostors, over a wide range of masses, as suggested by some recent exploratory models (Dessart et al. 2009). A relatively large amount of deposited energy compared to the binding energy would initiate a large hydrodynamic explosion, whereas a smaller amount of deposited energy may just temporarily increase the luminosity of the star above the Eddington limit, at which point the physics of continuum-driven SE winds becomes relevant, as discussed above. Observations show evidence for both phenomena. Further progress in this direction requires substantial effort in multidimensional and hydrodynamic simulations of stellar interiors, plus estimates

[9] Heger & Woosley (2002) did note a rare case where the PPI eruption can delay the resumption of nuclear burning, leading to intervals of as much as 10^3 yr between bursts, but this is not generally the case.

[10] This exact mass range, however, depends on mass-loss rates assumed in stellar evolution models throughout the lifetime of the star.

of the resulting observables. The observed radiation from SN impostor events coupled with the detailed kinematics of nearby circumstellar shells can provide important constraints on such models. Dessart et al. (2009) have argued that this type of energy deposition may be particularly likely in stars with initial masses of 8–12 $M_{\odot}$, with obvious possible implications for SN 2008S, N300-OT, and some of the sources discussed in the preceding section.

Failed SNe? Models that fail to generate successful core-collapse SNe may nevertheless produce partial explosions, and therefore, observable transient sources, as discussed recently by Fryer et al. (2009; see also Moriya et al. 2010). With a wide range of possible absolute magnitues around −14, these certainly may be applicable to some of the observed SN impostors, especially in cases with dense CSM discussed by Fryer et al. (2009). Such mechanisms are unlikely to explain the full diversity of SN impostors, however, since several examples exist of LBVs that have survived giant eruptions as relatively stable hot supergiant stars, and there is considerable evidence that these eruptions can repeat *multiple times* on a variety of timescales up to millenia. Nevertheless, such failed SNe remain viable explanations for distant SN impostors unless deep follow-up observations are available to establish the post-eruption state of the (surviving?) star.

Electron-capture SNe? This idea has been discussed above. It does not offer an attractive explanation for the diversity observed in most SN impostors, because this type of event is only expected for a narrow range of initial masses around 8 $M_{\odot}$. It does, however, provide a potential explanation for either faint SNe II-P (not discussed here) or some of the relatively faint transients discussed in §4.5.

Close binary interaction events? Through the course of post-main sequence evolution of a massive star, its luminosity goes up as the core contracts, its total mass goes down due to mass loss, and so its proximity to the Eddington limit becomes more precarious. This is presumed to lead — somehow – to the instability we see as LBVs, by making the star more susceptible to internal *or external* disturbances. But in addition, as a massive star evolves off the main sequence, it migrates to cooler temperatures, and so its radius increases by a huge factor. An increasing radius leads to inevitable dangerous encounters in binary systems with periods less than several years. Smith (2011) notes that in the case of η Car (5.5 yr orbital period), even with the *quiescent* pre-outburst luminosity of η Car and a likely temperature around 8000 K, that the companion star would plunge well inside the apparent photosphere of the primary during periaston passages. A violent periastron encounter is therefore inevitable, and may help explain the brief brightening episodes that occurred in 1838 and 1843; these two events are, in fact, closely associated with times of periastron (Smith & Frew 2010). Exactly how this works in unclear, and explaining the energetics is not trivial. Similarly, in the case of the eclipsing binary HD 5980, Koenigsberger and collaborators (see Koenigsberger 2004) have proposed that tidal interactions in the close binary may have triggered the eruption observed in the 1990s.[11]

Interacting binary events are attractive in the sense that the seemingly endless free parameters in binary models (mass ratios, stellar radii, orbital period, eccentricity, conservative vs. non-conservative mass transfer/mass loss, posible instability of either star, etc.) may provide a natural origin for the wide diversity observed in SN impostor outburst properties. Furthermore, close binary interactions could conceivably operate over a wide range of initial masses, even in stars that are not dangerously close to the Eddington limit on their own. Specifically, these enounters may occur for initial masses both above and below $8M_{\odot}$, regardless of differences in core evolution, providing a possible link between LBV eruptions and very similar transients from lower-mass stars (see §4.5). The detailed way in which binary encounters could account for the energetics of SN impostor events looms on the horizon as a major open question, however. A fruitful possibility for explaining SN impostors is that such a model would require two suitable conditions: 1) an evolved primary star that approaches instability anyway, and 2) a rather sudden increase in stellar radius so as to initiate a catastrophic encounter. Whether such binary interactions are the key to causing LBV eruptions or whether they simply modify the temporal behavior by triggering an instability that would have occurred anyway, is obviously a key question for future theoretical research. In the case of η Carinae, though, it seems clear that a simple mechanism such as kinetic heating of the primary star's envelope by the invading secondary is insufficient, since the gravitational binding energy of the binary orbit is substantially less than the kinetic energy of the expanding Homunculus nebula (Smith et al. 2003a). However, it must also be noted that binary interactions such as this are unlikely to explain *all* LBV eruptions; P Cygni, for example, has shown no evidence of binarity despite decades of detailed study. There must be some mechanism than can lead to eruptions of single massive stars as well.

A main emphasis of this paper has been to demonstrate the wide diversity in observed properties of SN impostors and their progenitors, but a fair question is whether the group is *too diverse*. In other words, can this group be explained by a single mechanism operating over a wide range of energy and mass, or must it be a collection of different mechanisms operating in different stars that are susceptible to perturbations? Can these different mechanisms give rise to transient sources that overlap in Figure 13 and have similar spectra? Is it *required* that multiple mechanisms work together to initiate an eruption? Since several potential mechanisms listed above seem at least plausible, there may be more than one cause of SN impostors. Inventing ways to connect observations to theory and to distinguish between these will be a major task for future work.

4.7 Summary and Future directions

While SN impostors are intrinsically fainter than SNe, and are therefore discovered less easily, their numbers are grow-

[11] Soker and collaborators (e.g., Soker 2001) have envisioned a much more complicated model for η Carinae, where the main-sequence secondary star accretes from the primary wind during close passages and blows a pair of collimated jets, as an attempt to explain the bipolar shape and kinematics of Homunculus; in their model, however, an eruption from the primary star was an assumed and necessary precondition.

ing. They will continue to be discovered in increasing frequency in upcoming surveys, and so a better framework to understand them is needed. In this paper, we have attempted to compile some of the basic observables of SN impostors and related transients known to date, including nearby historical examples and more recent events discovered in modern SN/transient searches. We also presented new spectra and light curves for a number of SN impostors.

Examining the full distribution of observed properties — including peak absolute magnitude, characteristic fading timescale, outflow velocity, spectral morphology, and progenitor properties — the most striking result is that SN impostors are extremely diverse, filling essentially all the available parameter space between SNe and novae. We find no clear correlations between spectral morphology, luminosity, or fading timescale, as exhibited by other transients like SNe and novae. Moreover, the diversity exhibited by well-studied cases where the progenitor is known to be an LBV fully encompases the range of parameter space occupied by transients that are supposedly not LBVs. In some cases, therefore, previous claims of new types of transients based on observed properties of the eruption appear to have been too strong. On the other hand, the mechanism behind these eruptions is still unknown, and so multiple different types of outburst phenomena may overlap in parameter space, so we are not arguing that all these sources are necessarily LBV giant eruptions. Indeed, LBVs may be a subset of a larger group of nonterminal eruptive phenomena. A great deal of theoretical work is needed before confident conclusions can be drawn.

Nevertheless, even though the distribution of SN impostor properties is very diverse, we did find one extreme outlier among the sample, which stood out in every measurable way: the supposedly prototypical impostor SN 1961V. We find that SN 1961V is more naturally explained as a true core-collapse SN of Type IIn, similar to SN 2005ip and SN 1988Z, but with delayed CSM interaction. We propose that the strange light curve shape of SN 1961V can be explained by a relatively normal SN II, followed by a late turn-on of CSM interaction luminosity that causes its rise to its peak luminosity after ∼100 days. That late peak luminosity was the same as SN 2005ip, and comparable late turn-on of CSM interaction has been documented in previous SNe IIn. This requires that the CSM shell had an interior cavity, and reasonable velocities would imply that the shell would have been ejected within a few years before core collapse. Indeed, the progenitor of SN 1961V was observed at an absolute magnitude of roughly −14 about a year before its main brightening, and we suspect that this was the *direct* detection of a precursor LBV-like outburst. This erradicates the notion that the progenitor of SN 1961V must have been an astoundingly massive star, and instead, suggests that it had an initial mass and luminosity comparable to η Carinae.

There is considerable room for improvement in our understanding of LBV eruptions and SN impostors. The most glaring deficiency is in our theoretical understanding. A theory for these eruptions should strive to identify a physical mechanism that can account for a range of ejected mass (0.01–10 $M_{\odot}$) and kinetic energy (10^{46} – 10^{50} ergs), total radiated energy (10^{46}–$10^{49.3}$ ergs), peak luminosity (−10 to −15 mag), outflow speeds (100–1000 km s^{-1}), and different spectral properties through all luminosities (relatively cool and hot, varying emission line strengths, etc.). This is admittedly a tall order. Although more realistic models for the structure of post-main-sequence massive stars are needed to assess the susceptibility and outcomes of various instabilities, it is also likely that simple toy models can be useful to investigate the hydrodynamics of envelope ejection and the star's dynamical and thermal response. Detailed radiative transfer calculations for these ejections are needed in order to connect observable spectra and luminosities to derived properties (see, e.g., Dessart et al. 2009). Finally, dynamical models of close binary interactions and the transients they might produce are sorely needed.

On the observational front, our understanding of SN impostor statistics will improve in the near future, since these kinds of transients will be a major emphasis of upcoming photometric surveys. In this paper we have only examined about 2-dozen SN impostors and a few additional cases whose nature is debated. While this has been sufficient to demonstrate the diversity in observed properties, it is not sufficient to examine their intrinsic statistical distribution. A prohibitive weakness is that this sample is not drawn from a uniform survey with understood systematics, so we have been careful not to draw conclusions about how common SN impostors with various peak luminosities are, for example, or how common they are compared to core-collapse SNe. Understanding the intrinsic rates of SN impostors is key, as has been done for SNe (e.g., Li et al. 2010), but it has been difficult to address for SN impostor statistics because they are so faint. The Large Synoptic Survey Telescope (LSST) will provide a critical advance in this area, allowing estimates of control times and completeness of a large sample.

It may seem discouraging that the diversity of SN impostors is so large, because it follows that there is limited utility from spotty observations of a transient's spectrum or a monochromatic light curve of only the time around peak luminosity. Follow-up spectroscopy and photometry are extremely useful, however, when combined with good coverage at late times or with cases where detections of a progenitor star are available. In particular, followup observations that may (eventually) detect a second outburst or multiple eruptions can be extremely useful for understanding the phenomenon, although this may take several years of monitoring. We should keep a watchful eye on all nearby and historical examples, in case they erupt again or explode as real SNe. Late-time data and upper limits can potentially help us understand the recovery of a star after a disruptive event, which is a problem that has received little attention so far.

Lastly, these transient sources are associated with substantial mass ejection. The resulting circumstellar shells are potentially observable for a much longer time than the outburst itself. Thus, continued detailed study of nearby examples of resolved circumstellar shells around all types of stars is needed, as it offers our only way (in the absence of good models for the outbursts) to evaluate the amount of ejected mass. Comparing the statistics of circumstellar shells to the properties of SN impostors and other transients may prove enlightening when a statistical sample is available. If nearby examples are any guide, then the mass ejection of SN impostors is probably not spherical. It is therefore likely that considerations associated with asymmetry (spectrapolarimetry, detailed line profiles, rotation, asymmetric explosions and

winds, binary encounters) will figure more prominently in upcoming studies.

ACKNOWLEDGMENTS

We thank A.J. Barth, S.B. Cenko, R. Chornock, A.L. Coil, R.J. Foley, C.V. Griffith, M.T. Kandrashoff, I.K.W. Kleiser, M. Modjaz, J. Bloom, A. Miller, D. Perley, and D. Poznanski for their assistance with some of the observations and data reduction. We thank S. Kulkarni and E. Ofek for providing us with their spectrum of M85-OT. A.V.F.'s group is supported by NSF grants AST-0607485 and AST-0908886, the TABASGO Foundation, US Department of Energy SciDAC grant DE-FC02-06ER41453, and US Department of Energy grant DE-FG02-08ER41653. KAIT and its ongoing operation were made possible by donations from Sun Microsystems, Inc., the Hewlett-Packard Company, AutoScope Corporation, Lick Observatory, the NSF, the University of California, the Sylvia & Jim Katzman Foundation, and the TABASGO Foundation.

REFERENCES

Appenzeller, I. 1986, IAU Symp. 116, 139
Appenzeller, I. 1970, A&A, 5, 355
Ayani, K., & Kawabata, T. 2002, IAUC, 7864, 1
Barbá, R., & Niemala, V.S. 1994, IAUC, 6099, 1
Barbá, R., Niemala, V.S., Baume, G., & Vázquez, R.A. 1995, ApJ, 446, L23
Barkat, Z., Rakavy, G., & Sack, N. 1967, Phys. Rev. Lett., 18, 379
Bateson, F.M., Gilmore, A., & Jones, A.F. 1994, IAUC, 6201, 1
Beckman, S., & Li, W. 2001, IAUC, 7596, 1
Berger, E. 2010, ATel, 2655, 1
Berger, E., et al. 2009a, ApJ, 699, 1850
Bertola, F. 1963, Asiago. Contr., 142, 29
Bertola, F. 1965, Asiago. Contr., 171, 29
Bertola, F., & Arp, H. 1970, PASP, 82, 894
Blondin, S., Modjaz, M., Kirshner, R., & Challis, P. 2006, CBET, 494, 1
Bond, H., Arnett, W.D., & Carr, B.J. 1984, ApJ, 280, 825
Bond, H., et al. 2003, Nature, 422, 405
Bond, H., et al. 2009, ApJ, 695, L154
Bond, H. 2010, ATel, 2640, 1
Botticella, M. T., et al. 2009, MNRAS, 398, 1041
Branch, D., & Greenstein, J.L. 1971, ApJ, 167, 89
Chu, Y. H., et al. 2004, AJ, 127, 2850
Chugai, N.N. 2001, MNRAS, 326, 1448
Davidson, K. 1987, ApJ, 3‘7, 760
Davidson, K., et al. 2005, AJ, 129, 900
Della Valle, M., & Livio, M. 1995, ApJ, 452, 704
Dessart, L., et al. 2009, MNRAS, 394, 291
Drake, A., Prieto, J.L., Djorgovski, S.G., Mahabal, A.A., Graham, M.J., Williams, R., McNaught, R.H., Catelan, M., Christensen, E., Beshore, E.C., Larson, S.M., & Howerton, S. 2010, ATel, 2897, 1
Drissen, L., Roy, J. R., & Robert, C. 1997, ApJ, 474, L35
Drissen, L., Crowther, P. A., Smith, L. J., Robert, C., Roy, J. R., & Hillier, D. J. 2001, ApJ, 546, 484
Duszanowicz, G. 2007, CBET, 1182, 1
Elias-Rosa, N., Benetti, S., Cappellaro, E., Dolci, M., & Pastorello, A. 2005, IAUC, 8498, 1
Faber, S. M., et al. 2003, Proc. SPIE, 4841, 1657
Filippenko, A.V. 1982, PASP, 94, 715
Filippenko, A.V. 1997, ARAA, 35, 309
Filippenko, A.V., Li, W., & Modjaz, M. 1999, IAUC, 7152, 1
Filippenko, A.V. 2003, in From Twilight to Highlight: The Physics of Supernovae, ed. W. Hillebrandt & B. Leibundgut (Berlin: Springer-Verlag), 171
Filippenko, A.V., Barth, A. J., Bower, G. C., Ho, L. C., Stringfellow, G. S., Goodrich, R. W., & Porter, A. C. 1995, AJ, 110, 2261
Filippenko, A.V., Li, W.D., Treffers, R. R., & Modjaz, M. 2001, in Small-Telescope Astronomy on Global Scales, ed. W. P. Chen, C. Lemme, & B. Paczyński (San Francisco: ASP), 121
Foley, R. J., et al. 2003, PASP, 115, 1220
Foley, R.J., Smith, N., Ganeshalingam, M., Li, W., Chornock, R., & Filippenko, A.V. 2007, ApJ, 657, L105
Foley, R.J., et al. 2010, submitted
Fox, O., Chevalier, R.A., Dwek, E., Skrutske, M.F., Sugerman, B.E.K., & Leisenring, J.M. 2010, arXiv:1005.4682
Frew, D. J. 2004, J. of Astron. Data, 10, 6
Fryer, C.L., et al. 2009, ApJ, 707, 193
Gal-Yam, A., & Leonard, D.C. 2009, Nature, 458, 865
Ganeshalingam, M., et al. 2010, ApJS, 190, 418
Gautschy, A., & Saio, H. 1995, ARA&A, 33, 75
Gautschy, A., & Saio, H. 1996, ARA&A, 34, 551
Glatzel, W., & Kiriakidis, M. 1993, MNRAS, 263, 375
Glatzel, W., & Kiriakidis, M. 1998, MNRAS, 295, 251
Glatzel, W., Kiriakidis, M., Chernigovskij, S., & Fricke, K.J. 1999, MNRAS, 303, 116
Gogarten, S., et al. 2009, ApJ, 703, 300
Goodrich, R. W., Stringfellow, G. S., Penrod, G. D., & Filippenko, A. V. 1989, ApJ, 342, 908
Groh, J.H., Hillier, D.J., Damineli, A., Whitelock, P.A., Marang, F., & Rossi, C. 2009, ApJ, 698, 1698
Guzik, J.A., Cox, A.N., & Despain, K.M. 1999, in Eta Carinae at the Millenium, ed. J.A. Morse, R.M. Humphreys, & A. Damineli (San Francisco: ASP), 347
Guzik, J.A. 2005, in ASP Conf. Ser. 332, The Fate of the Most Massive Stars, ed. R.M. Humphreys & K.Z. Stanek (San Francisco: ASP), 204
Haratyunyan, A., et al. 2007, CBET, 1184, 1
Heger, A., & Woosley, S.E. 2002, ApJ, 567, 532
Horne, K. 1986, PASP, 98, 609
Hubble, E. & Sandage, A. 1953, ApJ, 118, 353
Humphreys, R.M., & Davidson, K. 1994, PASP, 106, 1025
Humphreys, R.M., Davidson, K., & Smith, N. 1999, PASP, 111, 1124
Humphreys, R.M., et al. 2010, arXiv:1005.4356
Immler, S., & Pooley, D. 2006, ATel, 802, 1
Immler, S., Brown, P., & Russell, B.R. 2010, ATel, 2639, 1
Innes, R.T.A. 1903, Ann. Cape Obs., 9, 75
Ishibashi, K., et al. 2003, ApJ, 125, 3222
Jones, A.F., & Sterken, C. 1997, JAD, 3, 4
Kasliwal, M.M., et al. 2010, arXiv:1005.1455
Kiriakidis, M., Fricke, K.J., & Glatzel, W. 1993, MNRAS, 264, 50
Koenigsberger, G. 2004, RevMexAA, 40, 107
Koenigsberger, G., Pena, M., Schmutz, W., & Ayala, S. 1998, ApJ, 499, 889
Koenigsberger, G., et al. 2010, AJ, 139, 2600
Kulkarni, S.R., et al. 2007, Nature, 447, 458
Lamers, H.J.G.L.M., & de Groot, M.J.H. 1992, A&A, 257, 153
Lamers, H.J.G.L.M., & Fitzpatrick, E. 1988, ApJ, 324, 279
Landolt, A. U. 1992, AJ, 104, 340
Laskar, T., Berger, E., & Chornock, R. 2010, ATel, 2648, 1
Ledoux, P. 1941, ApJ, 94, 537
Leonard, D.C., et al. 2002, PASP, 114, 35
Li, W. 1999, IAUC, 7149, 1
Li, W., et al. 2002
Li, W., Filippenko, A. V., Chornock, R., & Jha, S. 2003, ApJ, 586, L9
Li, W., et al. 2010, MNRAS, in press
Mario, Vinko, & Wheeler, J.C. 2010
Matheson, T. 2005, in ASP Conf. Ser. 332, The Fate of the Most Massive Stars, ed. R.M. Humphreys & K.Z. Stanek (San Francisco: ASP), 86
Matheson, T., Filippenko, A.V., Ho, L.C., Barth, A.J., & Leonard, D.C. 2000, AJ, 120, 1499

Matheson, T., et al. 2001, IAUC, 7597, 1
Maund, J.R., et al. 2006, MNRAS, 369, 390
Meakin, C.A., & Arnett, W.D. 2007, ApJ, 667, 448
Miller, A.A., et al. 2010, MNRAS, 404, 305
Miller, J. S., & Stone, R. P. S. 1993, Lick Obs. Tech. Rep. 66 (Santa Cruz: Lick Obs.)
Monard, L.A.G. 2010, CBET, 2289, 1
Monet D. G., et al. 2003, AJ, 125, 984
Moriya, T., et al. 2010, arXiv:1006.5336
Munari, U., et al. 2005, A&A, 434, 1107
Nakano, S. 2010, CBET, 2299, 1
Nakano, S. 2010, CBET, 2161, 1
Ofek, E.O., et al. 2008, ApJ, 674, 447
Oke, J. B., et al. 1995, PASP, 107, 375
Owocki, S.P. 2005, in The Fate of the Most Massive Stars, ed., R.M. Humphreys, & K.Z. Stanek (San Francisco: ASP), 169
Owocki, S.P., Gayley, K.G., & Shaviv, N.J. 2004, ApJ, 616, 525
Owocki, S.P., & van Marle, A.J. 2007, in Massive Stars as Cosmic Engines, eds., F. Bresolin, P.A. Crowther, & J. Puls (Cambridge: Cambridge U. Press), 71
Pastorello, A., et al. 2007a, Nature, 449, 1
Pastorello, A., et al. 2007b, Nature, 447, 829
Pastorello, A., et al. 2009, arXiv:0901.2075
Pastorello, A., et al. 2010, arXiv:1006.0540
Petit, V., Drissen, L., & Crowther, P. A. 2006, AJ, 132, 1756
Phillips, M.M., Lira, P., Suntzeff, N.B., Schommer, R.A., Hamuy, M., & Maza, J. 1999, AJ, 118, 1776
Poznanski, D., et al. 2009, ApJ, 694, 1067
Prieto, J. 2008, ATel, 1550, 1
Prieto, J., et al. 2007, arXiv:0706.4088
Prieto, J., et al. 2008a, ApJ, 681, L9
Prieto, J., et al. 2008b, ATel, 1596, 1
Prieto, J., Sellgren, K., Thompson, T.A., & Kochanek, C.S. 2009, AJ, 705, 1425
Prieto, J., et al. 2010, arXiv:1007.0011
Prieto, J., & Khan, R. 2010, CBET, 2122, 1
Puckett, T., & Gautier, S. 2002, IAUC, 7863, 1
Rakavy, G., & Shaviv, G. 1967, ApJ, 148, 803
Rich, D. 2005, IAUC, 8497, 1
Schlegel, D. J., Finkbeiner, D. P., & Davis, M., 1998, ApJ, 500, 525
Schmidt, B.P., Kirshner, R.P., & Eastman, R.G. 1992, ApJ, 395, 366
Schmidt, B.P., Kirshner, R.P., Eastman, R.G., Phillips, M.M., Suntzeff, N.B., Hamuy, M., & Aviles, R. 1994, ApJ, 432, 42
Schwarzschild, M., & Härm, R. 1959, ApJ, 129, 637
Sehgal, A., Gagliano, R., & Puckett, T. 2006, CBET, 493, 1
Shaviv, N. 2000, ApJ, 532, L137
Shara, M.M., Zurek, D., Prialnik, D., Yaron, O., & Kovetz, A. 2010, arXiv:1009.2961
Silverman, J.M., et al. 2010, in prep.
Smith, N. 2005, MNRAS, 357, 1330
Smith, N. 2006, ApJ, 644, 1151
Smith, N. 2007, AJ, 133, 1034
Smith, N. 2008, Nature, 455, 201
Smith, N. 2010, MNRAS, submitted (arXiv:1010.3770)
Smith, N., & Conti, P.S¿ 2008, ApJ, 679, 1467
Smith, N., & Frew, D. 2010, MNRAS, submitted (arXiv:1010.3719)
Smith, N., & Hartigan, P. 2006, ApJ, 638, 1045
Smith, N., & Owocki, S.P. 2006, ApJ, 645, L45
Smith, N., Humphreys, R.M., & Gehrz, R.D. 2001, PASP, 113, 692
Smith, N., Davidson, K., Gull, T., Ishibashi, K., & Hillier, D.J. 2003a, ApJ, 586, 432
Smith, N., Gehrz, R.D., Hinz, P.M., Hoffmann, W.F., Hora, J.L., Mamajek, E.E., & Meyer, M.R. 2003b, AJ, 125, 1458
Smith, N., Vink, J., & de Koter, A. 2004, ApJ, 615, 475
Smith, N., Chornock, R., Li, W., Ganeshalingam, M., Silverman, J.M., Foley, R.J., Filippenko, A.V., & Barth, A.J. 2008, ApJ, 686, 467
Smith, N., et al. 2009a, ApJ, 697, L49
Smith, N., et al. 2009b, ApJ, 695, 1334
Smith, N., et al. 2010a, AJ, 139, 1451
Smith, N., et al. 2010b, ApJ, 709, 856
Soker, N. 2001, MNRAS, 325, 584
Sparks, W.B., et al. 2008, AJ, 135, 605
Stockdale, C.J., Rupen, M.P., Cowan, J.J., Chu, Y.H., & Jones, S.S 2001, AJ, 122, 283
Stothers, R.B., & Chin, C.W. 1993, ApJ, 408, L85
Sugerman, B., & Meixner, M. 2004, IAUC, 8442, 1
Tammann, G. A., & Sandage, A. 1968, ApJ, 151, 825
Thompson, T. A., Prieto, J. L., Stanek, K. Z., Kistler, M. D., Beacom, J. F., & Kochanek, C. S. 2009, ApJ, 705, 1364
Tully, R.B., Rizzi, L., Shaya, E.J., Courtois, H.M., Makarov, D.I., & Jacobs, B.A. 2009, AJ, 138, 323
Umana, G., Buemi, C.S., Trigilio, C., Leto, P., & Hora, J.L. 2010, ApJ, 718, 1036
Utrobin, V.P. 1984, Ap. & SS, 98, 115
Van Dyk, S.D. 2005, in ASP Conf. Ser. 332, The Fate of the Most Massive Stars, ed. R.M. Humphreys & K.Z. Stanek (San Francisco: ASP), 47
Van Dyk, S.D., Peng, C.Y., King, J.Y., Filippenko, A.V., Treffers, R.R., Li, W., & Richmond, M.W. 2000, PASP, 112, 1532
Van Dyk, S.D., Filippenko, A.V., & Li, W. 2002, PASP, 114, 700
Van Dyk, S.D., Filippenko, A.V., Li, W., & Challis, P.M. 2005, PASP, 117, 553
Van Dyk, S.D., Li, W., Filippenko, A.V., Humphreys, R.M., Foley, R., & Chllis, P. 2006, PASP, in press, astro-ph/0603025
van Marle, A.J., Owocki, S.P., & Shaviv, N. 2008, MNRAS, 389, 1353
van Marle, A.J., Owocki, S.P., & Shaviv, N. 2009, MNRAS, 394, 595
van Marle, A.J., Smith, N., Owocki, S.P., & van Veelen, B. 2010, MNRAS, arXiv:1004.2791
Vinko, J., Marion, G.H., Wheeler, J.C., Foley, R.J., & Kirshner, R.P. 2010, CBET, 2300, 1
Wade R. A., & Horne K. 1988, ApJ, 324, 411
Wagner, R.M., et al. 2004, PASP, 116, 326
Walborn, N.R., & Liller, M. 1977, ApJ, 211, 181
Whitney, C.A. 1952, Harvard Obs. Bull., 921, 8
Wild, P. 1961, IAUC, 1764, 1
Woosley, S.E., Blinnikov, S., & Heger, A. 2007, Nature, 450, 390
Yamaoka, H. 2005, IAUC, 8497, 1
Young, P.A. 2005, in ASP Conf. Ser. 332, The Fate of the Most Massive Stars, ed. R.M. Humphreys & K.Z. Stanek (San Francisco: ASP), 190
Zwicky, F. 1964, ApJ, 139, 514